AN INVESTIGATION INTO PISTON RING BLOWBY AND ITS EFFECT ON BIOGAS ENGINES.

Graham Peter Bush BSc (Hons), MRSC

Thesis submitted in partial fulfilment of the requirements for Doctor of Philosophy of the Council for National Academic Awards.

School of Mechanical and Production Engineering
School of Chemistry
Leicester Polytechnic.

October 1986

AN INVESTIGATION INTO PISTON RING BLOWBY AND ITS EFFECT ON BIOGAS ENGINES.

Graham Peter Bush BSc (Hons), CChem, MRSC

October 1986

ABSTRACT

This study has investigated the severe corrosion of Biogas engines by the blowby gases. The formation of blowby, its composition and flowrate have been measured and simulated. The nature of the piston ring sealing, lubrication and breakdown has been examined.

A study of Biogas engines showed that Copper corrosion of the small end and camshaft bearings by H_2S gas was the reason for engine failure. H_2S is present in all Biogas at a concentration of usually less than 1%, but succeeds in chemical attack despite its good combustion properties, and the expected reaction with the bases present in the lubrication oil. The H_2S was corroding in its gaseous state, but only those bearings with indirect lubrication. The solution to this problem is either to adopt force fed lubrication of the bearings, or to replace the alloy with Aluminium-Tin.

The experimental work used four engines of differing wear. The constant speed work showed that the fuel content of blowby gas increases with load despite any increase in fuelling rate. This trend was consistent for all gaseous fuels present including H_2S.

A series of computer calculations of piston ring blowby were completed, using conventional and novel input data. The resultant blowby flow was within an order of magnitude, confirming that two blowby mechanisms, ring gap blowby and ring seal breakdown, are present on worn engines. The composition results showed that the fuel content of blowby is subject to the complex nature of the quenching process in the combustion chamber.

A study of the oil present at the top ring showed that the oil is greatly modified when compared with the sump oil, as a result of thermal degradation and base depletion. The oil has a high acid TAN, which suggests it could encourage corrosive wear of the cylinder liner.

ACKNOWLEDGEMENTS

I would like to express my gratitude to my supervisors, Professor D J Picken and Dr M F Fox for their guidance and encouragement throughout the course of the research.

I would like to thank Mr L A Tibbs, Mr C English and Mr R J Smith from the School of Mechanical and Production Engineering, and Mr C Groves and Mr R White from the School of Chemistry for their technical assistance.

I would like to thank Dr D A Armitage for his lively debate.

I am indebted to the SERC for financing a research assistantship.

I would like to thank the following organisations for their assistance:

Anglian Water Authority
Applied Energy Systems
Austin Rover Group
Brooksby Agricultural College
Esso Chemicals, Abingdon
Ford Motor Company
MQAD, Harefield
Perkins engine company
Powertorque, Coventry
Severn-Trent Water Authority
Villiers Limited

Finally to my wife Sarah, for her assistance in preparing this thesis.

To my Parents

CONTENTS PAGE

Chapter 1. Introduction.

1.1 World Energy.

The sharp rise in crude oil prices in the early 1970's highlighted our dependence upon oil as the major source of energy, and was responsible for increased public interest in energy conservation and research. Statistical studies of present and future energy use and reserves, both worldwide and nationally, show that conventional energy sources will only sustain our energy needs for a finite time (the decline in oil production is predicted to be at approximately the year 2000). Table 1.1 shows a recent estimate of current and future world energy use. Such forecasts are constantly updated as technological and economic changes alter energy production and consumption patterns, and have, in the past, been inaccurate. However, all forecasts anticipate energy demand outstripping future energy provision by the oil industry. They clearly indicate the immediate need for research and development into alternative sources of energy.

The distribution of energy resources and their use varies considerably from one country to another. The industrialised nations have a high per capita consumption of high grade energy (e.g. electricity, gas and petroleum distillates). Fig 1.1 shows the pattern of U.K energy use over the last 35 years. The intelligent use of conservation measures within these communities is likely to produce an effective reduction in total world energy consumption (Ref 1.1). These nations also have the technological base from which conservation industries can grow, coupled with a large stable population who readily accept energy saving measures. However, the high degree of industrialization and large domestic market ensures a high demand for electricity in the future. Both established and novel alternative energy industries can compete in the market to supply electricity provided that the unit cost of its production is competitive with that of other technologies being developed to replace oil based power supplies.

In contrast, the developing countries depend on lower grade fuels, which are mainly used for cooking and heating. It has been suggested (Ref 1.2) that the shortage of firewood and the consequent defoliation of woodland and forest areas constitutes a larger and more difficult energy problem than the future decline in oil production. The developing countries are also experiencing a massive increase in population, which shows no signs of easing in the future. These two factors, combined with the commitment by governments to improve the living standards of their people, will generate an increasing energy demand in these countries. One important feature is common to most developing nations - a relatively low population density. This factor, combined with poor communications, promotes localised energy provision; national energy policies are poorly developed and those that exist are not particularly ambitious. Hence, conservation measures must also be on a localised basis, and this makes it harder to achieve large overall savings. However, the widespread use of alternative energy sources promises to provide a viable means of future supply because they can be tailored to suit local requirements. The large areas of available land space, the generally favourable climate and the need for small-to-medium sized installations are well suited to novel energy technologies, particularly those which are solar based.

It has been estimated that the annual solar radiation reaching the earth's surface has an energy content of 3×10^{24} J, which is equivalent to 75 times the world's proven fossil fuel reserves. Of this, 60% is available for absorption by plants, and 0.1% is actually collected by plant photosynthesis (Ref 1.3). Although the energy of the solar radiation reaching the earth's surface is dispersed, the trapping of sunlight, particularly in the otherwise unpopulated desert regions, is expected to be one of the major sources of electricity in the future. Research in several nations, notably the USA, has been undertaken into the direct use of sunlight to power steam turbines at desert based power stations (Ref 1.4).

Major solar energy projects, using the sun as a "primary" source, have been very successful in attracting finance for their development. The direct trapping and conversion of light energy is well suited to smaller scale installations (e.g domestic water and space heating) and shows potential with solar cells.

Supplementing these applications are the "secondary" solar technologies such as hydro-electric or wind power. These are well established techniques which are being tailored to suit modern needs. Several biological energy conversion technologies are also currently under development. As with other solar based energy projects they benefit from the virtually unlimited supply from the sun (via photosynthesis), simple technology, and also from a publicly approved ecological image. Along with geophysical projects such as geothermal power or hydro-electricity, biotechnology is renewable, promising potential long after the exhaustion of mineral supplies. However, the application is less advanced, with a few successful projects such as alcohol automotive fuel in Brazil or anaerobic digestion of animal wastes in India and China. Such projects illustrate that Biotechnology could become a very important source of energy because it can directly replace petroleum in its two major functions; motor fuel and chemical feedstock (Ref 1.4). There are many experimental biotechnology based proposals whose aim is to prove that they are viable and capable of a positive contribution towards future world energy needs. Only then will these proposals attract the financial backing required to exploit their potential.

1.2 Biotechnology.

1.2.1 The Bioenergy Conversion Technologies.

Fig 1.2 shows the general routes for the conversion of Biomass into high grade fuels or electricity. The application of, or research into, these areas is largely dependent on localised factors such as the availability of feedstock or the energy needs of the user. The feedstock, Biomass, is a variable material as it is dependent on

local climate, agricultural and industrial techniques, and also geographical conditions. The product generated is applied to satisfy specific needs, which depends on the society, climate and geography of the user. Therefore the development of a given Biotechnology will vary across the world.

This project is associated with the Leicester Polytechnic Anaerobic Digester Group's research into the anaerobic digestion of animal wastes. The anaerobic digestion of biomass is a long established process, as outlined in Section 1.2.2. The product "Biogas" contains CH_4 and CO_2 in roughly a 2:1 ratio, with up to 1% of H_2S and other trace gases such as H_2 and N_2 (see Section 1.2.4). The anaerobic digestion process is very tolerant to the type of feedstock, being able to produce Biogas from a very wide variety of natural materials. These range from sewage and animal excreta to plant matter (e.g water hyacinth, grass, algae) and industrial wastes (e.g brewery hops, paper sludge, cheese whey). On industrial sites, digestion is often used as a treatment step to break down an unpleasant effluent before disposal. It is often a viable process for this reason alone, as pollution control legislation can be satisfied by the anaerobic breakdown of the waste. Under these circumstances, the production of Biogas is an additional bonus, which can be used to contribute towards the energy needs of the treatment plant concerned.

Considerable research has been undertaken into the development of improved digestion technology and efficient gas output, with wide application to all sizes of digester. However, the utilisation of the gas produced always depends upon the needs of the individual site. As a result, digester design has been improved by both industrial and research projects, but the development of the technology to exploit the gas produced has remained site dependent. The lack of co-ordinated development of the gas utilisation techniques has had an important effect on the commercial development of the smaller scale digester, because its viability relies on the effective use of the gas produced.

1.2.2 The History of Biogas.

The production of marsh gas has been observed throughout history and is the simplest natural form of anaerobic digestion. The anaerobic breakdown of natural materials occurs in all de-oxygenated environments including lagoons, peat bogs, marshes and swamps. It has been estimated that natural sources produce at least ten times as much H_2S as man does. This occurs as a result of both anaerobic digestion and volcanic activity (Ref 1.5). Investigations of "air produced by substances putrefying in water" began as early as 1790 (Ref 1.6).

The first artificial digesters were sewage lagoons, created during the Industrial Revolution, where the effluent was left to process naturally. The subsequent increase in population, combined with increased technical knowledge, led to the development of more advanced systems for the processing of sewage sludge. The first known use for Biogas was for gas street lighting in Exeter in 1896 (Ref 1.7). This marked the start of the development of unheated sludge digesters. By the 1920's these digesters were becoming overloaded, and the heated digester was conceived. This development reduced the process retention time. Subsequent research was directed towards the refinement of this technique, and it was not until the 1950's that the "high rate" digesters were introduced. It is only recently that concerted research has begun to understand and refine the digestion process itself, although this is unlikely to produce a significant improvement in the rate of gas production. However, the emphasis has moved away from effluent treatment alone, and towards optimizing the production and utilisation of Biogas.

1.2.3 The Principles of Biogas Production.

Anaerobic digestion is the bacterial breakdown of organic molecules. It has been used to produce Biogas from a wide variety of natural materials, with varying degrees of success (Ref 1.3). The great

advantage of this process is that it occurs spontaneously once the anaerobic conditions have been established, as the bacteria are already present in the slurry mixture. The processing costs are therefore very low, the largest cost being the heat to keep the slurry temperature within the optimum range 30°C to 40°C (the process does not generate enough heat to counteract both the heat loss from the digester and also that incurred due to slurry replacement). The heat input required varies with both the local climate and seasons. This favours the operation of digesters in tropical or sub-tropical regions of the world where there is little seasonal temperature variation around a warm mean value.

The process by which methane is formed appears to involve three interdependent metabolic groups of bacteria; fermentative, H_2 producing acetogenic, and methanogenic (Ref 1.8). The role of a fourth group, the H_2-consuming acetogenic bacteria, is still unclear, but they do not make a major contribution to the digestion process (Ref 1.9). A schematic reaction is given in Fig. 1.3, but the exact mechanisms are still largely unknown, mainly due to the large variety of participant species and the complex interdependence of various types on one another. However, within the digester environment, the catabolism of organic plant matter forms a food chain, with each group using the breakdown products from the last.

The fermentative bacteria are responsible for the breakdown of organic materials into carboxylic acid salts, H_2, CO_2 and other product molecules. The concentration of H_2 in solution is critical to the amount of acetate produced; at higher H_2 concentrations, longer chain carboxylic acids are the favoured products.

The H_2-producing acetogenic bacteria are responsible for the production of acetate, H_2 and CO_2 from the longer chain carboxylic acids, alcohols and other organic acids which are formed as part of the first stage fermentation. A low H_2 concentration in the solution is critical for these reactions to occur.

The methanogenic bacteria catabolise the acetate and CO_2 into CH_4 using the H_2 produced by the other two metabolic groups, but this group can only perform the methanogenesis under strictly anaerobic conditions. The rapid consumption of the H_2 controls the other steps in the digestion process, and the activity of the methanogenic bacteria acts as a regulatory mechanism for the complete digestion process.

The formation of H_2 in solution is essentially a reduction of free H^+ during the first two stages of the digestion process. The formation of H_2S has been attributed to the reduction of dissolved sulphate under these conditions (Ref 1.8). The sulphide produced is an important source of sulphur for all of the bacteria present.

The conditions under which anaerobic digestion occurs are well documented, and a considerable amount of research has been directed towards the refinement of digester design, resulting in the modern high rate digesters. Apart from the establishment of strictly anaerobic conditions, there are several important factors to be considered for maximising the gas output from slurry digesters:

(a) The temperature of the digester must be maintained in the range $30^{o}C$ to $40^{o}C$ to encourage healthy methane production. This is easily achieved in warmer climates, but heating (often using the product Biogas) is usually required in the temperate zones during the winter. This is an important consideration, as during the winter months the energy demand is highest, and the Biogas used for digester heating is effectively a diversion of energy output during this period.

(b) The retention time for the slurry should be between 10 and 30 days, with some degree of mixing within the digester to homogenise the newer and partially digested sludge. The extent, method and rate of mixing depends on the design of the digester concerned, and the optimised rate of sludge homogenisation developed for that digester.

(c) In some digester designs, it is important to monitor the pH, the solids content and other physical or chemical parameters on which the operation is dependent. Such process control is inconvenient on small scale farm digesters, where simplicity is an essential factor.

1.2.4 The Nature of Biogas

The composition of the Biogas produced from Anaerobic Digesters depends upon both the digester design and its operating conditions, but mainly on the nature of the digested material. The methane content of Biogas is normally within the range of 60% to 70%, with the pre-treated feedstocks (e.g pig slurry) providing the highest content. The balance is carbon dioxide, with traces of H_2, N_2 and H_2S.

The analysis of Biogas is now a routine measurement by Gas Chromatography. An extensive programme of research by Grune and Chueh (Ref 1.10) established the technique using column packing materials commonly available in the early 1960's. The refinement of gas chromatographic analysis from this period onwards has yielded improved and specialised column packings, which give increased component resolution. Burgess and Wood (Ref 1.11) undertook a wider investigation of Biogas properties. Their work covered the composition, water content, explosion risk and a safety appraisal of Biogas use in the sewage industry. This paper has been the basis for most of the analysis and handling techniques which have been devised since its publication. With the development of porous polymer chromatographic packings, their improved gas handling capabilities were quickly adopted for use with Biogas. A recent description of Biogas analysis is presented in Warren Springs Laboratory WRC Report TR85 (Ref 1.12).

The methane content of Biogas can vary considerably, but all Biogas is flammable and can be used to generate heat or power. The simplest

use for the gas is to produce heat for cooking, which is favoured in the developing countries, where there is a constant need for this type of low grade energy. The extensive anaerobic digester programmes in India and China provide small scale digesters, which yield Biogas to be used on a local basis for cooking. One of the major advantages of direct heat use by burning the gas is the simplicity of the technology involved with inherent low cost and minimal maintenance. However, in a more complex industrialized society, with centralized gas distribution, there are important failings in the use of biogas to supplement or replace existing gas sources. The most fundamental problem is the quantity and quality required of the gas supply. At best, Biogas can be envisaged as a "top up" supplement to the mains distribution system; in this country the demand for gas would drastically outstretch potential Biogas production. Raw Biogas is unsuitable for supplementing the mains supply, first because of its inconsistent composition, and second because of the potential corrosion and reliability problems associated with the introduction of H_2S and water vapour into the gas mains. The gas would first require scrubbing (see Section 2.2.1), drying and then compression and the processing costs involved in this purification process would make the project unprofitable. These shortcomings rule out the use of Biogas as a direct source of energy within industrialized societies. The gas must either be used on a localized basis, or its chemical energy must be converted into another form of energy.

1.2.5 Gaseous fuels in Internal Combustion Engines

The use of gaseous fuels in Internal Combustion engines is a well established practice, the most common fuels being liquified Propane and Methane. As such there is an established source of technology to provide I.C engines tailored for use with Biogas. Such engines can be used in two major areas; the production of power from static engines, usually producing electricity and heat, or automotive use, supplementing or replacing conventional fuels.

The major constituent of both Biogas and Natural Gas is methane. The use of Natural Gas engines in static applications is common and they are often used as a source of standby power. The use of Liquid Natural Gas (LNG) and Compressed Natural Gas (CNG) in automotive applications has gained support recently, because of the recent oil price rises. CNG has been used in Italy for over 30 years (Ref 1.14), and is currently used in almost 200 000 vehicles (Ref 1.15). Recent development of CNG fuel networks have been undertaken, notably in both the USA and New Zealand.

The motivation for these developments is the combination of low to competitive cost, and the very low pollution characteristics. The use of gaseous fuels enables a simpler design of induction system to be used. The gas does not have to be vapourized, and therefore a simple gas mixing device can be used to combine the air and fuel prior to its entry into the combustion chamber. The efficiency of mixing is very good, offering an even mixture distribution across multi-cylinder engines (Ref 1.16).

There is a reduction, in theory, in the air breathing capacity when using methane fuel. This is because the fuel gas occupies a larger volume within the induced mixture than when a comparable atomized liquid fuel is used. Methane also has a relatively slow flame speed when compared with gasoline. Both these factors could adversely affect the performance of a converted engine. These disadvantages can be overcome by the optimization of the engine calibration (ignition timing, valve timing etc), and the excellent anti-knock characteristics of methane allow the use of very high compression ratio engines. The combustion of methane is highly efficient, giving very low exhaust emissions, particularly for the CO and HC values.

1.3 Project Aims

The Biogas industry has been very successful in implementing large scale centralized digesters, with correspondingly large I.C engine generation facilities. In contrast, the efficient use of the small scale digester, producing useful power and heat, has not been fully exploited.

The aims of this project were:

(a) To examine the type of engine design used with digesters, and determine why so many small scale digester projects suffer from engine failures.

(b) To investigate the factors affecting the actual cause of failure and to propose solutions to the problem.

(c) To investigate the basic principals which affect the failure mechanism, and to determine the effect of differing stages of engine wear.

References Chapter 1

1.1 BEIJDORFF A.F, Energy Efficiency publ. Shell International Petroleum Co., 1979.

1.2 AUER P.L et al, "Unconventional Energy Resources" in World Energy Resources 1985 - 2020. publ. IPC Scientific and Technical Press 1978, pp 135 - 179.

1.3 SLESSER M, LEWIS C, Biological energy resources publ. E & F.N Spon Ltd 1979.

1.4 RAHMER B.A, "Fuels for the future" publ. Petroleum Economist 1980 pp 41 - 49.

1.5 STRAUSS W, MAINWARING S.J "Air Pollution" publ. Edward Arnold 1984 p 3.

1.6 PRIESTLEY J Experiments and observations on different kinds of air Vol 1, (publ) Birmingham, 1790.

1.7 TIEJTEN C, "From Biodung to Biogas - A historical review of the european experience". Energy, Agriculture and Waste Management, 1980, pp 247 - 259.

1.8 McINERNEY M.J, BRYANT M.P, "Review of methane fermentation fundamentals" in WISE D (ed) Fuel gas production from Biomass Vol 1 CRC Press, 1983, pp 19 - 46.

1.9 HAWKES F "The biochemistry of anaerobic digestion" in BUVET R, FOX M.F, PICKEN D.J (eds) Biomethane, production and uses (publ) Turret Wheatland 1984, pp 41 - 60.

1.10 GRUNE W.N, CHUEH C.F "Sludge gas analysis using Gas Chromatography" A report in 8 parts in Water and Sewage Works December 1962 to July 1963.

1.11 BURGESS S.G, WOOD L.B "The properties and detection of sludge gas" J Inst Sew Purif 1964 pp 24 - 46.

1.12 Water Research Centre Report TR85, Warren Springs Laboratory, 1980.

1.13 TISON R, SPRAFKA J et al. "Safety issues surrounding the use and operation of CNG vehicles." SAE 831078.

1.15 JOYCE T.J "Research and developement needs for CNG fuelled vehicles." SAE 831065.

1.16 KARIM G.A, WIERZBA I "Comparitive studies of Methane and Propane as fuels for S.I and C.I engines" SAE 831196.

1.17 Department of Energy Digest of United Kingdom energy statistics 1985 HMSO pp 10 - 11.

1.18 FRANCIS W, PETERS M C "Fuels and Technology" (2nd Edn) Pergamon Press p 473.

Figures Chapter 1.

Fig 1.1 Diagram of U.K energy consumption (Ref 1.17).

Fig 1.2 General routes for Biomass conversion (Ref 1.3)

Fig 1.3 Schematic diagram of the digestion process (Ref 1.9)

Tables Chapter 1

Table 1.1 Current energy patterns in developed and underdeveloped countries (Ref 1.18).

Energy source	Date of 90% depletion	Date of major use (>1%)	Use in third world	Use in devel. world	Use world wide
	(A.D)	(A.D)	(1980)	(1980)	(2100)
VEGETABLE			75	2	21
Food			30	2	9
Food residues			25		
Wood			20		
Peat	2000				
Biomass		1990			8
FOSSIL			16	89	19
Gas	2040	1940	2	12	1
Oil	2020	1920	1	47	2
Coal	2500	1700	13	17	11
Oil shale		2000			5
RENEWABLE			9	6	42
Solar		1980			12
Wind		1300	2		3
Hydro		1000	7	6	3
Wave		2000			5
Tidal		1990			2
Geothermal		2010			15
Oceanic		2050			2
NUCLEAR			Nil	3	18
Thermal reactors	2050	1960		3	3
Fast reactors		2000			14
Fusion reactors		2050			1

TABLE 1.1 ENERGY PATTERNS IN DEVELOPED AND UNDERDEVELOPED COUNTRIES

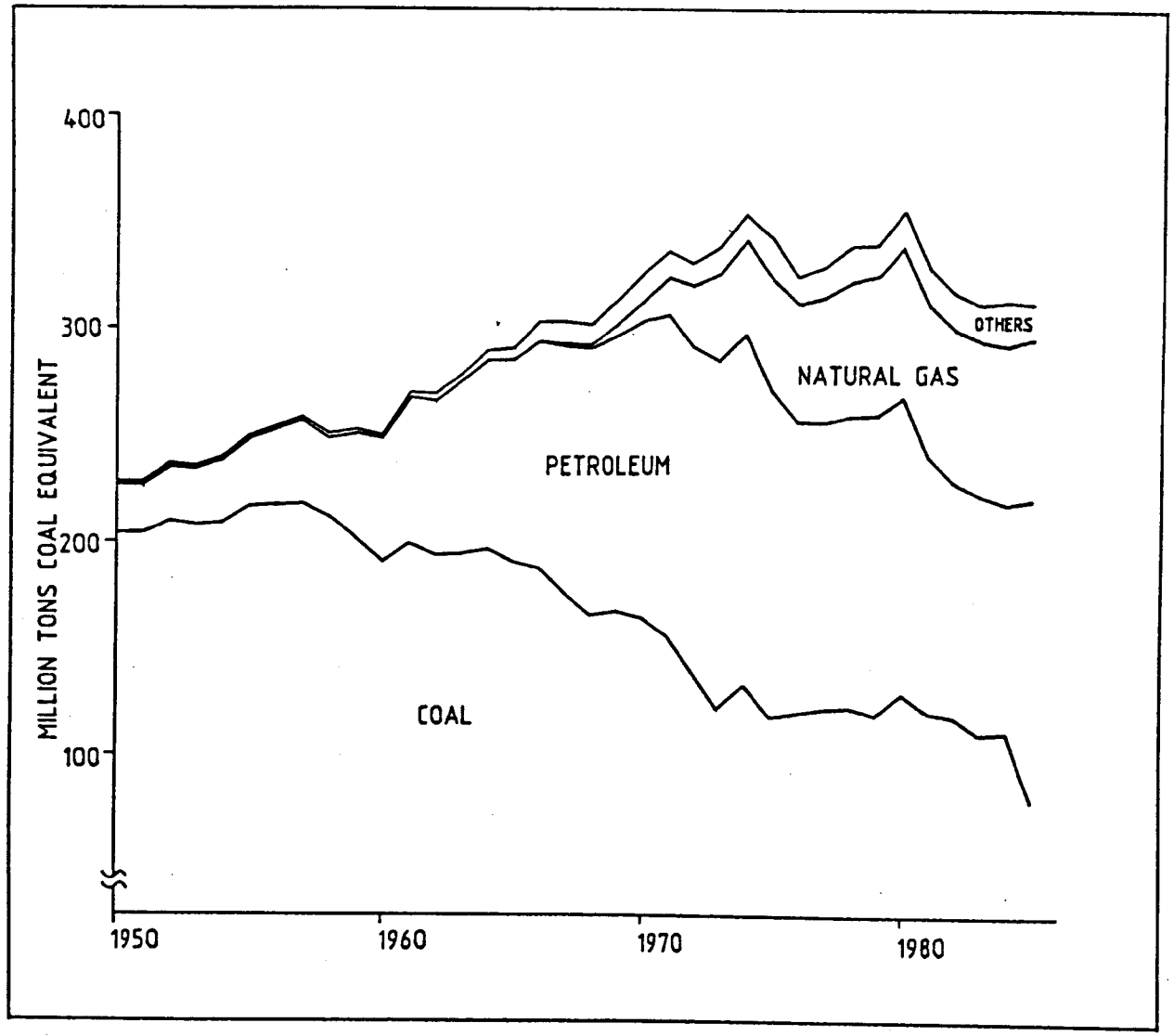

FIG 1.1 DIAGRAM OF U.K ENERGY CONSUMPTION (REF 1.17)

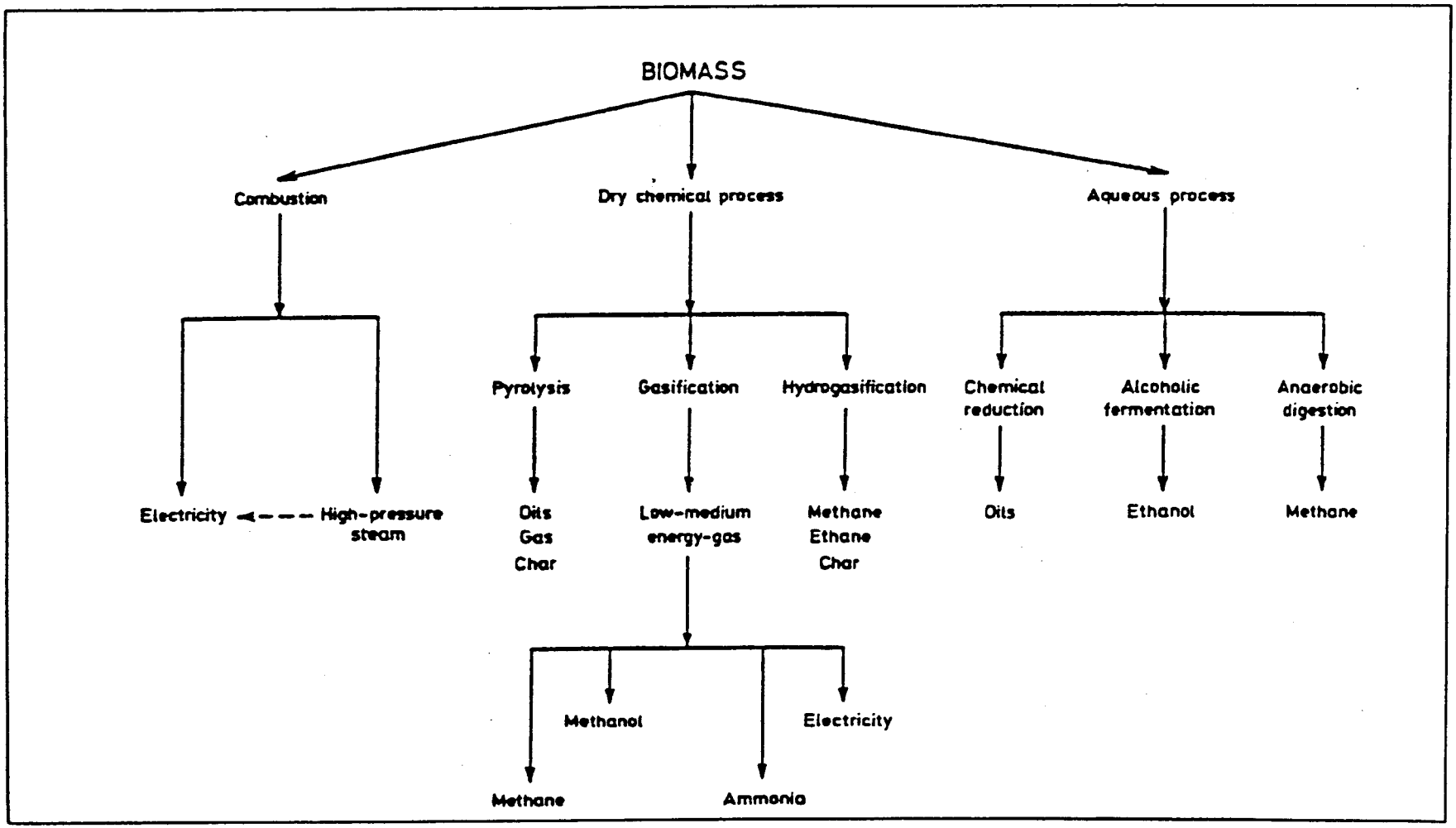

FIG 1.2 GENERAL ROUTES FOR BIOMASS CONVERSION (REF 1.3)

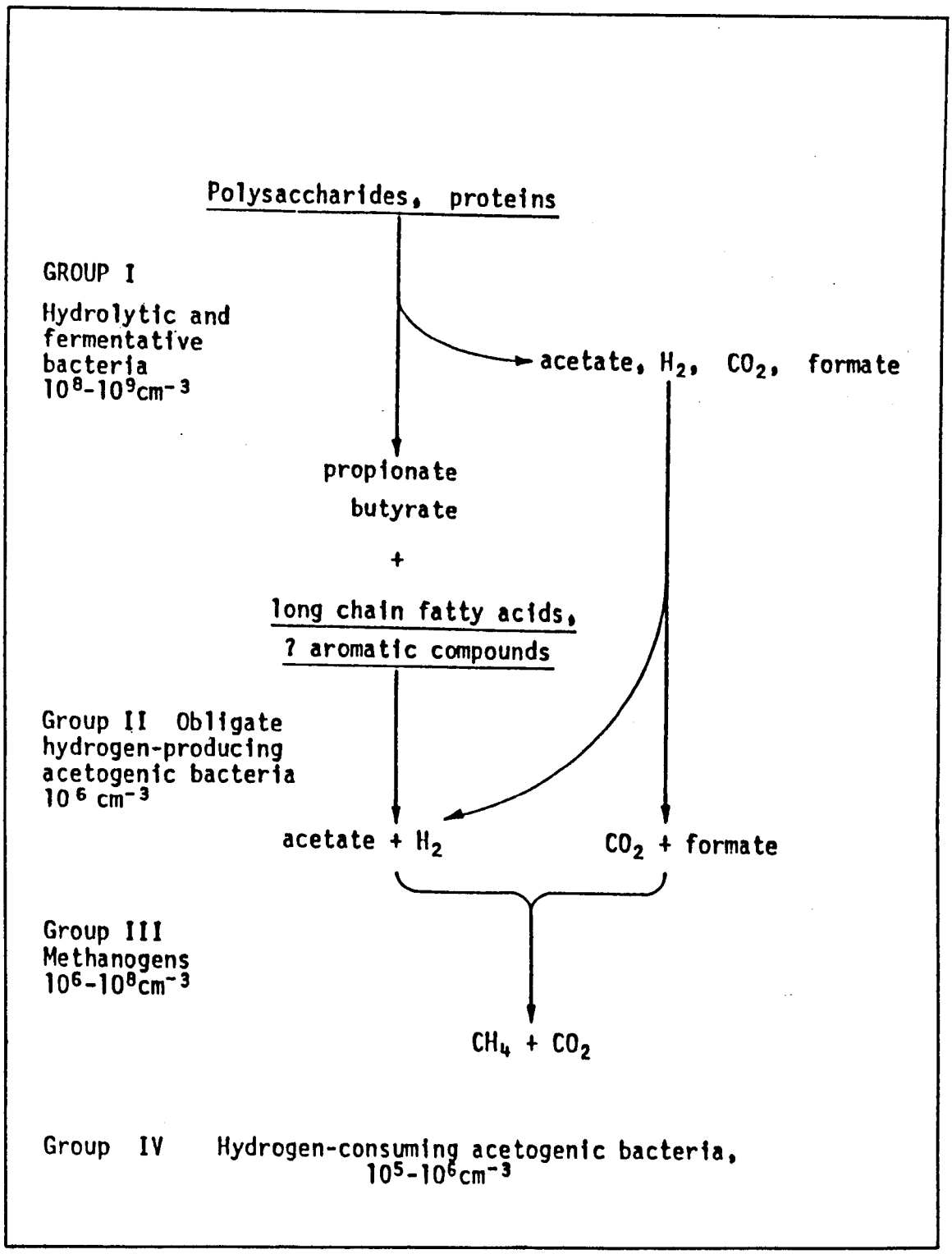

FIG 1.3 SCHEMATIC DIAGRAM OF THE DIGESTION PROCESS.

Chapter 2 Analysis of failures and experimental engine work.

2.1 Introduction.

2.1.1 Corrosion in Biogas Engines.

The success of Biogas as an alternative energy source depends upon its ability to become a viable replacement for future conventional supplies. Central to this aim is the reliable production of Biogas and the continuity of electricity generation by engines running on a fuel mixture containing H_2S, which is very corrosive. In the industrialized nations, the use of Biogas as a fuel for engine-generator sets producing electricity and heat has highlighted a reliability problem related to the size of engine used.

The large diesel dual-fuel (Diesel/Biogas) engines in municipal sewage works run very reliably with few, if any corrosion problems. This is partly due to the fact that sewage Biogas (at up to 0.1% H_2S) is relatively low in H_2S content compared to farm Biogas. The Thames Water Authority have Sewage digesters which have been producing electricity since the 1930's. In 1979/80, their sewage works produced over 9×10^7 m^3 of gas and their dual-fuelled engines generated 1.26×10^2 MWh of electricity (Ref 2.1). In the paper by Burgess and Wood (Ref 2.2), Mogden sludge gas was quoted as being between 0.02% and 0.05% H_2S. At this concentration no engine corrosion was reported.

A successful example of the municipal use of Biogas is the Severn-Trent Water Authority's Wanlip water reclamation works near Leicester. Four large steel digester tanks with a total capacity of 19093 m^3 of sewage sludge are used to generate Biogas. In 1984, on average, a daily throughput of 1040 m^3 of sewage sludge held for 13.5 days, produced 12060 m^3 of Biogas per day. The Biogas is fed to five Harland and Wolf 860 bhp dual-fuelled diesel engines installed in a purpose-built generator house. The engines annually produce 10.2×10^6 KWh of electricity which is approximately 80%

of total site usage. The cooling water from the engines is used to heat the digesters. The engines are regularly maintained with a short service every 1,000 hours and a major overhaul and oil change every 20,000 hours. A recent 100,000 hour stripdown revealed that the small end bearing surfaces had no abnormal wear or Biogas corrosion (Ref 2.3). The Biogas at this site has between 0.15% and 0.18% H_2S content.

The large quantity of Biogas produced from this reclamation works justifies the massive investment in large marine derived engines. At smaller rural sewage works or on farms, the engines used must be correspondingly smaller. These small scale digester engines suffer from extensive corrosion, particularly of copper-based bearing materials. Farm-sized digester engines are usually automotive engines modified to run on gas, either as spark ignition or dual-fuelled diesel engines. Typically, the smallest biogas engines are natural gas engines converted from automobile applications. The pioneer commercial project in this area was the Fiat "Totem" system based on their 903cc spark ignition engine. Similar conversions have been done to the Ford Cortina OHC and Land Rover 2.2 litre engines. However, none of these have appeared in a corrosion resistant form, and consequently suffer failure when used with Biogas.

The STWA's Retford sewage works has a small digester producing Biogas. This was fed to a Perkins G 4.236 gas engine installed in a generating room adjacent to the gas holder. The engine ran for a period of just over two years, completing 9597 hours with the only major shutdowns associated with ignition component development problems. During this period it annually produced 5.87×10^4 KWh of electricity from 4.68×10^4 m^3 of gas. Regular oil analysis of the high TBN oil was performed. However, increasing engine noise led to an engine stripdown and it was found that the phosphor-bronze small end bearings had suffered severe corrosion - in some parts total disintegration. These bearings have recently been replaced and the manufacturer has consulted their bearing supplier (Glacier

Metals) to obtain an aluminium alloy alternative. The Biogas at this site is high in H_2S, within the range 0.35% to 0.40%. This concentration is unusual for a sewage farm, and is in the range normally encountered at agricultural sites. The engine is now on standby only, as the changes in CEGB tariffs have made it uneconomic to run (Ref 2.4).

The photographs (Figs 2.1, 2.3 - 2.6) show typical H_2S corrosion of copper based bearings; in this case the camshaft bearing shells from a Ford Dover dual-fuelled diesel engine (a "Powertorque" customized gas engine). The bearing surface has large areas of severe abrasion parallel to the direction of camshaft rotation (dark areas), interdispersed between regions of the original metal (lighter areas). The surface cross section A - D from Fig 2.1 was measured by a Talysurf and is shown in Fig 2.2. This clearly shows that the damaged surface has been stripped of parent metal to leave a large trough containing the corrosion products. The scanning electron micrographs (Figs 2.3 - 2.6) of the abraded region give a detailed view of the surface corrosion. The metal is initially attacked at weak points in its structure, and pitting occurs, leaving an uneven surface from which fragments flake away. The movement of the camshaft, using these fragments suspended within the oil film, removes the upper layer of metal and corrosion products to reveal a fresh metal surface. This is then attacked by the H_2S to continue the corrosion process. This mechanism is similar to that for the failure of small end bearings, where the combination of high temperature, high bearing pressure and oil agitation (as a result of the cyclic movement of the piston) encourages the rapid corrosion of the copper alloy. This is similar to, but far more severe than, the corrosion of bearing alloys observed at high temperatures with sulphurised oil additives (Ref 2.5).

The corrosion product, analysed by powder X Ray crystallography, is Copper Sulphide. This is a black solid whose appearance on all copper and brass components is common at all Biogas installations. The corrosion of Copper by Sulphur compounds, including H_2S, has

been extensively recorded. The reaction has been used in the automotive industry in the "Copper Strip Test" (ASTM D 130/ IP 154) for determining the organic Sulphur content of fuels (the presence of elemental Sulphur, H_2S and Carbonyl Sulphide can cause inaccuracies in the test results). Research into the atmospheric corrosion of Copper has been comprehensive because of its implications in the use of electrical switches and contacts. This is particularly important in the telecommunications industry, where the need for low maintenance, long life contacts is essential.

The reaction between Copper and H_2S is very rapid, the product being Copper (I) Sulphide as shown in Equation 2.1. This reaction is enhanced by the presence of atmospheric oxygen and water. With excess H_2S, Copper (II) Sulphide can be formed by a reaction of the initial corrosion product (Equation 2.2). This reaction is normally restricted to the outer surface of the sulphide layer, as Cu_2S is relatively impervious to the penetration of H_2S.

$$2Cu + H_2S = Cu_2S + H_2 \qquad (2.1)$$

$$Cu_2S + H_2S = 2CuS + H_2 \qquad (2.2)$$

The corrosion of bearing alloys in Biogas engines is encouraged by the oil stirring, relative movement of the loaded bearing surfaces, and the temperature of the reaction surface. The removal of the corrosion product by the oil film and the continuous supply of H_2S from the blowby gases ensures a high rate of surface deterioration. The small end and camshaft bearings are both subject to this type of H_2S corrosion. However, the big end bearings are not attacked in this manner, and appear to be suitable for use with Biogas. Both the big end bearings, and all the bearings in the larger (marine derived) Biogas engines, have force-fed lubrication systems which provide a continuous supply of oil directly to the bearing surfaces. However, the vulnerable bearings rely on indirect lubrication mechanisms which are less efficient. This difference suggests that the corrosion is by gaseous H_2S present at the

bearing surface, and not as a result of H_2S dissolved in the oil. Moreover, the oil additive package appears unable to neutralise the H_2S.

It has been shown that small internal combustion engines have severe corrosion problems. The research and industrial projects involved have attempted to overcome this failure. There are two distinct approaches to solving the corrosion problem:

(A) Modification to the engines in an attempt to reduce or prevent the attack by H_2S.

(B) Remove the H_2S from the fuel gas before it enters the engine. This can be further broken down into:

(a) Preventing the production of H_2S.

(b) Removal of H_2S from the Biogas once generated.

(A) One possible solution to the problem is to modify the smaller engines so that all their bearings have force-fed oil lubrication. It is unlikely that the engine manufacturers would instal such a modification, because it is not required for those engines which are used in normal applications. The low volumes and low profits associated with such a specialised use would deter such companies from designing and producing an upgraded oil supply system. This factor immediately increases the potential cost of such a modification, as, with no standardized Biogas engine components, Biogas engines would be produced by the replacement of standard parts by small specialist firms. On the technical side, there is very little room to run an oil channel up through the small section con-rod, and the precision drilled oilway would be expensive to produce. It may, however, be possible to run an external small diameter oil pipe from the big end up the con-rod to the small end. Such modifications are not only expensive, but may require further changes such as the need for an upgraded oil pump. The maintenance

of these modified engines is unlikely to be acceptable to the farmer, who wants to use the simpler standard engine. The supply of excess oil to the small end will also lead to greater oil consumption and increased hydrocarbons in the exhaust gases, because the amount of oil entering, and burnt in, the combustion chamber increases. This occurs because the excess of oil floods the drain holes in the piston skirt, and this splashes excess oil onto the cylinder wall. This, in turn, overcomes the control of the oil supply to the cylinder wall by the oil scraper rings, leaving an excess of oil on the upper liner which is then swept into the combustion chamber by the compression rings. The supply of oil to this region is further discussed in Chapter Four.

Another possible modification is to change the bearing alloy to one without copper, or a copper alloy which is resistant to corrosion by H_2S. This solution has the same disadvantages as outlined above in that it introduces non-standard parts into the engine at increased cost. It is, however, a simpler solution, requiring no major redesign of the engine components involved, providing the correct alloy can be found. One alternative is that of an Aluminium-Tin based bearing, but the engine would have to be de-rated to reduce the stress on the modified small end. This, in turn, means increased capital costs (for a given power output) on top of the engine modification costs. However, there may be an increase in overall engine life by only partly loading the engine. Hassaan (Ref 2.6) has shown that the limiting factor on engine service life is the wear at the top of the cylinder bore. De-rating the engine extends its service life and could therefore provide a long term capital saving.

The rapid failure of the small end and camshaft bearings leads to increased maintenance costs and lost running time, reducing the project viability and acceptability (Ref 2.7). On the other hand, the increased capital cost of engine modifications makes the initial investment in Biotechnology less attractive, particularly as the modifications suggested above are, as yet, unproven and therefore do

not have the support of the engine manufacturers. For these reasons, many Biogas projects have attempted to use engine-generator systems with components largely unmodified, or alternatively have bought the commercial packages described earlier and have tolerated high service costs. Large capital investment in improving the engine technology has not been undertaken, with financial resources being used to improve digester technology.

(B) The alternative to engine modifications is the removal of H_2S from the Biogas supplied to it. This approach also increases both capital and running costs, and also detracts from the concept of Biogas as a free fuel. Biogas is produced from materials which would be treated in a similar manner during non-productive disposal. Industrial organic waste material and sewage has to be treated, or disposed of, to satisfy health and pollution control requirements. Long term storage of farm manure is common, before it is spread on the land as a fertilizer. Therefore industrial, municipal and agricultural waste materials can be stored and treated in a productive way to generate Biogas at little additional cost. Furthermore, the digestion process improves the quality of the slurry, both chemically and physically. Chemically, the slurry is broken down and both its Chemical Oxygen Demand (COD) and its Biological Oxygen Demand (BOD_5) are greatly reduced. These are, respectively, the measures of the oxidizable organic matter present and the oxygen consuming activity of the waste material. Physically the slurry is homogenised, producing a solution which is far easier to handle and to spread evenly on farmland as a fertilizer.

In the discussion so far, the gas has been considered as an untreated by-product, as any gas treatment process immediately increases the unit production costs. However, the removal of H_2S from the fuel gas is an alternative to engine modifications, and many experimental digesters have used gas treatment equipment in an attempt to combat their corrosion problems. There are two ways of removing the corrosive H_2S from the gas.

(a) Modify the digestion process to prevent the production of H_2S.

Our understanding of the digestion process has increased rapidly in the last few years, and many strains of bacteria have been isolated as described in Chapter One. However, the formation of H_2S occurs as a result of the biochemistry of the deoxygenated digestion environment which favours the formation of sulphide from the reduction of both organic sulphur and dissolved sulphate. An obvious sludge treatment is to inhibit or remove the sulphur from the solution. This is likely to be counterproductive because all of the bacteria present require sulphur as a basic element for reproduction, and its removal would prevent the anaerobic digestion from occurring. Any sludge treatment must be based on removal of the sulphide following its formation. One such treatment could be the introduction of transition metal ions into the sludge in order to form metal sulphides. The concentration of Iron in sewage sludge, for example, has been shown to reduce the H_2S content of the Biogas produced from its digestion (Ref 2.2). The transition metal sulphides, because of their low solubility in water (typically less than 10^{-7} gcm^{-3}), would settle in the base of the digester and could be separated (Ref 2.8). This is likely to fail because, in most digester designs, the slurry is agitated to ensure complete digestion and to prevent solids from caking within the digester. A study is also needed of both the effect of added metal ions on the digestion bacteria and on the environment where the output slurry is eventually spread.

A recent paper by Kobayashi et al (Ref 2.9) has investigated the use of anaerobic photosynthetic bacteria to oxidize the sulphide to sulphate within the digester. This approach is simple and relatively inexpensive, but as the authors point out, requires a large amount of development. The controlling factor is the supply of light to the slurry, and this technique requires a new design of digester. It would be constructed from a transparent material, with a complex external shape in order that it has a relatively large surface area. This is to maximise the amount of light available for

photosynthesis. The novel materials and unusual design also provide new technical and maintenance challenges.

All of these modifications or additions within the digester require further research to examine their feasibility, cost and environmental consequences. In conclusion, there appears to be no acceptable method of preventing the formation of H_2S during digestion, and its presence in the Biogas produced.

(b) Removal of the H_2S from the Biogas.

The natural gas industry is an available source of technical expertise which can be adapted for use with Biogas. The technology, previously used to sweeten coal gas, can be used to scrub H_2S from Biogas. Proven designs are readily available for scrubbers for medium to large scale digesters. As a result, a large amount of effort has been directed towards the removal of both H_2S and CO_2 from Biogas. The advantages of this approach are:

(i) The calorific value of the Biogas is increased by the removal of the inert CO_2.

(ii) The H_2S is poisonous, corrosive and produces SO_2 as a combustion product. Its removal solves most of the problems associated with the use of Biogas.

(iii) The removal of CO_2 combats the problem of its solidification at constrictions in the pressurisation equipment used when Biogas is compressed (the use of compressed Biogas in automotive applications is being investigated by the Anglian Water Authority).

The H_2S is regarded as a nuisance to be removed mainly because of the health hazard that it poses. With large scale industrial digesters, the unit cost of gas scrubbing is relatively low, particularly if low grade steam, as a by-product of the industry

concerned, can be used for the scrubbing or regeneration of scrubbing reagents. In contrast, the H_2S removal process is a threat to the viability of the small digester, where the economics of scrubbing are less favourable. Several systems have so far been tried.

Liquid absorption (e.g by water) in scrubbers. These are typically shower type devices allowing the thorough mixing of the Biogas and the scrubbing solution. This technique takes up both CO_2 and H_2S, as they are both readily soluble in aqueous solutions (3.3 and 9.8 x 10^{-3} mol/100 cm^3 H_2O respectively). Both of these gases dissolve to give an acidic solution which subsequently requires safe disposal. A variation of this technique uses an alkali solution such as Sodium Hydroxide, where the scrubbing involves an acid-alkali reaction following the dissolution of the gas. The capital cost of providing a (corrosion resistant) scrubbing booth and waste container is high. However, the processing costs are relatively low if water is used.

Solid absorption e.g by zeolites or activated carbon. This is achieved by passing the gas through a packed vessel containing the absorption medium. The CO_2 and H_2S are separated from the Biogas as it passes through the molecular framework of the absorbant material. This occurs because of chemically active sites attracting the electron-rich Oxygen and Sulphur atoms. Once attracted into the solid matrix, the gas molecules are held in low chemical potential energy wells associated with electronic interactions. They require an input of energy to be released, usually in the form of heat. The methane gas molecules, which lack the available electron pairs, do not interact with the solid's activated sites so easily, and therefore the absorption is selective. However, the solid eventually becomes saturated with absorbed gas molecules. It then requires regeneration. Both solids are comparatively expensive to buy, and there must be two scrubbing units alternating between the scrubbing and regeneration phases. For these reasons, the capital cost of this system is quite high. Both materials have a limited

regeneration life. Both (particularly the zeolites) are water sensitive, and the gas must be dried before treatment. The regeneration process is by thermal desorption. These two factors increase the processing costs and decrease the net energy gain. However, activated carbon does show some preference for H_2S over CO_2 (Ref 2.8).

Iron hydroxide. Iron hydroxide selectively reacts with H_2S to form Iron sulphide (Eqn 2.3), which subsequently requires regeneration. Hot, wet air is used in the regeneration step producing solid sulphur (Eqn 2.4). The equations for these reactions are:

$$2Fe(OH)_3 + 3\ H_2S = Fe_2S_3 + 6H_2O \qquad (2.3)$$

$$2Fe_2S_3 + 6H_2O + 3O_2 = 4Fe(OH)_3 + 3S_2 \qquad (2.4)$$

The capital cost of this system is low. The regeneration step is also inexpensive. It is the oxidation of the sulphide by air, producing solid sulphur, which ultimately clogs the scrubber. The resulting mixture presents a pollution problem on disposal, because there is no ready market for sulphur waste. This is because sulphur is a major by-product of the oil refineries, and there is a world glut of refinery sulphur.

A variation of this reaction is the use of iron turnings or wire wool (Eqn 2.5). The product is an unpleasant mixture of unreacted iron coated with a gelatinous layer of Iron Sulphide which cannot be regenerated in the same manner as above. Periodic closure of the scrubber is required, and the mixture is disposed of.

$$Fe + H_2S = FeS + H_2 \qquad (2.5)$$

All these scrubbing systems yield a product which eventually poses a disposal problem, and increases both the capital and running costs of gas production. Not all are selective for H_2S, and the

solid-based scrubbers suffer from deactivation due to their interaction with Biogas, and thus require periodic stripdown for replacement or regeneration of their active agent.

As yet the economics of Biogas scrubbing are still in doubt for the farm-sized digester. The techniques outlined above were originally developed for use on large installations where the economics of scale are favourable. However, the unit cost of gas scrubbing increases as the scale of the Biogas installation is reduced. The cost of scrubbing on industrial sites can be justified as part of a complex industrial package in which Biogas production is only a minor part of the overall process. The treatment (by both digestion and gas scrubbing) of unpleasant waste materials may be cost effective in itself, without including the potential benefits from the Biogas produced. At sites where the economics of digestion rely on the successful production and use of Biogas, rather than the treatment of an effluent, the cost of scrubbing can make the whole project unprofitable. To the average farmer, for example, the maintenance of a gas scrubber as well as a digester would occupy too much time. Added to this, the scrubber does not produce a useful by-product, but only generates an unwanted and often unpleasant pollutant which will raise further charges for disposal.

In order for the small-scale digester to be profitable, it must reliably produce and use gas to produce cheap electricity. The farm digester must be shown to be providing low cost energy with the minimum of maintenance from simple and therefore easily accepted technology. The system that approaches this ideal is the basic digester and engine-generator, where the engine effectively acts as a scrubber as well as producing electricity and heat. Under these circumstances, the farmer gains electricity and homogenised sludge to spread as a fertilizer, in exchange for only routine maintenance of the installation. The important factor is the reliability of the engine, which should be as cheap as possible to instal and run on untreated Biogas. As previously discussed, it is this part of the small scale Biogas system which is unsatisfactory.

The major factor in the failure of small displacement Biogas engines has been established as the H_2S corrosion of copper-based bearing alloys. The H_2S enters the crankcase as blowby past the piston rings. The alternative solutions (scrubbing or engine modifications) are largely untried or uneconomic for small scale applications. The understanding of the mechanism of blowby of, and the subsequent corrosion by, the H_2S has not been investigated. The following sections examine the formation of crankcase gases, with particular interest in the H_2S content.

2.1.2 Biogas and crankcase gas in engines.

In Section 2.1.1, the alternatives facing the small, farm-sized, digester have been introduced, with every addition to the installation increasing the capital and running costs. In order to operate an efficient system, which can show its profit potential and attract large scale commercial exploitation, the degree of corrosion protection must be carefully controlled. However, there is no guide as to what extent of system modification is really necessary. Individual research projects have observed the corrosion without trying to quantify its extent. Henry (Ref 2.10) concluded that 0.15% H_2S was the maximum concentration to be tolerated in the fuel supply to gas engines. However, this value is exceeded on many Biogas installations, and is notably independent of any engine classification.

There has recently been some interest in trying to inhibit the engine corrosion by adding extra overbased oils, but, although these oils are ideal for neutralising the strong acids formed from the combustion products, they are not specifically formulated to combat the threat from H_2S attack. For example, Waukesha specify the TBN range of the oil, depending on the H_2S concentration. They also encourage regular oil analysis for both TBN and TAN and specify acceptance criteria for oil retention. This approach is acceptable

to the water treatment industry, for example as practiced at Retford (Ref 2.4). However, it is unlikely that such specialised oils would be readily accepted by the farmer, who will already have a stock of his preferred tractor oil.

The comparison of H_2S and CH_4 in Table 2.1 (Ref 2.11) indicates that the H_2S is a fuel gas that should burn under normal combustion conditions as it has a lower auto-ignition temperature and has wider combustion mixture tolerances in air than those for methane. However, the corrosion evidence indicates that some H_2S must be entering the crankcase.

A literature search revealed that the mechanism of crankcase gas formation has not been identified; the major area of interest being that of crankcase gas as a source of vehicular emissions. Payne and Sigworth (Ref 2.12) identified the crankcase contribution towards overall hydrocarbon emissions, and attempted to quantify its extent under different driving conditions. As crankcase gas was not considered to be a threat to the internal components of small engines, most of the work in the late 1950's and early 1960's also concentrated on the crankcase contribution towards hydrocarbons in the atmosphere. The common practice at that time was a vent pipe leading fumes to the underside of the vehicle. Bennett (Ref 2.13) quickly realised that this pollution problem could readily be solved by recirculating the crankcase gas through the intake system. The hydrocarbons from a range of vehicles were reduced by up to 70%, and crankcase recirculation has is now adopted as a standard automotive feature. Early development of crankcase ventilation concentrated on overcoming oil fouling of the induction system, and the prevention of sludge formation in cooler parts of the engine. Improvements in both oil and fuel additives were demanded (Refs 2.14 and 2.15). Wentworth (Ref 2.16) investigated the relationship between piston ring gaps, blowby flowrates and exhaust hydrocarbon emissions (without quantifying blowby composition). The results showed that the flowrate was proportional to ring gap size and that blowby had a major effect on exhaust hydrocarbons.

The few ideas that Bennett (Ref 2.13) raised about the mechanism of blowby were not investigated further, although it was known that unburnt fuel entered the crankcase in large quantities from the combustion chamber. It had been assumed that crankcase gas was a simple mixture of combustion gases and exhaust gases. Spearot and Gallopoulos (Ref 2.17) investigated crankcase NO_x levels, (oxides of nitrogen are formed within the flame front during combustion), and their work indicated that the mechanism was not as simple as originally believed. Crankcase NO_x concentrations were shown not to be proportional to crankcase CO_2 concentrations. It was originally assumed that crankcase NO_x originated from the blowby of burnt gases, but the quench zone in the combustion chamber played an important role in crankcase NO_x formation. Their work concluded that the mechanism of crankcase NO_x formation was not simple, and suggested that the variation of NO_x concentration within the combustion chamber had a large influence. This paper is notable because the investigators were concerned with the the degradation of oil by the NO_x in crankcase gas, and therefore had a similar objective to this work - to study the attack by crankcase gas on the internals of an engine. The adoption of crankcase recirculation in automotive applications reduced the hydrocarbon emissions by a simple engineering solution. However, although recirculation is useful in controlling the external emissions from Biogas engines, particularly in enclosed spaces, it does not solve their internal corrosion problems.

The corrosion of bearing alloys by crankcase H_2S threatens the economic operation of small engine-generators on Biogas. However, there appears to have been no work on the mechanism of crankcase gas formation, for either conventional or Biogas fuels. Although H_2S should burn, no work has been found on its performance as a fuel in Biogas engines. The costly removal of H_2S from Biogas attempts to combat practical problems without initial consideration of its role in the Biogas engine.

2.2 Experimental.

2.2.1 Objectives.

The experimental work detailed in this chapter has attempted to quantify the relationship between crankcase gas composition, engine load and engine wear. The variation in composition has been used to investigate the mechanism of crankcase gas formation. Measurements using H_2S (Section 2.4) illustrate the amount of H_2S entering the crankcase under a range of conditions. The assumptions that have been made in the experimental work are:

(a) That crankcase gas flow and composition, as measured at the breather, is directly related to the blowby gas passing through the ring pack.

(b) That by isolation of the valve train from the sampled crankcase no valve guide blowby enters the crankcase and that this engine modification has no effect on piston blowby.

The Villiers engines used are governed to run at a fixed speed (3,000 rpm). Hence the research programme has investigated the behaviour of blowby with load at a constant engine speed, unlike the limited automotive work described in the previous section. The experimental objectives were:

(a) To measure the blowby flowrates for each engine, and to investigate the change of flowrate with both engine wear and engine load.

(b) To measure the blowby composition and to investigate the change in composition with both engine wear and engine load.

(c) To compare the trends in crankcase gas composition with those of the inlet and exhaust gas compositions over load range.

(d) To introduce H_2S into the fuel in a controlled manner and to observe the effect that H_2S has on the combustion process, and also on the crankcase gas composition.

H_2S is an obnoxious, toxic gas which is inconvenient to use for prolonged research under the controlled conditions required. Of the experimental objectives outlined above, (a), (b), and (c) can be achieved without the use of H_2S in the fuel mixture. The initial investigation of crankcase gas formation used methane fuel only (as natural gas). This approach assumed that the methane would behave in a similar fashion to H_2S, i.e that unburnt gaseous fuel found in the crankcase is present through the same basic mechanism. Further engine tests were then performed on fuel with H_2S added, in which the main objective was to study the behaviour of the H_2S (Section 2.4).

The combustion of methane produces CO_2 and water. It is reasonable to assume that the crankcase concentrations of methane and CO_2 will change with engine conditions in a mutually opposite manner. This approach can be extended to consider all aspects of the formation of crankcase gas - that blowby occurs with a mixture of unburnt fuel and combustion products.

Villiers C-30 engines were used for the experimental measurements. These are single cylinder, air cooled, four stroke, side valve, spark ignition engines. Four cylinder/valve/piston combinations were interchanged on a common crankcase-generator assembly. These have a known life history, as the result of a previous research project into cylinder liner wear and its effect on the limits of engine life by Hassaan (Ref 2.6). In that work, the engines were run for extended periods under selected operating conditions which resulted in differing cylinder wear rates. This library of cylinders was ideal for the study of crankcase blowby at the various stages of engine deterioration. They were previously used as listed overleaf.

Engine A New components which were briefly commissioned before this experimental programme.

Engine B Run at 74% maximum load at 2250 rpm for 1100 hours.

Engine C Run at 74% maximum load at 3000 rpm for 1100 hours.

Engine D Run at 100% maximum load at 3000 rpm for 690 hours when it partially siezed (without serious damage to the bore). A new set of piston and rings were fitted for this work because the original components were unserviceable.

2.2.2 Experimental Technique.

It was found during the initial running of the engine that the valve assembly required isolation from the main crankcase, to avoid valve guide blowby mixing with piston blowby. The chamber containing the valve springs, cam followers and shim/bucket adjusters was filled with valve guide blowby which mixed with piston blowby as it entered the crankcase through the oil splash lubricating hole. This hole was sealed, and the cam followers had therefore to be provided with their own separate lubrication. This was the only modification to the standard gas engine (Fig 2.7, 2.8, Table 2.2, Ref 2.18).

The inlet gas was metered by a purpose made single venturi, downdraught gas carburettor (Ref 2.6, 2.19) which was mounted onto the cylinder block and governed to run at 3000 rpm. The inlet fuel pipeline was constructed to British Gas standards (Ref 2.20), and the flowrate was monitored both by an industrial gasmeter and by a rotameter positioned before the pressure regulator.

The Villiers engine drove a Markon generator, the power output from which was fed, via a switching unit, to a loading board equipped

with 100 W bulbs and 500 W heating bars. The generator efficiency, from the calibration graph supplied by the manufacturers (Fig 2.9), was between 74% and 77% (Ref 2.21). The load measurements assumed that there was negligible power loss through the crankshaft-rotor coupling. The applied load was monitored with a RS heavy duty moving iron ammeter and voltmeter mounted to the loading board. The engine test bed is summarised in Fig 2.10 and Table 2.3.

The crankcase vent was positioned at the top of the main engine casing, below the cylinder barrel gasket face (Fig 2.7). The gas passed through a ball bearing non-return valve in the crankcase tapping, and a demister mounted on the side of the engine. The crankcase gas flowrate was measured by the timed inflation of a large Tedlar gas sampling bag (as used for exhaust emission testing - max volume 150 litres) and subsequent measurement of the volume collected using a calibrated Lange volumetric flowmeter. This technique allowed the measurement of average crankcase flowrate without any restriction from the metering device. It was found that continuous flow measurement by rotameter was impossible because of the rapid fluctuation of the blowby rate from the single cylinder engine.

The compositions of the inlet, exhaust and crankcase gas samples were measured by Gas Chromatography. The gas was sampled by the direct connection of the inlet, exhaust or crankcase sample ports to the gas chromatograph sampling system. The vacuum in the inlet line was overcome by a small pump which withdrew a sample at a slow controlled rate. Both exhaust and crankcase flowrates were sufficient to fill the sampling system, but the gas injected into the G.C was controlled by the pump by withdrawing the sample from the main flow through a side pipe (Figs 2.10 and 2.11). This ensured the consistency of the sampling technique.

A Pye Unicam 104 series Gas Chromatograph using a thermal conductivity detector was used for the gas analysis. Although this detector is not the most sensitive, it is ideal for the analysis of

both fuel and combustion gases at the concentrations measured in this project. The sample was passed through an oil/water de-mister and through a 6-way Pye Unicam headspace gas valve with a 0.5 cm^3 sample loop. When pneumatically switched, a precise volume of gas is flushed from the sample loop into the G.C by the helium carrier gas. The valve is a low "dead volume" device with inert stainless steel and PTFE internal components specifically designed for precision gas transfer.

The separation was accomplished by a 4 m length of 3 mm internal diameter glass column packed with Chromosorb 106 porous polymer. This packing material was chosen for its ability to separate CH_4, CO_2 and H_2S from the other component gases. The columns (sample and reference) were maintained at the minimum normal operating temperature for the machine (45 ^{o}C). Such low temperature operation allows the maximum detector sensitivity because the relatively cool gases enable the Katharometer current to be set to its highest value (250 mA).

The thermal conductivity detector is composed of two pairs of gold plated filaments, each pair situated at the exit of the sample or reference columns. These filaments form a Wheatstone bridge (Fig 2.12); the changing thermal conductivity of the gas in the detector cell causes a change in the temperature of, and therefore the resistance across the filaments concerned. The cell effectively compares the thermal conductivity of the sample gas stream with that of the Helium carrier gas. The resulting resistance change alters the potential across, and induces a current through, the ammeter. Helium carrier gas is used because of its relatively high thermal conductivity compared with the solute gases (Table 2.4, Ref 2.22). This yields two important advantages:

(a) It allows a high katharometer current setting for better resolution of trace gases.

(b) The difference in thermal conductivity also increases the effective sensitivity of the detector.

Because this technique is comparative, the detector requires frequent calibration, as it is very sensitive to gas flowrate, column and detector temperatures. A purpose made calibration gas of certified composition was bought from BOC Special Gases. Its analysis is given in Table 2.5 (Ref 2.23). This gas was used throughout the experimental period to calibrate the Katharometer. The layout of the analysis system is shown in Fig 2.11.

For a typical sampling run, the engine was started and allowed to warm up for ten minutes to allow thorough flushing of the crankcase. The crankcase volume was 3.8 litres, which, even at the slowest measured blowby rate of 2×10^{-5} m^3s^{-1}, would have been flushed three times in ten minutes. Gas samples were taken independently during a run, and the running conditions were not altered until all the measurements for those conditions had been made. Hence the inlet, crankcase and exhaust samples were collected under comparable conditions. Once new running conditions were selected, the crankcase was thoroughly flushed in the same way as for the warm up period.

2.3 Results using Methane

The experimentation with methane was designed to provide a quantitative baseline, against which the H_2S results could be compared. Several repeat runs at the selected loads were completed, to provide enough data to establish the trend in blowby flow and composition. The blowby composition is compared with both inlet and exhaust gas samples (Fig 2.13, 2.14).

The blowby flowrates (Fig 2.15) show an increase with load for each engine, but a substantial increase with increasing wear (from engine A to D). It is interesting to note the decrease in the flowrate for engine D from the previous measurement (15.4×10^{-5} m^3s^{-1} to

8.65×10^{-5} m^3s^{-1} at full load, Ref 2.6). This is purely as a result of fitting a new piston and rings. This result is to be expected. The new piston rings will have the ability to closely follow the cylinder liner surface because they have not lost their elasticity as much as the older rings they replace. However, the blowby has not dropped to a rate comparable with engines A and B. This indicates that the quality of seal is not as good as that found on the younger engines, and that the blowby must be a combination of ring gap blowby and some ring seal breakdown. This can be rationalized by comparison with engines A and B. The gradual increase in flowrate for engines A and B with load indicates that the higher combustion pressures experienced at higher loads do not significantly alter the blowby flowrate in these low wear engines. The engine has been run at constant speed. Therefore all the results for blowby flow relate to the response of the combustion chamber gases to the combustion chamber pressure whose peak value increases with load (Figs 3.6, 3.7, 3.8). The results for engines A and B show that, despite the increase in combustion chamber pressure, the flowrate is limited to a near constant value. This is consistent with the blowby flow occurring through the piston ring gaps, with the new piston rings maintaining a good seal to the cylinder liner. Conversely, for the more worn engines C and D, the flowrate does alter significantly at the higher loads, indicating that blowby is occurring not only through the piston ring gaps, but also past the rings themselves as the piston ring seal breaks down at the higher combustion chamber pressures. Hence the flowrate results show that:

(a) The engine undergoes blowby through the piston ring gaps at all loads, and under all conditions of wear.

(b) At very high loads and/or high wear, a partial failure of piston ring seal leads to additional blowby.

The composition of the blowby gas also shows some interesting trends. The methane composition curves (Figs 2.16 - 2.18) show a

large increase with load for each engine (composition curves for engine C were completed with H_2S injection only). The engine wear affects the overall methane content, with detail differences in the shape of the curves. This result shows that the blowby gas contains a significant quantity of unburnt fuel, when compared to the inlet gas composition. All the curves show a large increase in methane content at the higher loads, with a "transition" from low to high rate of increase.

The corresponding carbon dioxide composition curves show no clear trend (Figs 2.19 - 2.21). The scatter of results for this analysis was very wide, indicating an uneven degree of blowby from the burnt gases. The curves show that the CO_2 content is approximately constant for all the engines. These composition results indicate that the relationship between the methane and CO_2 content of the blowby gases is not simple or necessarily direct.

A derived curve (Fig 2.22) shows the methane blowby flowrate calculated by combining the averages from the data in Figs 2.15 to 2.18 using equation 2.6. The calculation for engine C is based on the results in Fig 2.25.

$$[\%CH_4][\text{Blowby flow}]/[100] = [CH_4 \text{ Blowby flow}] \qquad (2.6)$$

These curves clearly show the combined effect of flow and composition lead to a large difference between the newer and older engines. It also emphasises the difference between the newer engines with blowby mainly through the ring gaps, and the older engines which have breakdown of piston ring seal. It should be noted that the inlet methane flowrate is two orders of magnitude higher than the blowby methane flowrate (4 to 5 x 10^{-4} m^3s^{-1} as compared with 1 to 6 x 10^{-6} m^3s^{-1}). A comparable graph for CO_2 (Fig 2.23) shows a rising trend of CO_2 flowrate with load, which is mainly derived from the rising overall blowby flowrate with load. The curves highlight the detail differences in the blowby CO_2 content.

2.4 Experimentation using H_2S in the fuel.

2.4.1 Equipment modifications.

Due to the high toxicity of H_2S gas (Ref 2.24), the engine test bed was extensively modified to provide safe working conditions. The H_2S gas was injected into the inlet gas stream before the regulator via a small bleed pipe (compare Fig 2.10 and Fig 2.24). Various techniques were tried to inject a controlled amount of H_2S gas to constitute 0.2% of the fuel supplied, a composition comparable to the H_2S content of Biogas. This proved to be very difficult because of a combination of the small H_2S gas flowrate required, the high pressure of the source H_2S cylinder, and the minor fluctuations in induction vacuum experienced at the injection point in the fuel pipe. The continuous metering of the H_2S flowrate proved to be the controlling factor; the small rotameter necessary was useless in an undamped form. Eventually, a water displacement system was found to give the best approximate flowrate. The use of "wet" gas was not considered inappropriate because Biogas is normally stored in gas holders or digesters which themselves contain water. However, the amount of water vapour carried into the fuel was assumed to be negligible, because the static water level in the control system never changed during the experimental period. The H_2S injection pipe had a solenoid shut off valve opened by the generator output voltage as a failsafe safety feature.

The gas carburettor was fitted with an air induction pipe over the open bell-mouth to prevent any H_2S being released into the atmosphere by a misfire. The pipe's cross sectional area was four times that of the exhaust system, and was only 400mm long, designed not to alter the combustion characteristics of the engine. All exhaust and crankcase gases were carried outside the laboratory, as were all the waste gas samples after passing through the G.C sample and analysis system.

As a result of the difficulty experienced with H_2S injection, it was decided to monitor the inlet composition by gas sampling only, with no continuous monitoring of the amount of H_2S being used. The flow of H_2S through the final metering system proved to be steady and the approximate percentage could set for the following experiment with reasonable accuracy before analysis. A trial run was completed with several inlet gas samples taken at one H_2S flow setting. Four samples were taken and were measured using the G.C as 1.26% +/- 0.02% H_2S.

Only engine C was used for this experiment because it was considered that a prolonged series of experiments with H_2S was unwise and inconvenient with the limited test bed resources available. The experimental technique was similar to that used before with the exception that the crankcase sample was collected in the "Tedlar" gas sampling bag at the same time as the inlet sample was injected into the G.C. This was to reduce the running time to a minimum and also so that both inlet and crankcase samples were collected simultaneously. Particular attention was paid to the flushing of the crankcase both before analysis with H_2S on, and after analysis with H_2S off. This was to ensure accuracy of results, and so that the engine was not left standing with H_2S inside the combustion chamber or the crankcase. This ensured that the test engine did not suffer bearing corrosion problems during the test period.

The Gas Chromatograph analysis system was operated as before, with the same column conditions. The analysis timespan was extended to include the H_2S peak following that of ethane (C_2H_6) a trace constituent fuel in the natural gas supply. The behaviour of the ethane fuel was also studied during this part of the experimental programme, in order to provide further information on the formation of crankcase gas.

2.4.2 Results using H_2S.

The results were obtained from experimental runs where the H_2S content of the fuel mixture varied between 0.8% and 5.0%. The corresponding reduction in calorific value of the fuel was between 0.3% and 1.8% (Eqn 2.7) and observation of engine behaviour within this composition range indicated that the addition of H_2S made no appreciable difference to the engine's performance. The reduction in calorific value is given by the equation below. The calorific values used are given in Table 2.1.

$$\% \text{ Reduction} = 100 - [[33.95(100 - x)] + [21.82x]]/33.95 \qquad (2.7)$$

where $x = \%\ H_2S$ in the fuel mixture.

Fig 2.25 shows the variation in crankcase composition of all fuel gases with load. The change in methane content is consistent with the results from engines A, B and D. The ethane and H_2S concentrations both show an increase with load, although the smaller absolute rise reflects their smaller inlet content.

The inlet and crankcase gas samples were analysed with particular attention to the concentration of H_2S. However, any comparison between different engine runs was difficult because the H_2S concentration in the inlet fuel mixture varied. There are two approaches to interpreting these results.

Assume that the concentration of H_2S measured in the crankcase is proportional to the concentration of H_2S in the inlet fuel for any given engine operating condition. The crankcase gas H_2S concentration values can be corrected to represent the results which would be expected from runs using a fuel with a constant H_2S content. This correction is given by equation 2.8, and Fig 2.26 shows the result of the correction for the H_2S and ethane crankcase content assuming that the inlet fuel contained 0.2% H_2S. The trend shown by methane is repeated by both ethane and

H_2S, with an increase in crankcase concentration with increasing load.

$$H_2S(d) = H_2S(m) \times 0.2 / H_2S(i) \qquad (2.8)$$

where $H_2S(d)$ = derived crankcase percentage.
$H_2S(m)$ = measured crankcase percentage.
$H_2S(i)$ = measured inlet percentage.

The object of this correction is to relate the individual readings to one another by assuming a constant inlet fuel mixture and a proportional relationship between the inlet and crankcase fuel gas compositions. The second approach is to compare individual readings as ratios of the crankcase : inlet gas composition. This approach is independent of the actual value of the H_2S and ethane inlet concentration and indicates, moreover, the degree of proportionality of inlet and crankcase fuel gas composition used as the basis of equation 2.8. Fig 2.27 shows this comparison of the inlet and crankcase gas concentrations. All the curves rise with load, indicating that the unburnt fuel content in the blowby is rising faster than the rise in inlet fuel rate. The increase in H_2S is pronounced at higher load when compared to the other two gases. This suggests that the combustion of H_2S is less complete at higher loads. The ethane curve shows a similar trend, with a very high crankcase content up to the 0.7 ratio at maximum load.

2.5 Discussion of Experimental Results

The experimental results obtained from the Villiers engines have shown that:

(a) The fitting of a new piston and rings in a badly worn engine reduces blowby. The results also indicate that the improved ability of the piston rings to follow the bore has only a partial effect on the flowrate, with the unaffected proportion of the flow passing mainly through the piston ring gaps.

(b) The blowby flowrate increases with load (at constant speed) for any given engine wear condition. However, worn engines show a greater rate of flow increase, particularly at higher loads, and in spite of their lower peak combustion pressure, when compared with newer engines. All the flowrate results suggest that two types of mechanism act in parallel - ring gap blowby and ring seal breakdown blowby.

(c) The methane content of the blowby increases with load for all the engines at a rate faster than the increase in fuelling rate. This effect is greater for worn engines.

(d) The CO_2 content of blowby appears to be constant across the load range for all engines. The composition curves do not show a consistent trend, and are independent of the fuel gas concentration results.

(e) Both the Ethane and H_2S content of blowby also increase with increasing engine load.

(f) The comparison of inlet and crankcase concentrations of the fuel gases shows that the fuel content of blowby increases despite the change in fuel rate, with load. The H_2S fuel shows the greatest blowby increase of the three fuel gases considered. The ethane fuel achieves the highest ratio of 0.7.

The mechanism of crankcase blowby has been proposed as the passage of combustion gases through the piston ring gaps (Ref 2.12, 2.13, 2.16, 2.25, 2.26). In an appendix to their paper Bennett (Ref 2.13) also refers to the blowby as a combination of circumferential gas transfer and ring gap blowby. The role of valve guide blowby should not be ignored (Ref 2.27) although in this work this factor has been eliminated, reflecting the improvement in valve guide sealing of modern engine designs. In analysing the results, the blowby measured in this work is the summation of:

(a) Blowby through the piston ring gaps.

(b) Blowby around the piston rings as they move away from the sealing surface on the piston groove as the piston passes through TDC.

(c) Blowby between the piston ring outer face and the cylinder liner as a result of the breakdown of piston ring seal.

The results from engines A and B show little change in the blowby flowrate across the load range. These engines represent a new and nearly new engine assembly, where the ability of the piston rings to follow a relatively unworn cylinder liner is good. Hence the overall mechanism will be dominated by ring gap blowby, with the breakdown in piston ring seal being confined to the ring flutter caused by the change in direction of piston travel near the dead centre regions of the stroke (refer to Section 4.1.2 for a detailed analysis of piston ring lubrication and sealing).

The results from engines C and D show greater flowrates, and also considerable variation across the load range. Due to the higher wear of the cylinder liners, it is likely that greater piston ring seal breakdown contributes to this increased flowrate.

The fitting of a new piston and piston rings has reduced the blowby flowrate from the previously measured value (Ref 2.6) indicating that the improved ability of the new rings to follow the cylinder liner surface has prevented the passage of some gas across the ring pack. However the reduction is not down to the flowrates measured for engines A and B. This can be explained by:

(a) The worn profile requires the piston ring to respond to changes in bore diameter during its passage near to TDC. This does not allow the new rings to seal as well as those in engines A and B.

(b) The piston ring gap opens further as the rings expand into the worn regions of the liner, thereby providing a larger opening for the passage of blowby through the ring gaps.

Fig 2.28 shows the piston ring gaps measured for the cylinder liner for engine D, and its corresponding top compression ring. The measurements were made by positioning the engine barrel on a measuring table, inserting the loose piston ring into the cylinder bore and vertically positioning the ring using a depth gauge. The ring gap was then measured with slip blocks to an accuracy of 0.001 ins. This procedure was repeated for the entire travel of the top ring. The graph shows the range through which the piston ring gap alters as the piston ring follows the worn liner profile, with the largest opening near to TDC.

Fig 2.29 indicates the effect of material fatigue on a used piston ring. The graph shows the change in the piston ring gap when the piston ring is subjected to a load. The piston ring was clamped in the vertical plane, with the clamp at the lowest point on the ring. The ring gap was positioned at 90^{o} to the clamping point (horizontally) and a load was applied to the top of the ring directly above the clamping point. The ring gap was measured using slip blocks to an accuracy of 0.001 ins. The experiment was carried out for a new compression ring (all three are identical) and the top ring from engine C. The worn ring has a degree of permanent deformation, as indicated by the smaller gap at rest. A comparison of the slopes of the two curves shows that the worn ring closes to a greater extent under a given load than does the new ring. These two factors indicate that once compressed within the cylinder bore, the worn ring would exert a lower force onto the liner wall, and would be less likely to provide a good seal in response to changes in bore diameter.

For an engine with greater wear, the blowby mechanism will tend towards a combination of ring seal breakdown and ring gap blowby. The breakdown of the piston ring seal will be strongly dependent on

the combustion chamber pressure, because it is encouraged by the blowby gases attempting to pass through the piston ring pack. The degree to which breakdown occurs, will be dependent on the condition of the piston rings, piston grooves and cylinder liner wear. Hence, the increase in blowby flow with load is more pronounced for engines C and D.

Fig 2.30 is a graph of the ratio of blowby flowrate (Fig 2.15) to peak combustion chamber pressure (Figs 3.6, 3.7 and 3.8). The curves for A and B are similar and indicate that the same mechanism - piston ring gap blowby - is occurring. The blowby flowrate is proportional to the peak pressure. For engine D the blowby flowrate is proportional to pressure at low loads, but increases as the piston ring seal breaks down. The effect is clearly shown as a change in shape of the curve.

The fuel content of blowby gas increases with both engine load and engine wear. The measurements are taken from samples which have been collected over a number of engine cycles. Under normal running conditions (where there is no misfire, knock, etc) the crankcase samples can be considered as a summation of the blowby occurring during each of those cycles (the 0.5 cm^3 sample loop is equivalent in volume to the blowby of between 4 and 25 power strokes). The composition of crankcase gas can be explained by discussing the mechanism of blowby at various stages during the engine cycle.

Blowby occurs as a result of the physical forces experienced by the gases in the combustion chamber, cylinder bore and crankcase. The blowby flow of both fuel and combustion products is driven by the pressure difference across the ring pack, which alters considerably during the engine cycle. It is therefore important to consider the formation of crankcase gas at the various stages in the combustion cycle. As, by definition, the fuel gases have not burnt, it is reasonable to assume that they have passed the piston ring pack as one of the three categories overleaf.

(a) Blowby of the fuel mixture before the flame front has engulfed the gases in the main volume of the combustion chamber.

(b) Blowby of the quench zone gases formed as the flame front approaches the combustion chamber surface.

(c) Blowby of the residual fuel in the combustion products after combustion has occurred.

The relative significance of these sources of unburnt fuel is important. Blowby occurring during the early stage of the combustion cycle will lead to a large amount of unburnt fuel mixture entering the crankcase. The early stage of combustion coincides (by design) with the rapid compression of the combustion mixture and also with the physical breakdown of the piston ring seal near TDC. The ignition of the fuel mixture occurs late into the compression stroke, and the flame front takes a finite time to engulf the compressed gases, this flame travel time being particularly long with a side valve engine design. The piston and rings experience a large change in velocity (including a change in direction), combined with high pressures and temperatures. The resultant breakdown of the piston ring seal near TDC is well documented (Ref 2.25). A combination of all these factors leads to a large amount of unburnt gas passing the piston ring pack during the part of the engine cycle where the flame front is crossing the combustion chamber from the ignition source.

As the flame front approaches the combustion chamber surfaces, the blowby of unburnt fuel will be superseded by the blowby of the quench zone gases. The quench zone theory implies that a layer of unburnt fuel is present both on and near to all metal surfaces during and after the combustion, as a direct result of flame quenching (Refs 2.28, 2.29). This occurs as a result of the flame (at over $900^{o}C$) approaching the relatively cool combustion chamber wall (at less than $250^{o}C$), the sudden cooling of the reaction leads to flame quenching, and a layer of unburnt mixture remains

adjacent to the cooler surface within a "Quench Zone". The nature of the quench zone is dependent on the fuel concerned, the dynamics of combustion and the design of the combustion chamber. The fuels considered in this work are all gases at the conditions of quenching, and behave in a similar manner to the vaporised liquid fuels commonly used in internal combustion engines. The piston ring crevice (particularly the region above the top ring between the piston and the cylinder wall), the edge of the piston crown and the cylinder wall above the piston crown are the quench zones of particular importance to blowby gas formation. The likelihood of gases from this region entering the crankcase is high, as the cylinder pressure will be high during and slightly after combustion, and the piston will be near to TDC in the region of high bore wear. The flowrates measured were in the range 2 to 8.7 x 10^{-5} $m^3 s^{-1}$.

$$\text{Blowby flowrate} = 2 \text{ to } 8.7 \times 10^{-5} \ m^3 s^{-1}$$

$$\text{Volume per revolution} = 0.2 \text{ to } 1.74 \ cm^3$$

$$\text{Volume per firing stroke} = 0.4 \text{ to } 3.48 \ cm^3$$

These values can be compared with the quench zone volume in the crevice above the top ring. The radial gap between the piston and bore is 0.5 mm, and the top ring is 3.5 mm below the piston crown surface.

$$\text{Crevice volume} = 3.5 \times \quad \times ((35)^2 - (34.5)^2)$$

$$= 0.38 \ cm^3$$

This value is significant when compared with the blowby volumes quoted above. For relatively unworn engines, the blowby occurs through the piston ring gap. This consists of a small amount of crevice quench gas from near the top ring gap, which is high in unburnt fuel. Blowby from the bulk volume of the combustion chamber follows, with a composition dependent on the extent of the quench

zone and also on the dynamics of the combustion process. On worn engines with piston ring seal breakdown, crevice quench gas from the whole circumference of the piston ring is likely to enter the crankcase, and constitutes a larger percentage of blowby. This may increase the fuel content of the crankcase gas. In all cases, the blowby of the quench zone gases will be followed by the products of combustion formed in the main volume of the combustion chamber.

The contribution from combustion products is likely to be significantly smaller. The blowby of combustion products can only occur after combustion has occurred in the region near to the piston crown, which, as a result of the spark plug location in the side valve head, occurs late into the stroke - beyond TDC (this principle applies to all conventional SI and many CI engines because the ignition source, if any, is situated opposite to the piston crown in the cylinder head). The actual amount of unburnt fuel in the combustion products is small. The blowby flowrate of combustion products is low because the cylinder pressure drops as the power stroke continues, and the piston is moving away from the region of high cylinder wear near to TDC. As the piston travels down the cylinder, the oil layer and motion will re-establish hydrodynamic lubrication of the piston rings. This, and the comparatively unworn cylinder bore away from TDC will combine to give a better piston ring seal, thus hindering blowby. A combination of all these factors will greatly reduce the combustion products' contribution towards unburnt fuel in the crankcase. The blowby of combustion products can also occur on the exhaust stroke of a four stroke engine. However, throughout this stroke, the valves are open, and the pressure in the combustion chamber is low. Hence this stroke is unlikely to contribute significantly to crankcase gas formation.

The composition curves obtained from the experimental work with methane show that blowby fuel content increases with load for all engines. However there are detail differences in the shape of the curves.

Engine A has a gradual increase in blowby methane content throughout the load range until approaching the maximum load reading, where there is a sudden increase (Fig 2.16). This does not correspond to an increase in total blowby flowrate at the same load (Fig 2.15).

Engine B has a gradual increase in blowby methane content across the whole load range, without the dramatic increase at maximum load measured with Engine A (Fig 2.17). This is complemented by a slight rise in total blowby flowrate with load (Fig 2.15).

Engine C has a high methane content at low load, which rises gradually up to 2.0 kW, whereafter the methane content rises rapidly (Fig 2.25). This parallels the behaviour of the blowby flow curve.

Engine D has a high methane content at low load, which rises gradually up to 2.3 kW. Above this load, the rate of methane content rise changes dramatically, yielding a high fuel content at maximum load (Fig 2.18). This transition is complemented by a corresponding change in the total blowby flow curve (Fig 2.15).

Fig 2.31 is a graph of the ratio of the methane content of the blowby to the peak combustion pressure. No clear trend is observed for all the engines, apart from a common increase in ratio above 2.5 kW indicating that the methane content is increasing despite the increase in combustion pressure. This feature, and the flow : pressure relationship from Fig 2.30 are highlighted in Fig 2.32, a graph of the ratio of methane content of the blowby to the blowby flowrate. The curves for engines A, B and D all show that the ratio is constant across the load range, with an increase at high load for engines A and B. Moreover, the position of the curves show an overall decrease in ratio from engine A to engine D. As the engine wears, the blowby flowrate increases, with a lesser increase in unburnt fuel entering the crankcase, the increase in gas flow with wear being comprised of gases with a lower fuel content.

The corresponding CO_2 results show no conclusive trend, with a blowby content which is approximately constant across the load range. Engine A (Fig 2.19) has considerable scatter in the readings. Engine B (Fig 2.20) has a very slight rise with increasing load. Engine D (Fig 2.21) shows a rise in CO_2 content at 2.3 kW, which drops off at maximum load.

The CO_2 is derived mainly from the blowby of combustion products. There are two basic approaches which can be used to analyse the CO_2 content.

(a) Coincident blowby of burnt and unburnt gases. If the total measured blowby is divided in this manner, the concentration of CO_2 in the crankcase will fall in direct proportion to the rise in methane content. This effect does not occur.

(b) Blowby of the unburnt gases occurs late into the power stroke, when the combustion chamber pressure is low. All blowby earlier in the cycle is either unburnt inlet mixture or quench zone gas. The CO_2 content can be considered separately from the fuel content.

Neither approach is satisfactory. The carbon balance of the blowby gases is not achieved across the load range for any engine (see equation 2.9). This result is consistent. The results clearly show an increase in blowby fuel content without the corresponding reduction in CO_2 content expected if the composition of the gases in the ring zone is similar to the induction and exhaust mixtures. This effect has no easy explanation. However, the complex nature of quench zone gas, and the possibility of the CO_2 dissolving in the engine oil may contribute to this result. The equation of stoichiometric combustion is given in equation 2.9 below.

$$CH_4 + 2O_2 + 7.52N_2 = CO_2 + 2H_2O + 7.52N_2 \qquad (2.9)$$

The analysis of the crankcase gas composition is dry in that the water, which is a gas as it passes through the piston ring gaps, is condensed before the gas sample is analysed. However this will have no effect on the ratio of CH_4 to CO_2 measured in the gas samples.

The composition results from this work confirm that the unburnt fuel enters the crankcase to give a high crankcase fuel concentration, whose level is dependent on the load applied. The blowby mechanism includes a complex combination of fuel mixture, quench zone gas and combustion products. Further detailed work is required to resolve the magnitude and source of these components of the blowby gases.

References Chapter 2.

2.1 DUDLEY T.C, "Sludge digestion and gas utilisation in the Metropolitan Public Health Division of the Thames Water Authority." in BUVET R, FOX M.F, PICKEN D.J (eds) Biomethane, production and uses (publ) Turret Wheatland 1984, pp 219 - 229.

2.2 BURGESS S G, WOOD L B, "The properties and detection of sludge gas" J Inst Sew Purif 1964 pp 24 - 46.

2.3 LALAND J, District Controller, Soar Division, Severn Trent-Water Authority. Personal communication.

2.4 THORNTON H, Divisional Engineer, Lower Trent Division, Severn-Trent Water Authority. Personal communication.

2.5 WOOD C.P "How crankcase oil additives function" presented at "Lubricants for Automotive Engineers" London 1969.

2.6 HASSAAN H.A, "An investigation into the absolute life of an Internal Combustion engine". PhD Thesis, Leicester Polytechnic, 1983.

2.7 FOX M.F, "Safety and corrosion in Anaerobic Digestion." in BUVET R, FOX M.F, PICKEN D.J (eds) Biomethane, production and uses (publ) Turret Wheatland 1984, pp 201 - 208.

2.8 WHEATLEY B.I, "Adsorbers, scrubbers and strippers - An introduction with particular reference to Biogas." (unpublished paper presented at the BABA workshop on Biogas scrubbing, June 1980).

2.9 KOBAYASHI H.A, STENSTROM M, MAH R.A, "Use of photosynthetic bacteria to remove H_2S, from Biogas" Water Research Vol 17 No5 1983 pp 579 - 587.

2.10 HENRY C.R, "Hydrogen Sulphide in sludge gas." J Water Poll Control Fed Vol 33 1961 pg 136.

2.11 ROSE J.W, COOPER J.R (eds) Technical Data on Fuel (1977) (publ) Scottish Academic Press pg 267.

2.12 PAYNE J.Q, SIGWORTH H.W "The composition and nature of blowby and exhaust gases from passenger car engines." Proc 2nd Nat Air Poll Symp 1952 Vol 2 pp 62 - 70.

2.13 BENNETT P.A et al., "Reduction of air pollution by control of emission from automotive crankcases." SAE Transactions, Vol 68, pp 514 -536.

2.14 TRACY C.B, FRANK W.W, "Fuels, lubricants and positive crankcase ventilation systems." Paper 874A presented at SAE summer meeting Chicago June 1964.

2.15 PEARCE A.F, SHANNON H.F "PCV - Problems, cures, variables." Paper 874B presented at the SAE summer meeting Chicago June 1964.

2.16 WENTWORTH J.T "Piston and ring variables affect exhaust hydrocarbon emissions." SAE 680109.

2.17 SPEAROT J.A, GALOPOULOS N.E, "Concentrations of Nitrogen oxides in crankcase gases." SAE 760563.

2.18 Villiers Industrial Engines Ltd., Marston Road, Wolverhampton.

2.19 SOLIMAN H.A "The effect of Methane/Kerosene mixtures as spark ignition engine fuels". PhD Thesis, Leicester Polytechnic 1978.

2.20 Code of Practice for Natural Gas fuelled Spark Ignition and dual fuel engines. Publication IM/17, British Gas, Feb 1981.

2.21 Markon Generators Ltd, Oakham, England.

2.22 WEAST R.C (ed) Handbook of Chemistry and Physics (53rd Ed) CRC Press, Cleveland, Ohio, 1972, pg E-2.

2.23 B.O.C. Special Gases, 24 Deer Park Road, London SW19.

2.24 MUIR G.D (ed) Hazards in the chemical laboratory (2nd Ed) (publ) Royal Society of Chemistry, London, 1977, pg 284.

2.25 Department of Industry Report TRD 162, Piston Ring Design 1974.

2.26 FURUHAMA S, TADA T "On the flow of gas through piston rings". Bull of JSME 1961, Vol 4, pp 684 - 690.

2.27 BULL B, VOISEY M.A "An investigation of the sources of blowby in single cylinder supercharged diesel engines". Proc Inst Mech Eng 1978, Vol 192, pp 39 - 48.

2.28 DANIEL W.A "Flame Quenching at the walls of an internal combustion engine." 6th Symposium on Combustion, The Combustion Institute, Pittsburg 1956 pp 886 -893.

2.29 SCHEFFLER C.E "Combustion chamber surface area, a key to exhaust hydrocarbons." in Vehicle Emissions Part II (Progress in Technology Vol 12) SAE 1968 pp 60 - 70.

Figures Chapter 2

Table 2.1 Comparison of CH_4 and H_2S (Ref 2.11)

	CH_4	H_2S
Limits of flam. in air (%)	5 - 15	4.3 - 45.5
Autoignition Temp (^oC)	532	260
Calorific Value (MJ/m^3)	33.95	21.82

Table 2.2 Specification of Villiers engine (Ref 2.18)

Type	Single cylinder, 4 stroke
Bore	70 mm
Stroke	66.7 mm
Capacity	256 cc
Piston	Aluminium, flat topped
Piston rings	3 Compression, 1 oil
Ignition	4.75 mm (27.6^o B.T.D.C)
Compression Ratio	6.5 : 1

Table 2.3 Details of the experimental apparatus.

Parameter	Equipment Used
Engine speed	Toothed steel disc bolted to generator shaft and magnetic pickup aligned to the disc edge. The voltage "spikes", which were generated by the magnetic pickup were counted using an Orbit Controls 72 C1 Counter-Timer. The engine speed was maintained at 3000 rpm.
Engine Load	The crankshaft was connected directly to a Markon 240V, 50 Hz generator; power being switched to 500W heating bars and 100W bulbs on a remote loading board. The combined current was measured by using a moving iron ammeter and the output voltage by voltmeter.
Inlet Methane Flowrate	The gas passed through a Marconi X series Rotameter positioned before the regulator. Slight induction flutter gave a reading error of +/- 1.0%.
Crankcase Gas Flowrate	The gas inflated a Tedlar gas sampling bag over a timed period of 20 minutes. The volume collected was then measured, using a Lange volumetric flowmeter.

Table 2.4 Thermal Conductivities at 45°C (Ref 2.22)

Helium	0.156	
Methane	0.037	
Oxygen	0.028	
Nitrogen	0.027	
Ethane	0.024	
Carbon Dioxide	0.018	
Hydrogen Sulphide	0.016	($J\ s^{-1}\ m^{-1}\ K^{-1}$)

Table 2.5 Calibration Gas Composition (Ref 2.23)

CH_4	61.33 %
CO_2	28.63 %
N_2	8.04 %
H_2S	2.00 %

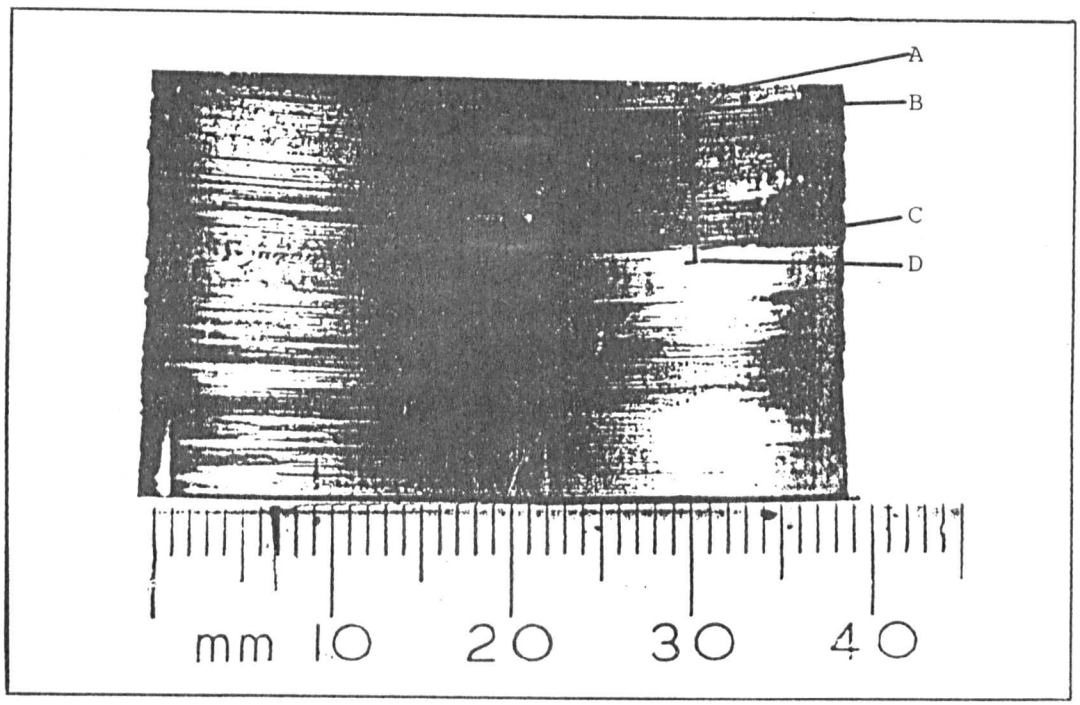

FIG 2.1 PHOTOGRAPH OF FORD DOVER CAMSHAFT BEARING CORROSION.

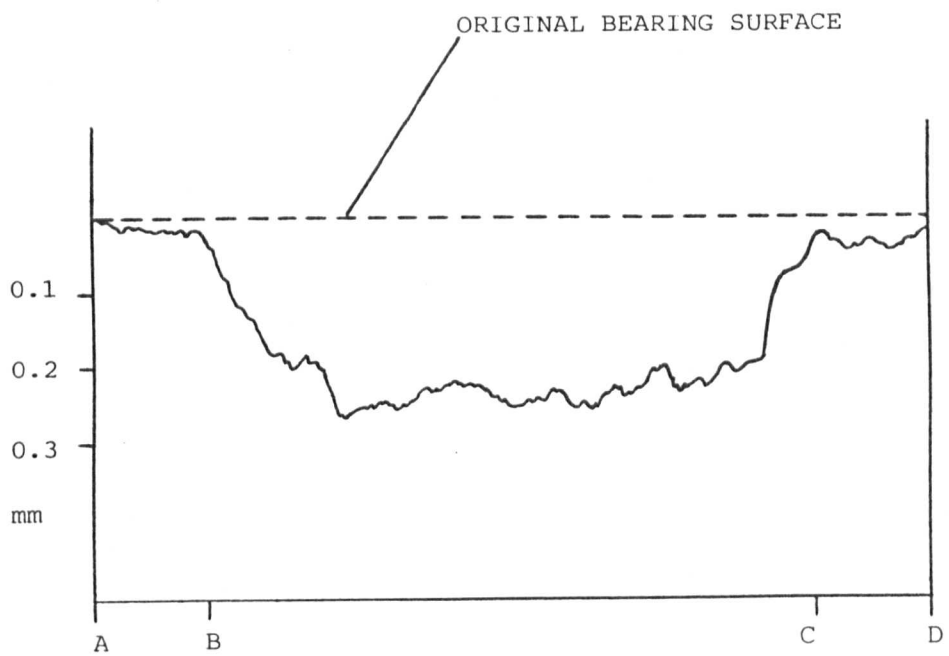

FIG 2.2 CROSS SECTION OF THE BEARING SURFACE.

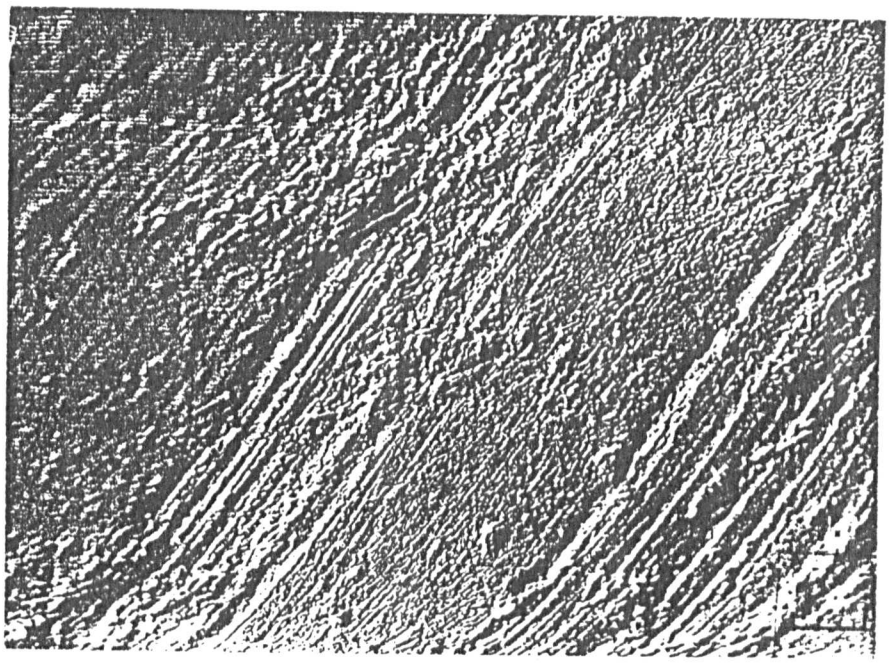

FIG 2.3 ELECTRON MICROGRAPH OF THE DAMAGED SURFACE.

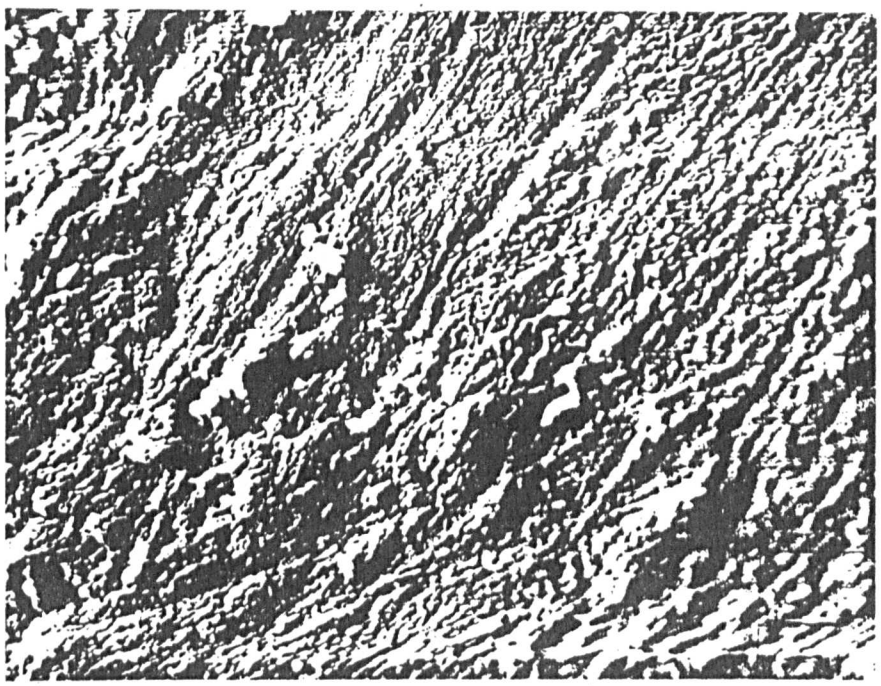

FIG 2.4 ELECTRON MICROGRAPH OF THE DAMAGED SURFACE.

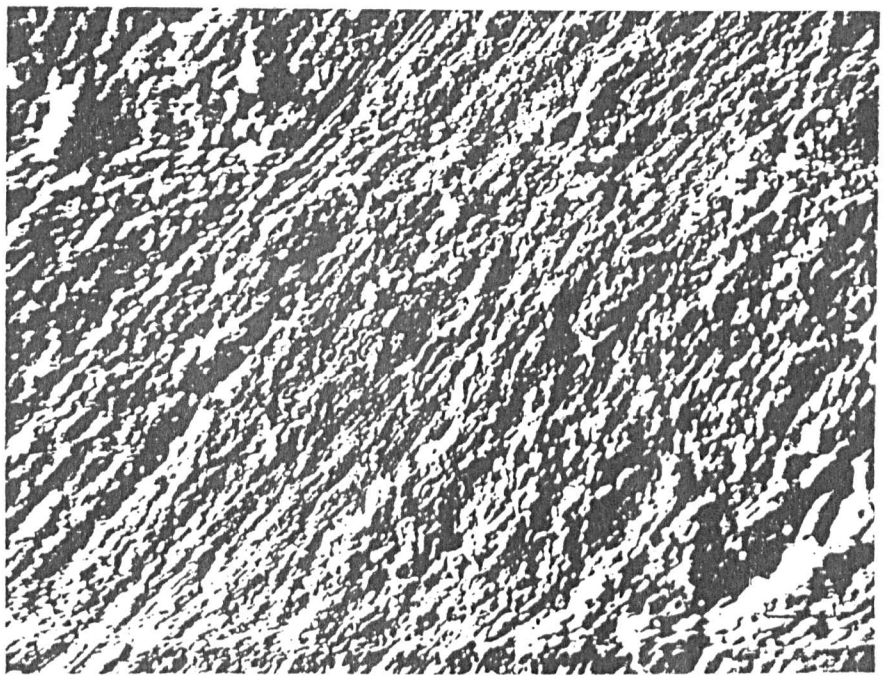

FIG 2.5 ELECTRON MICROGRAPH OF THE DAMAGED SURFACE.

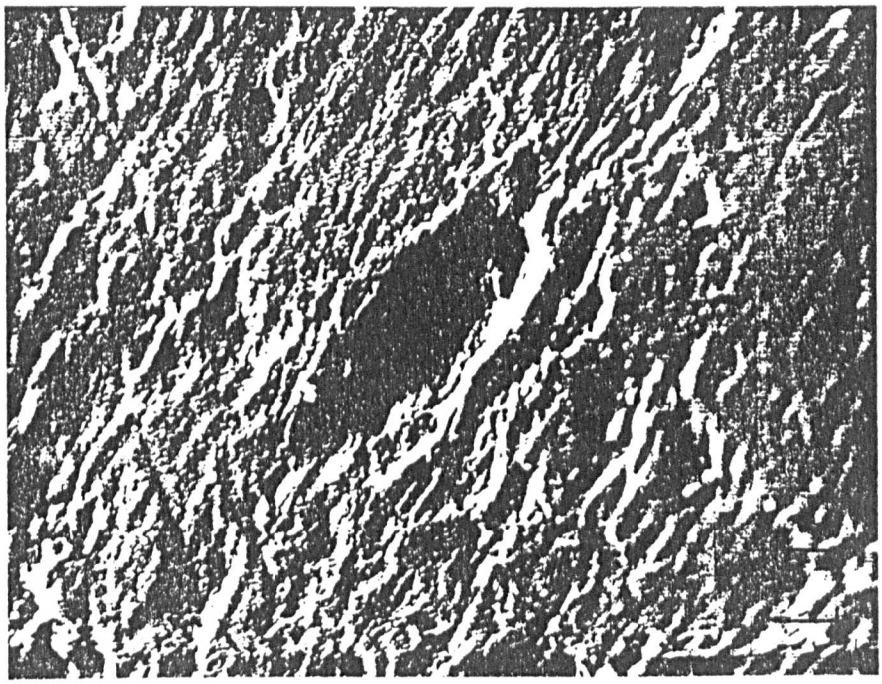

FIG 2.6 ELECTRON MICROGRAPH OF THE DAMAGED SURFACE.

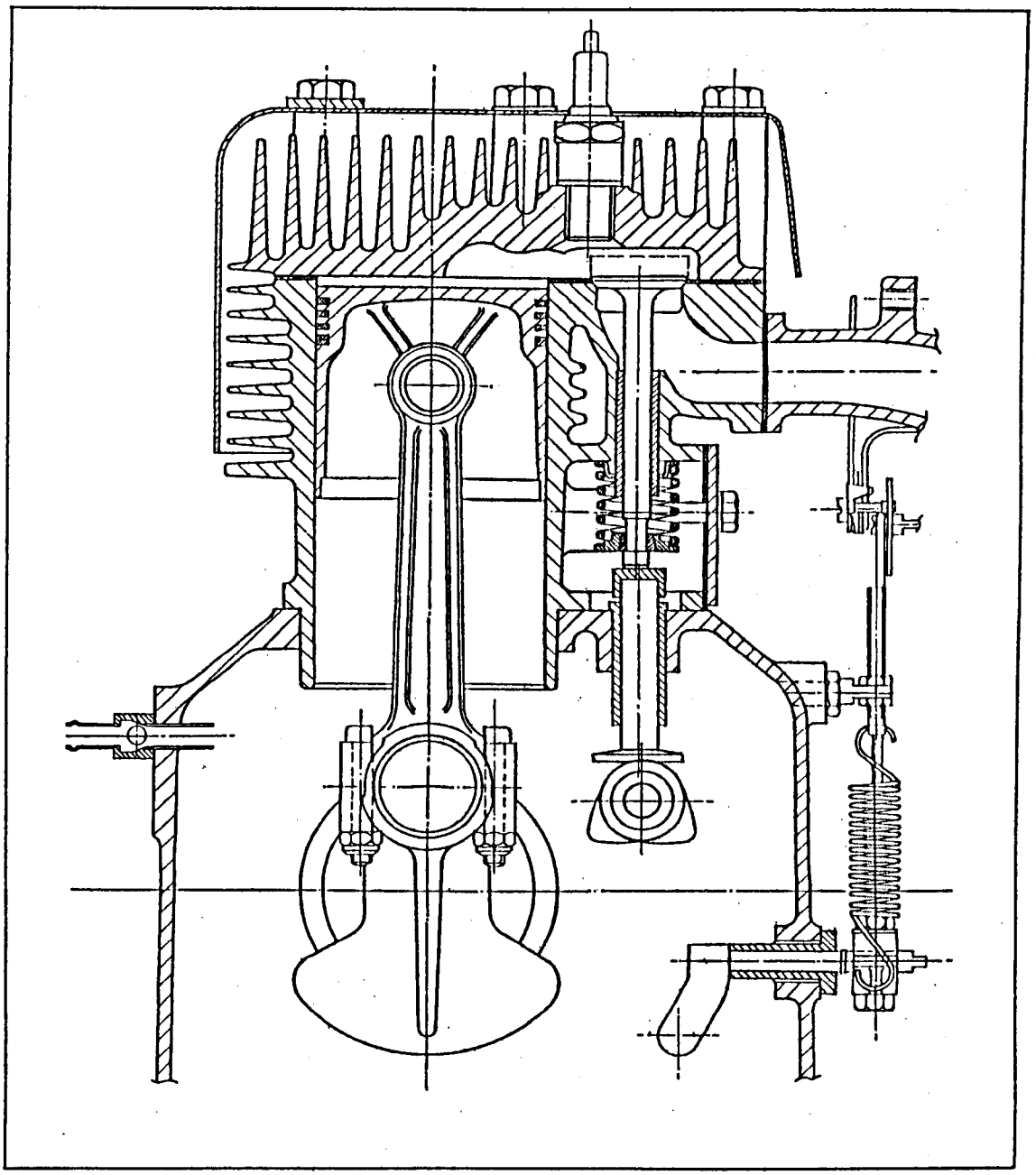

FIG 2.7 SECTION OF VILLIERS C-30 ENGINE

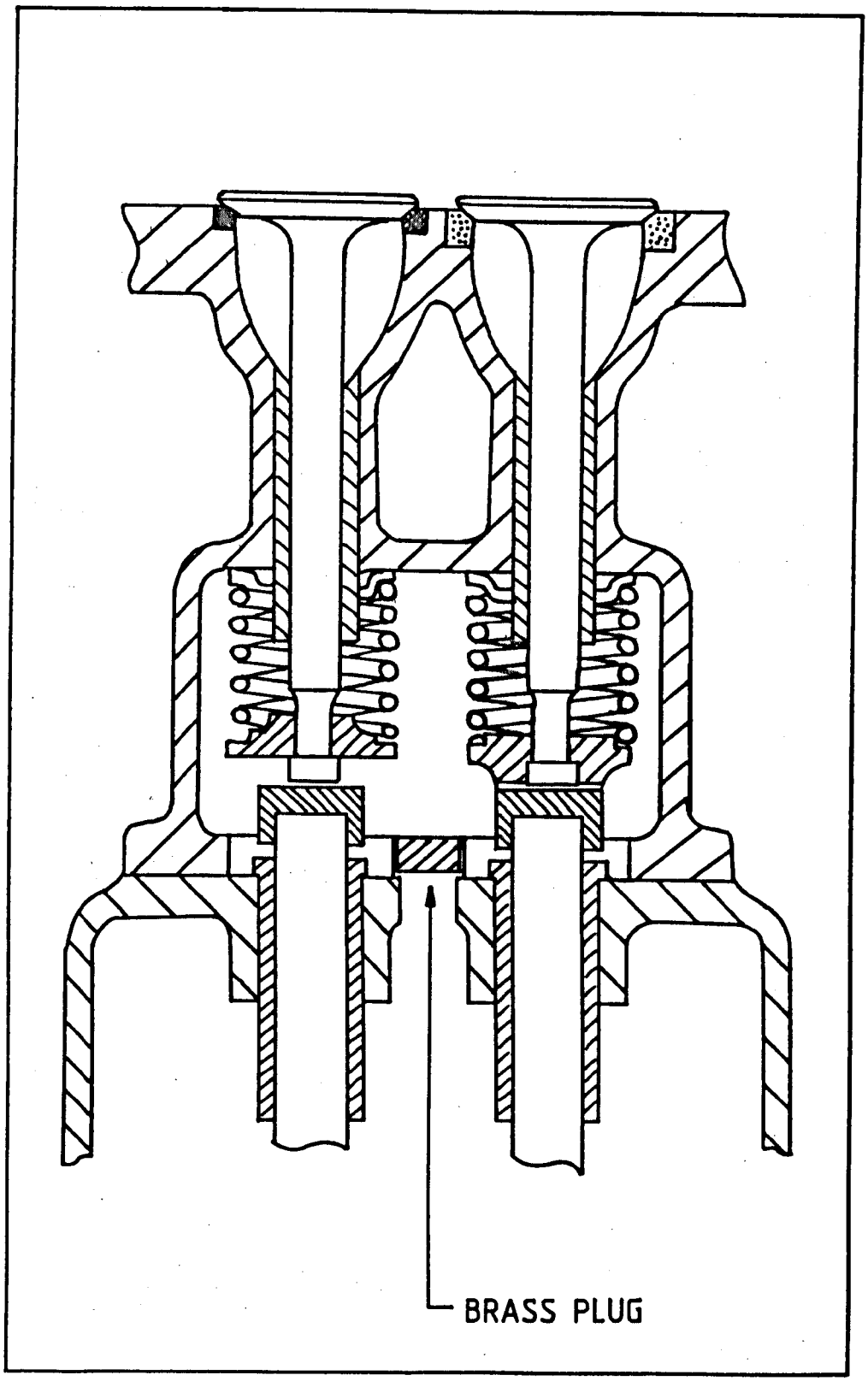

FIG 2.8 SECTION SHOWING MODIFIED TAPPET HOUSING

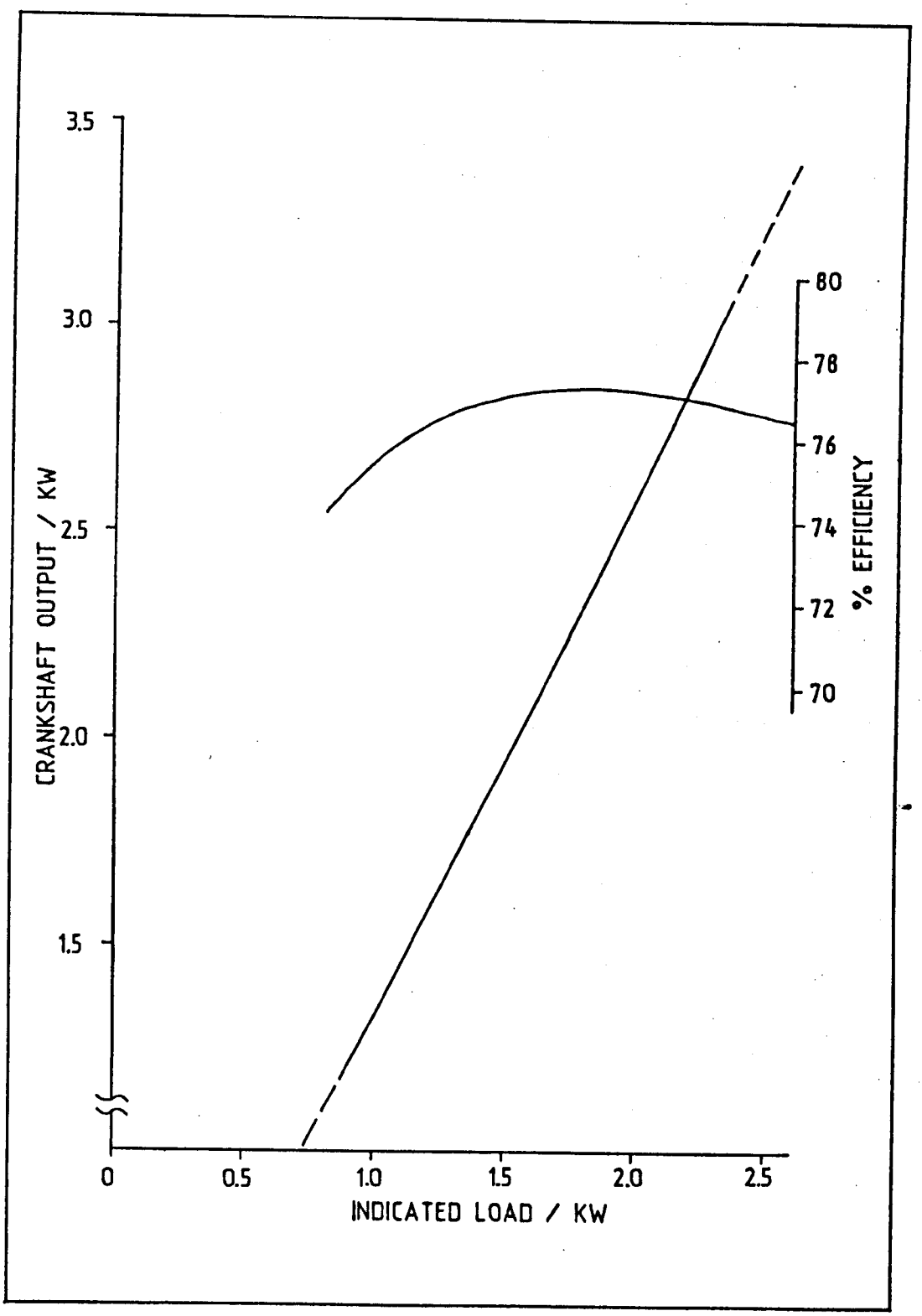

FIG 2.9 CALIBRATION GRAPH FOR THE GENERATOR

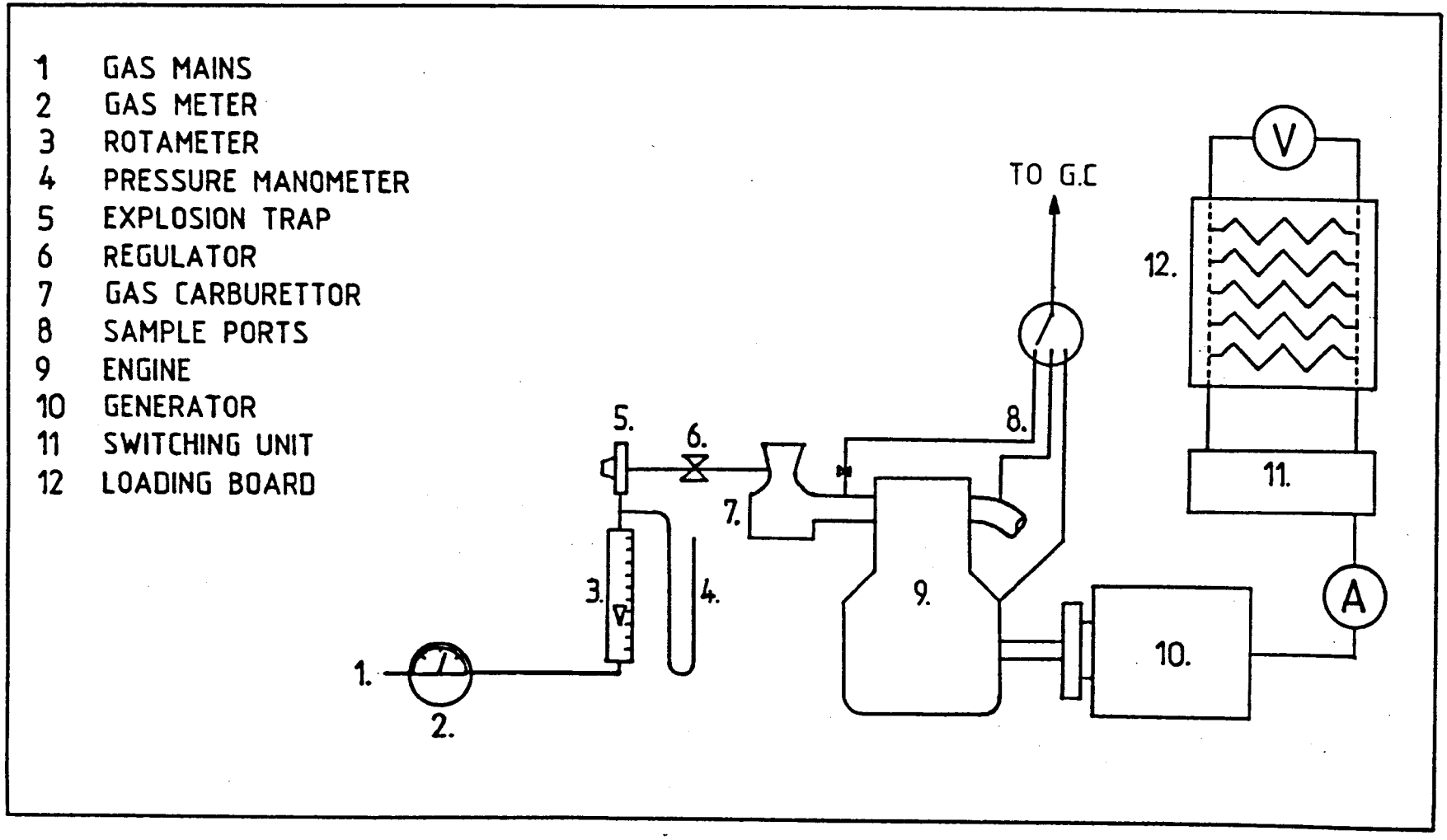

FIG 2.10 DIAGRAM OF THE ENGINE TEST BED

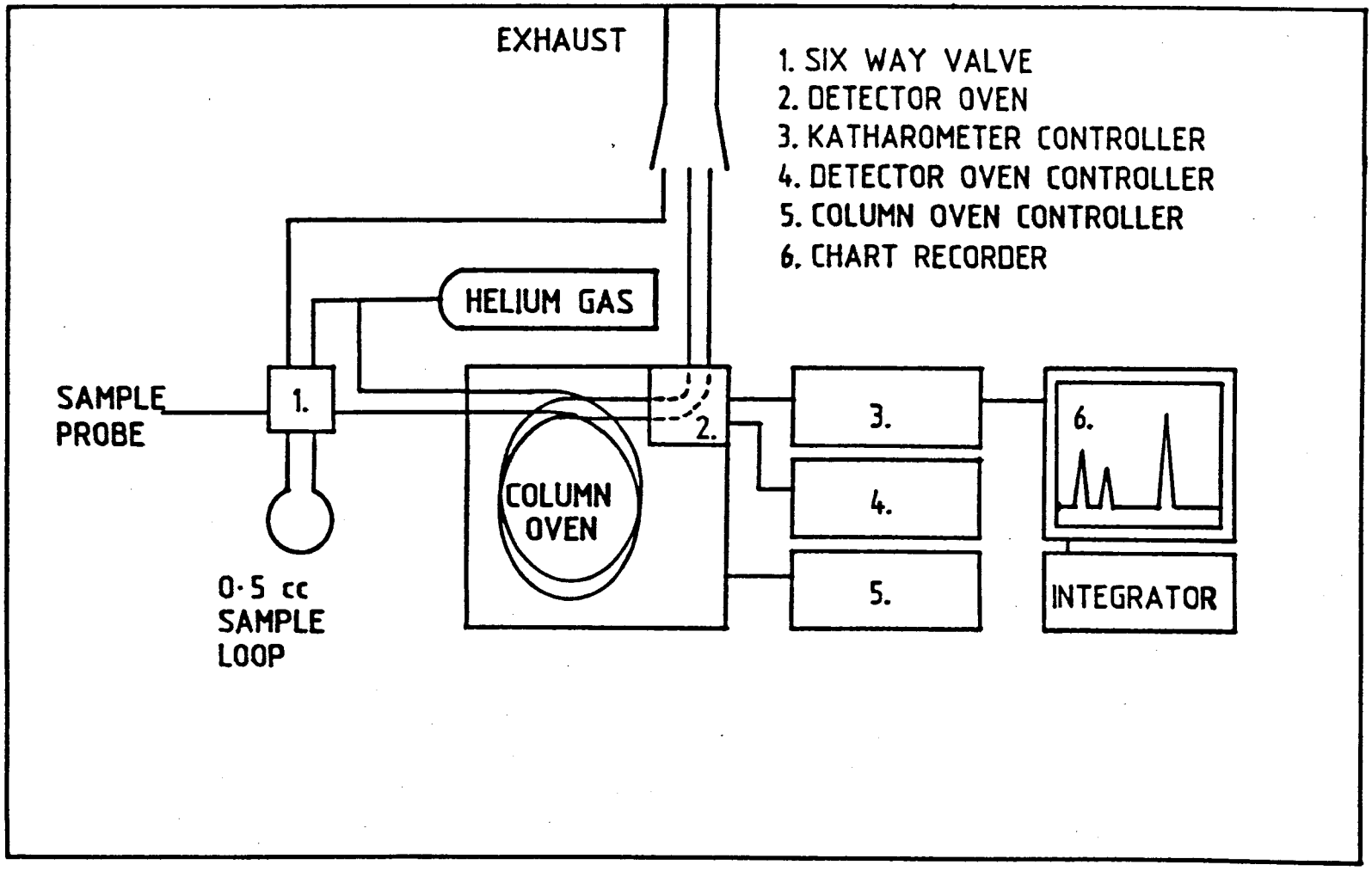

FIG 2.11 DIAGRAM OF THE SAMPLE GAS ANALYSIS SYSTEM

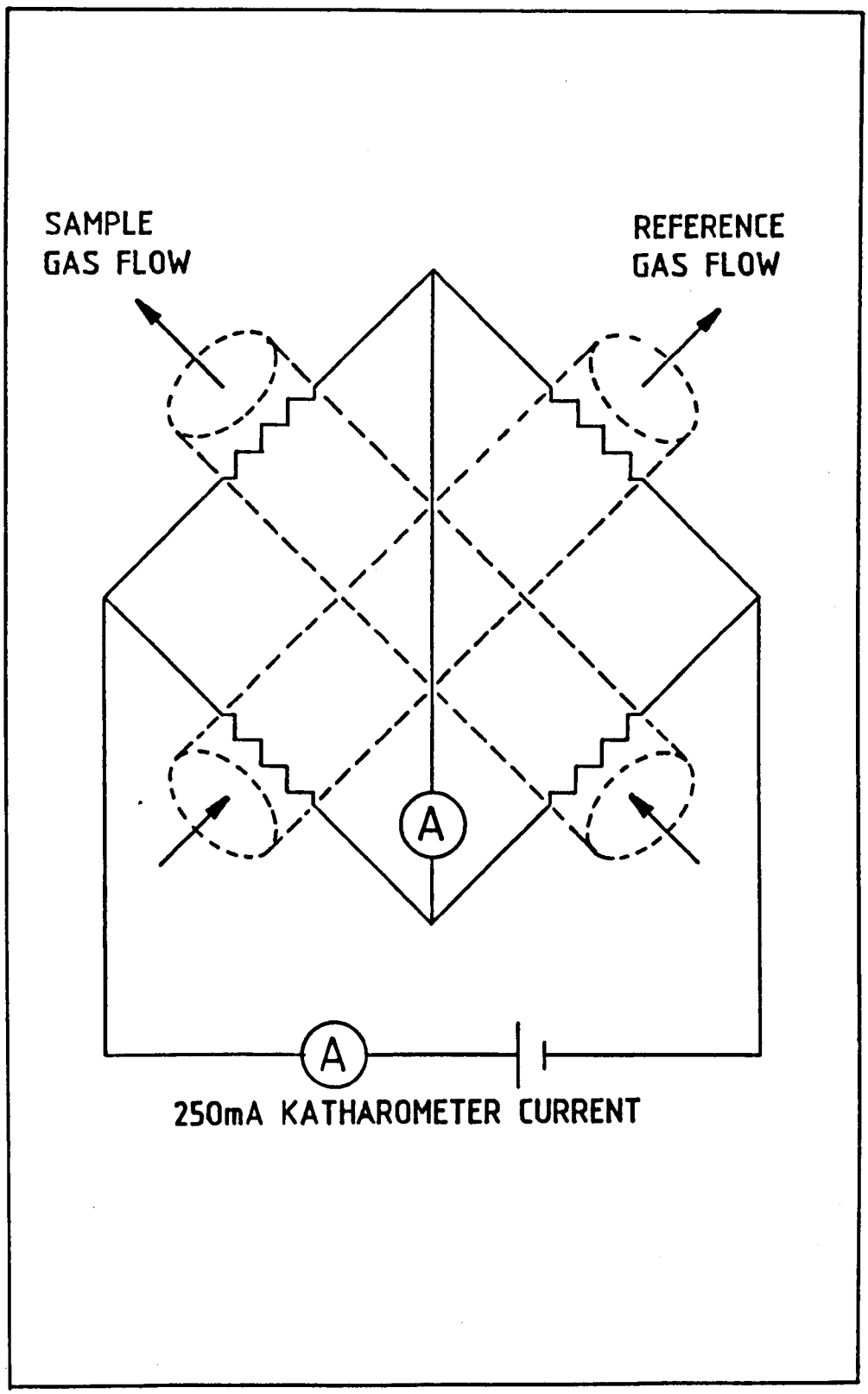

FIG 2.12 DIAGRAM OF THE WHEATSTONE BRIDGE DETECTOR.

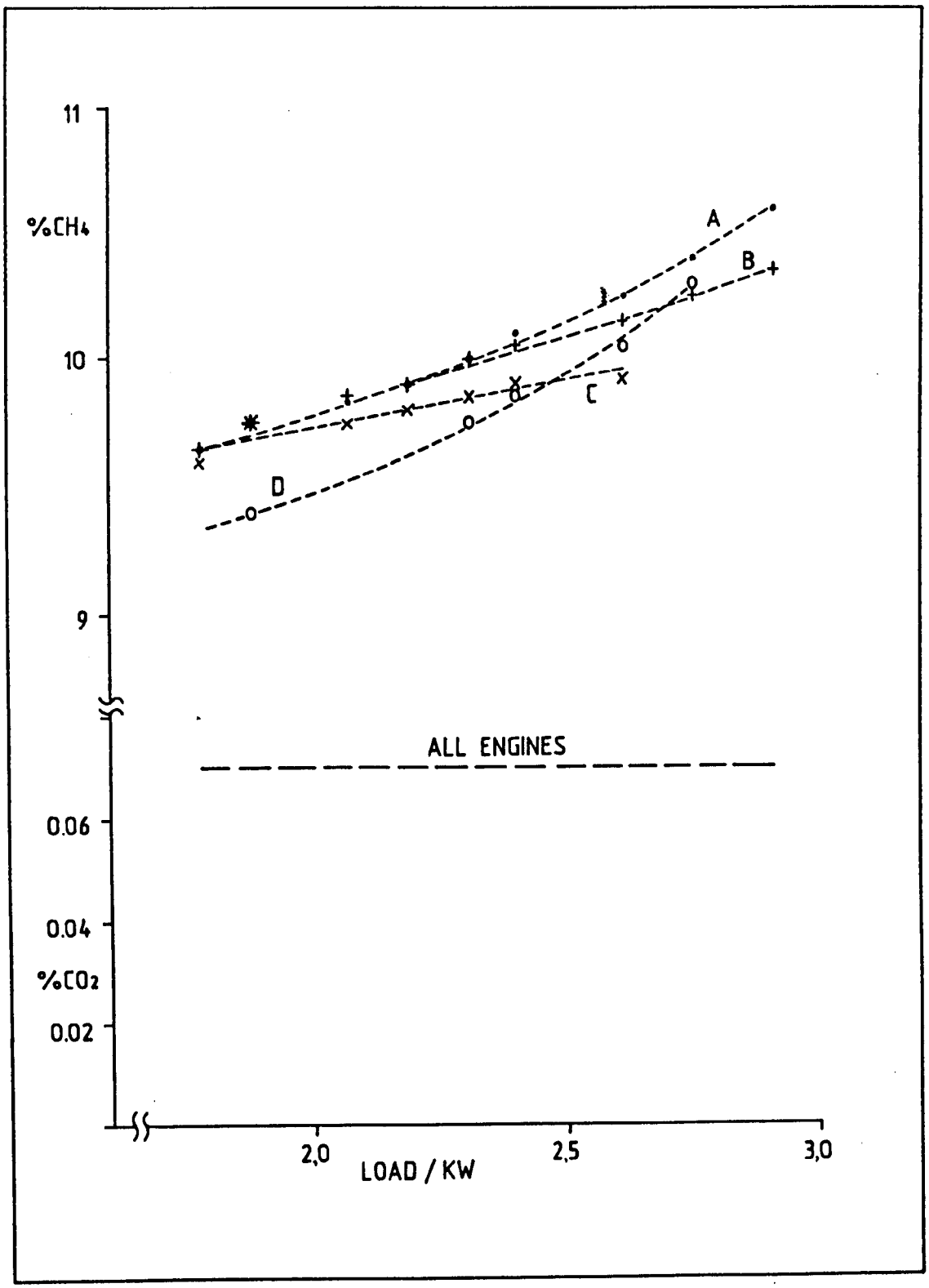

FIG 2.13 GRAPH OF THE INLET GAS COMPOSITION

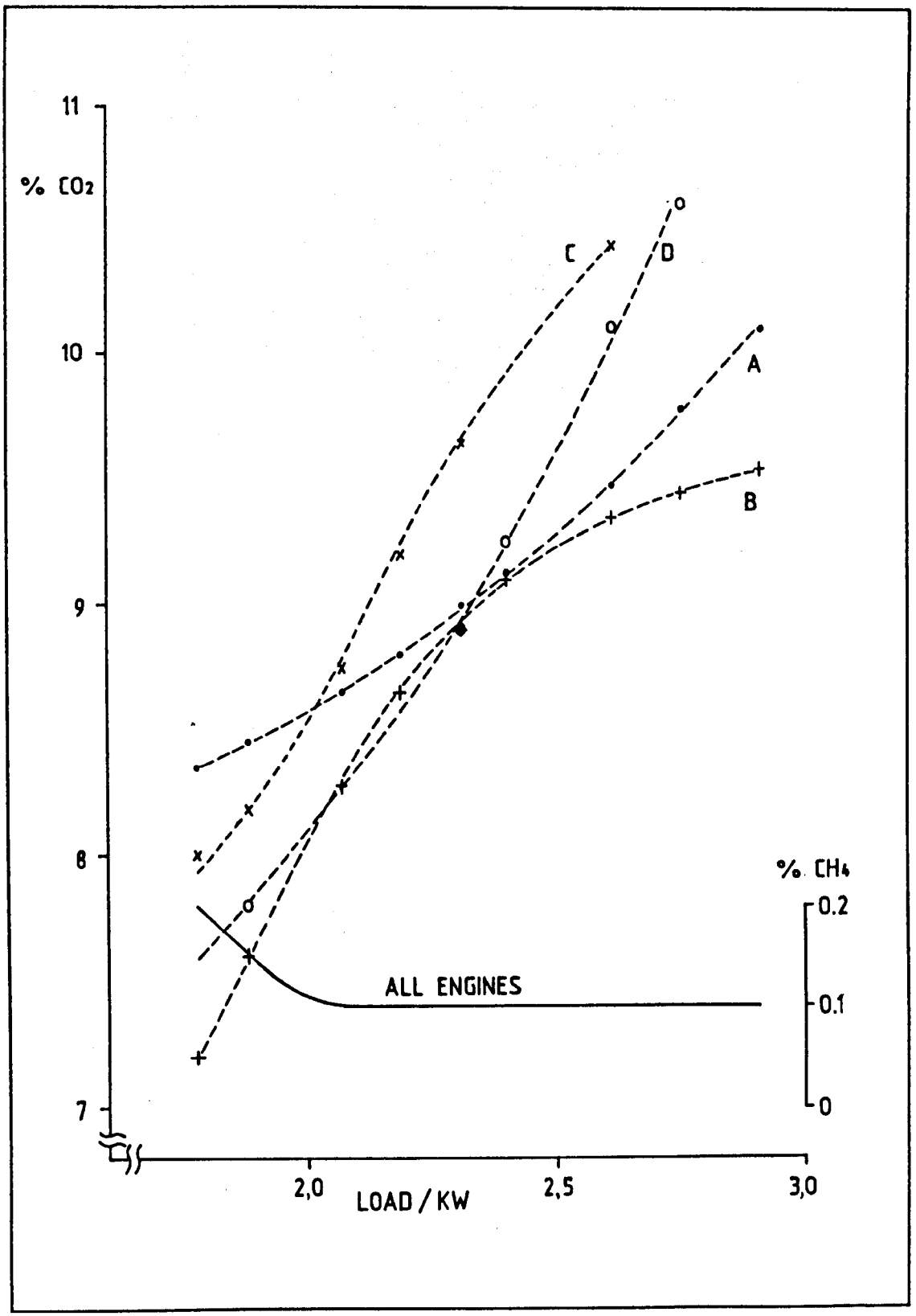

FIG 2.14 GRAPH OF THE EXHAUST GAS COMPOSITION

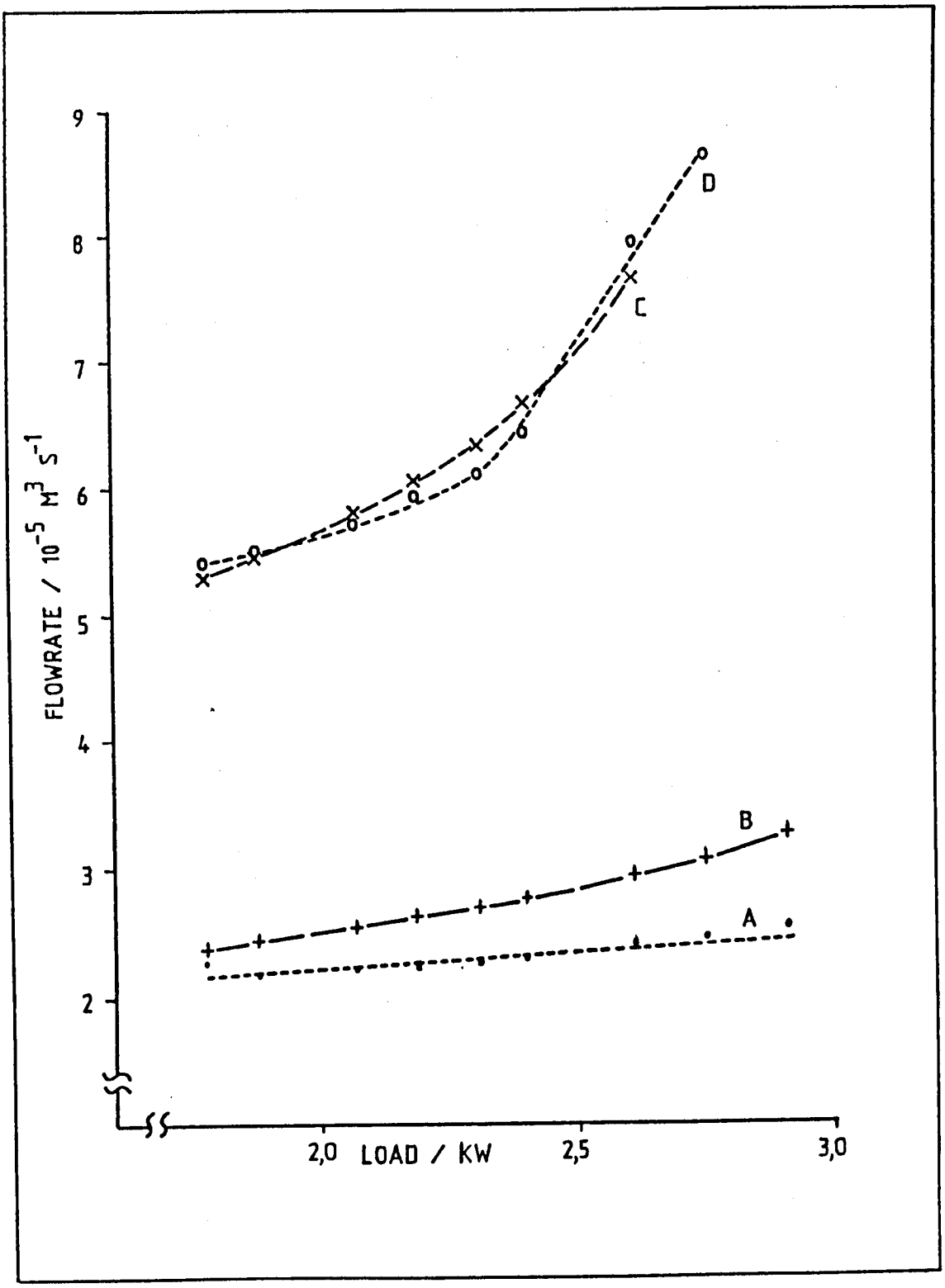

FIG 2.15 GRAPH OF THE BLOWBY FLOWRATES

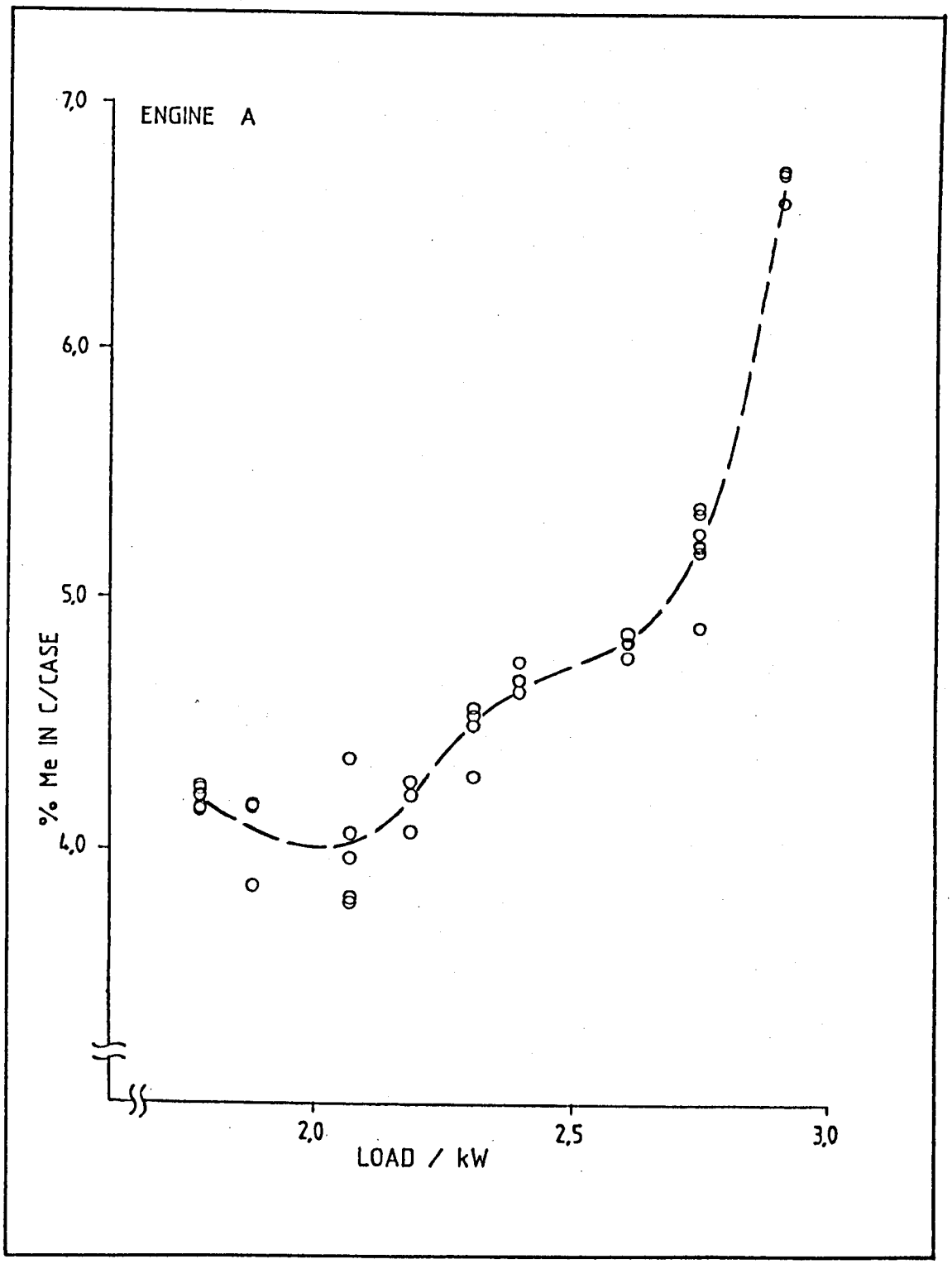

FIG 2.16 GRAPH OF BLOWBY METHANE CONTENT - ENGINE A

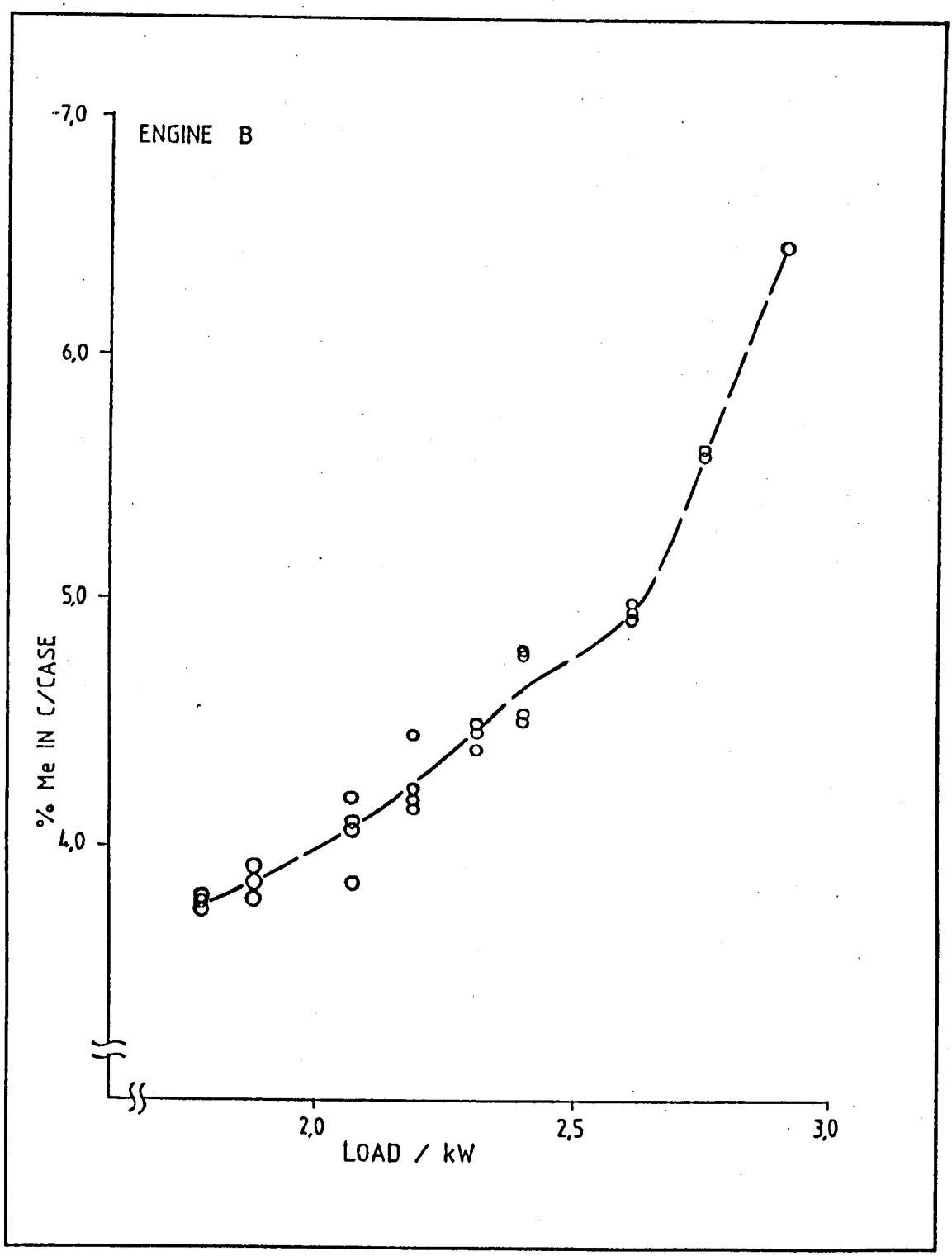

FIG 2.17 GRAPH OF BLOWBY METHANE CONTENT - ENGINE B

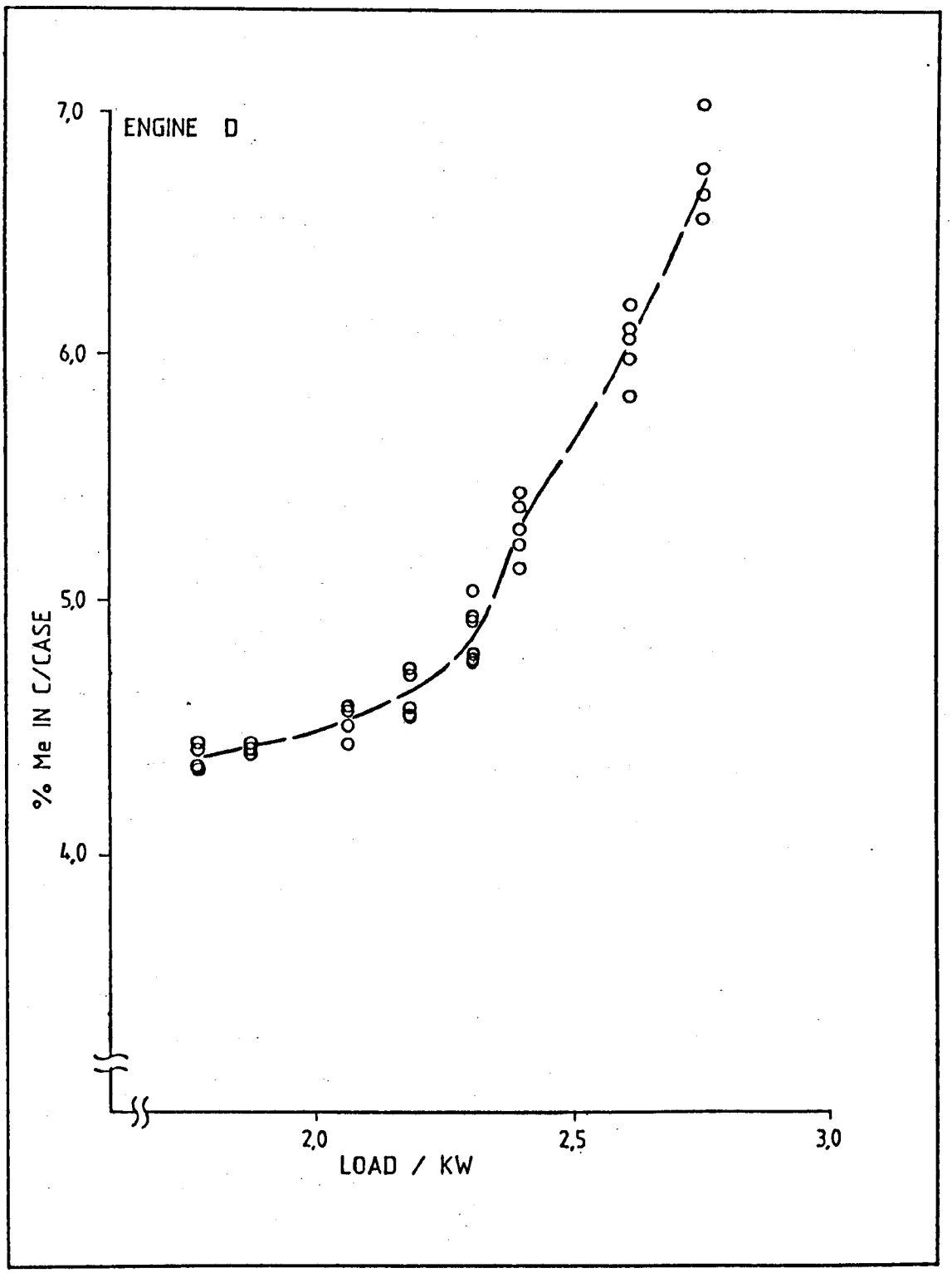

FIG 2.18 GRAPH OF BLOWBY METHANE CONTENT - ENGINE D

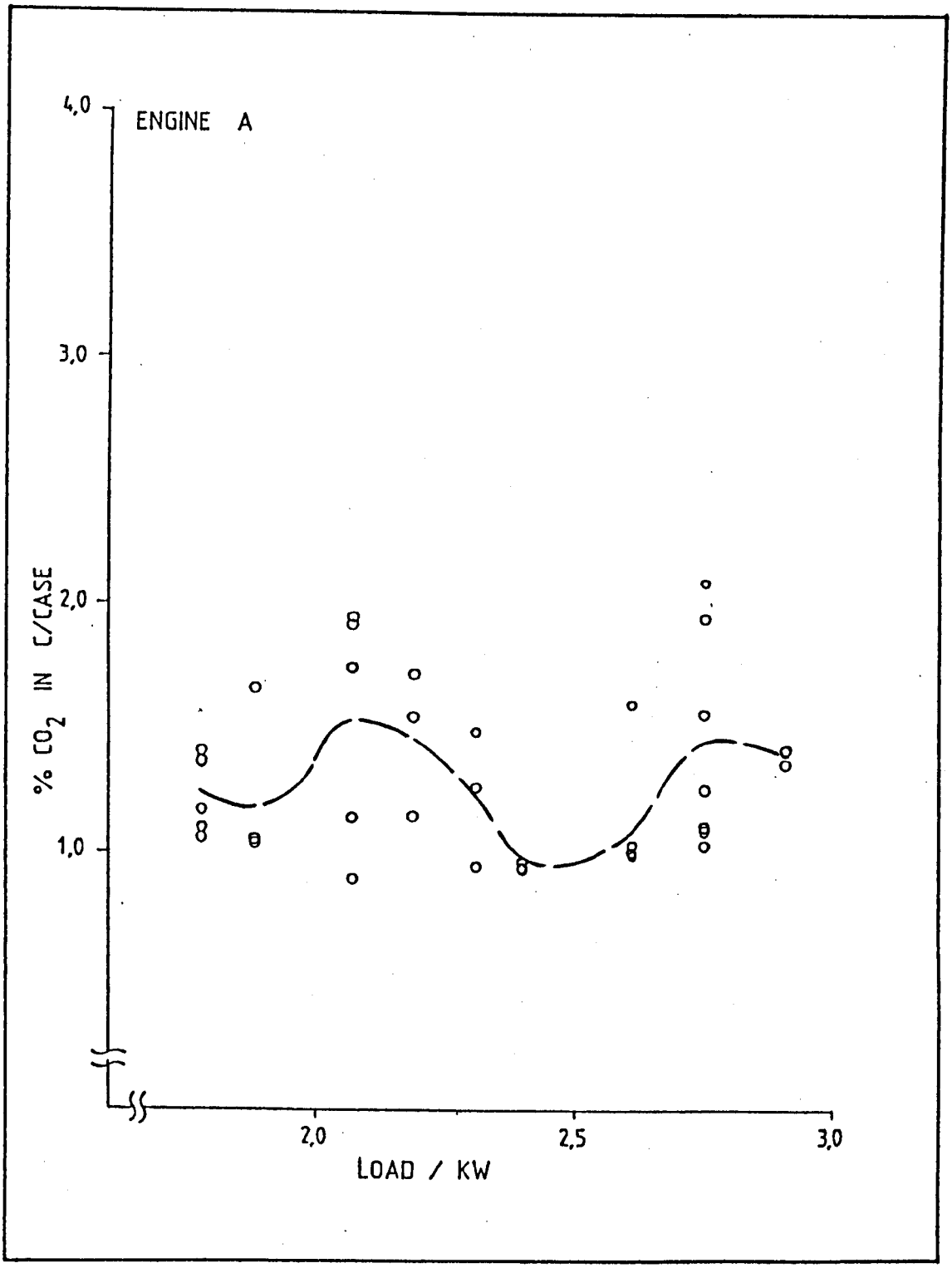

FIG 2.19 GRAPH OF BLOWBY CO_2 CONTENT - ENGINE A

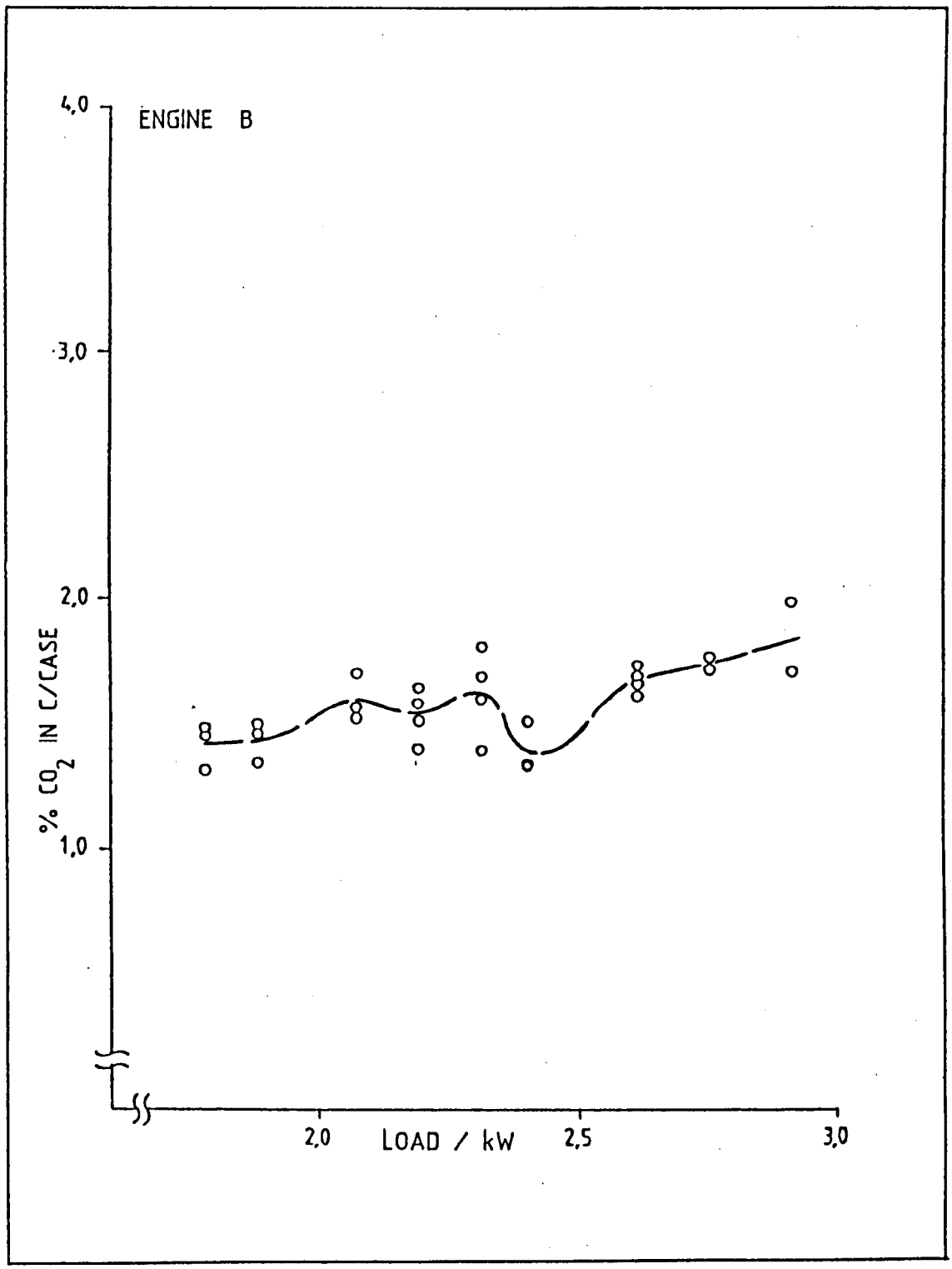

FIG 2.20 GRAPH OF BLOWBY CO_2 CONTENT - ENGINE B

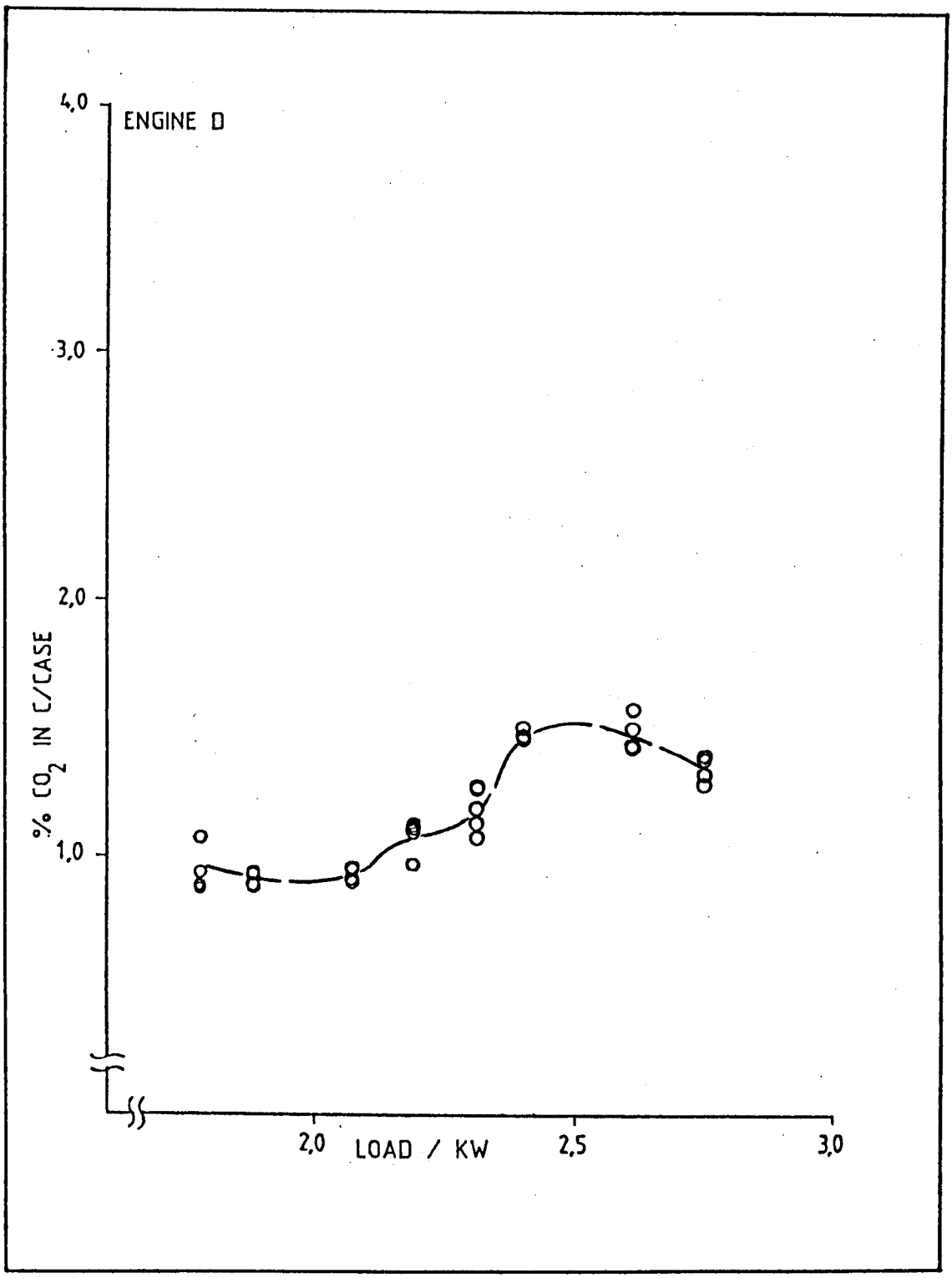

FIG 2.21 GRAPH OF BLOWBY CO_2 CONTENT - ENGINE D

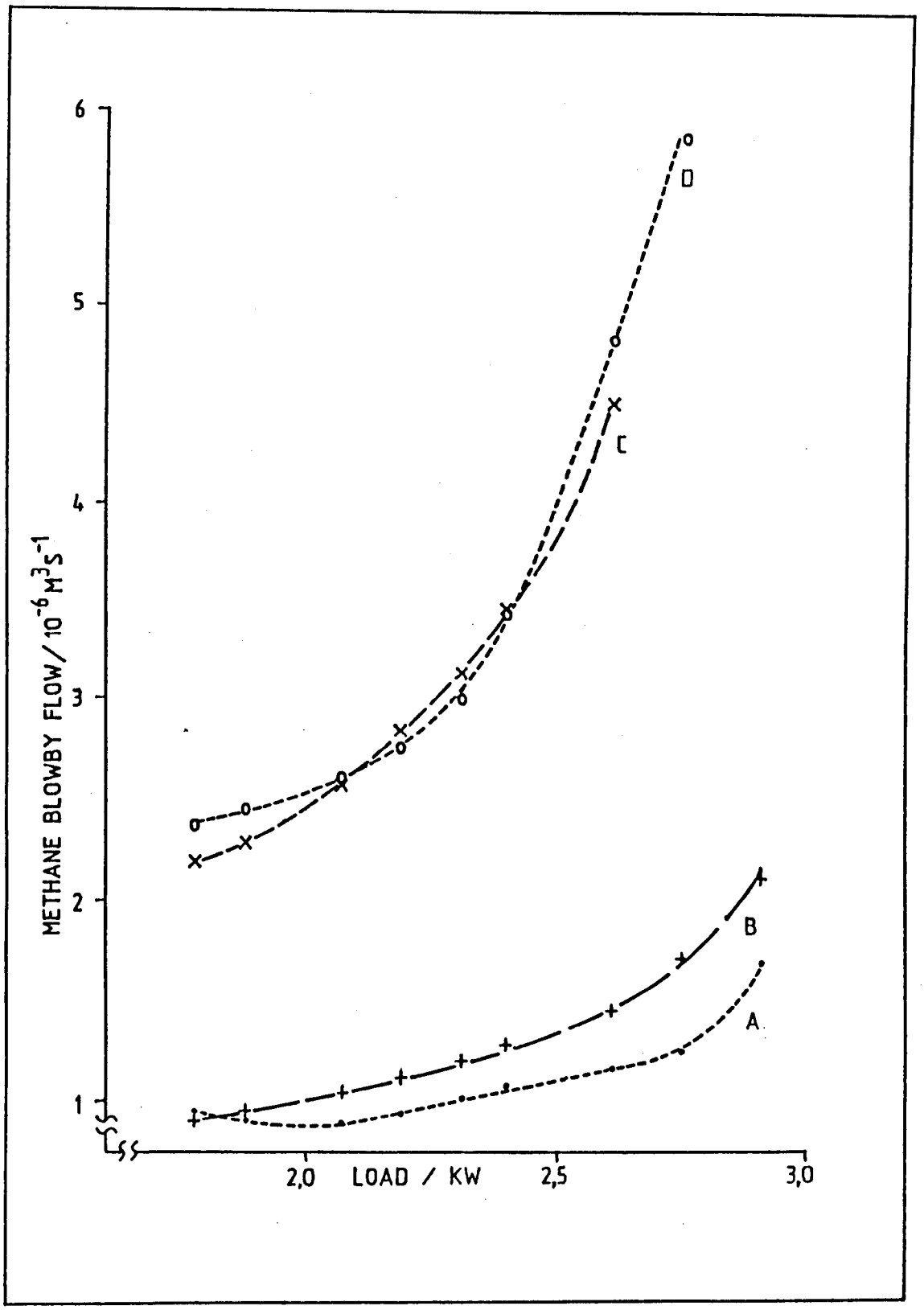

FIG 2.22 GRAPH OF METHANE BLOWBY FLOWRATE

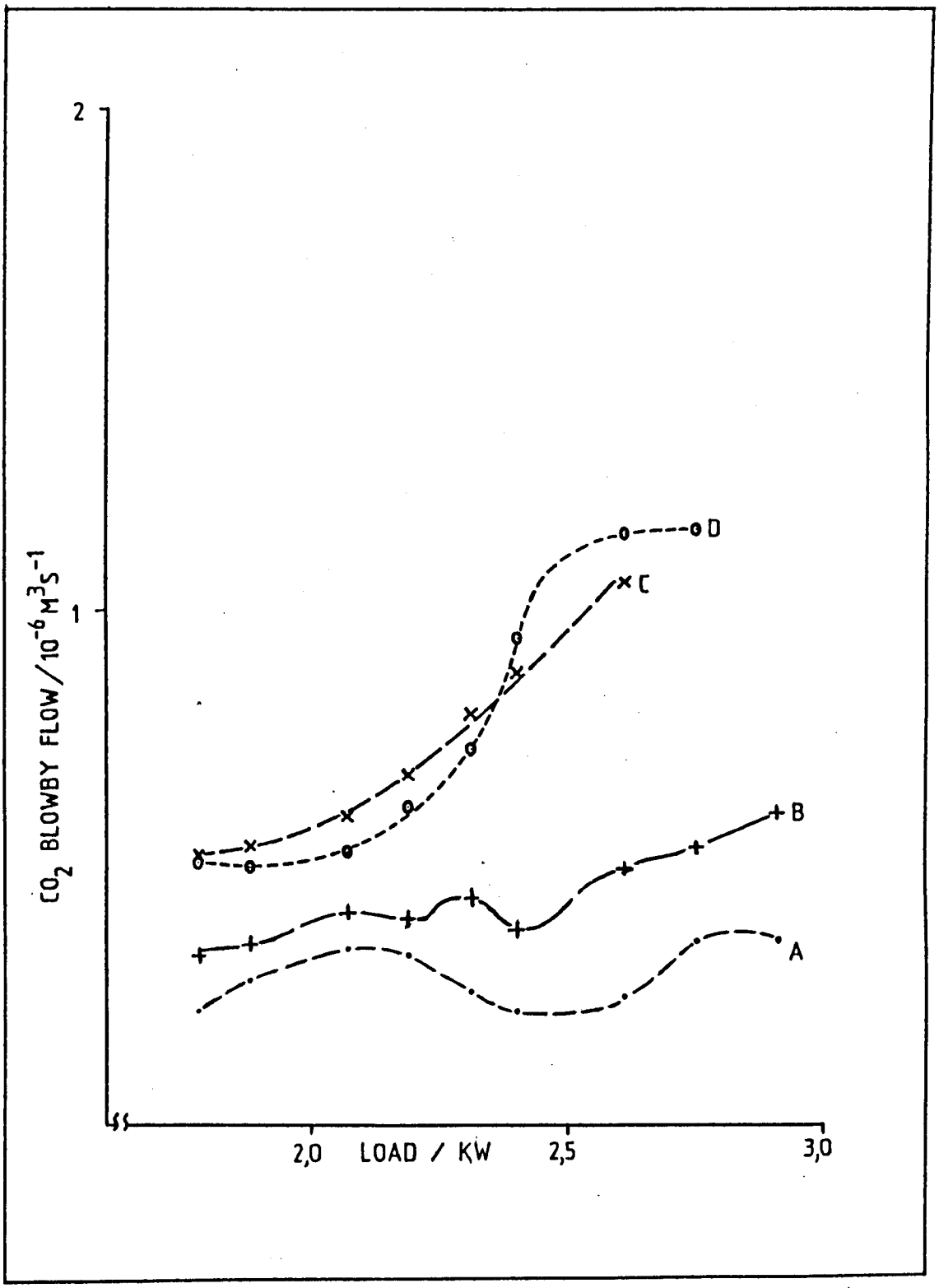

FIG 2.23 GRAPH OF CO_2 BLOWBY FLOWRATE

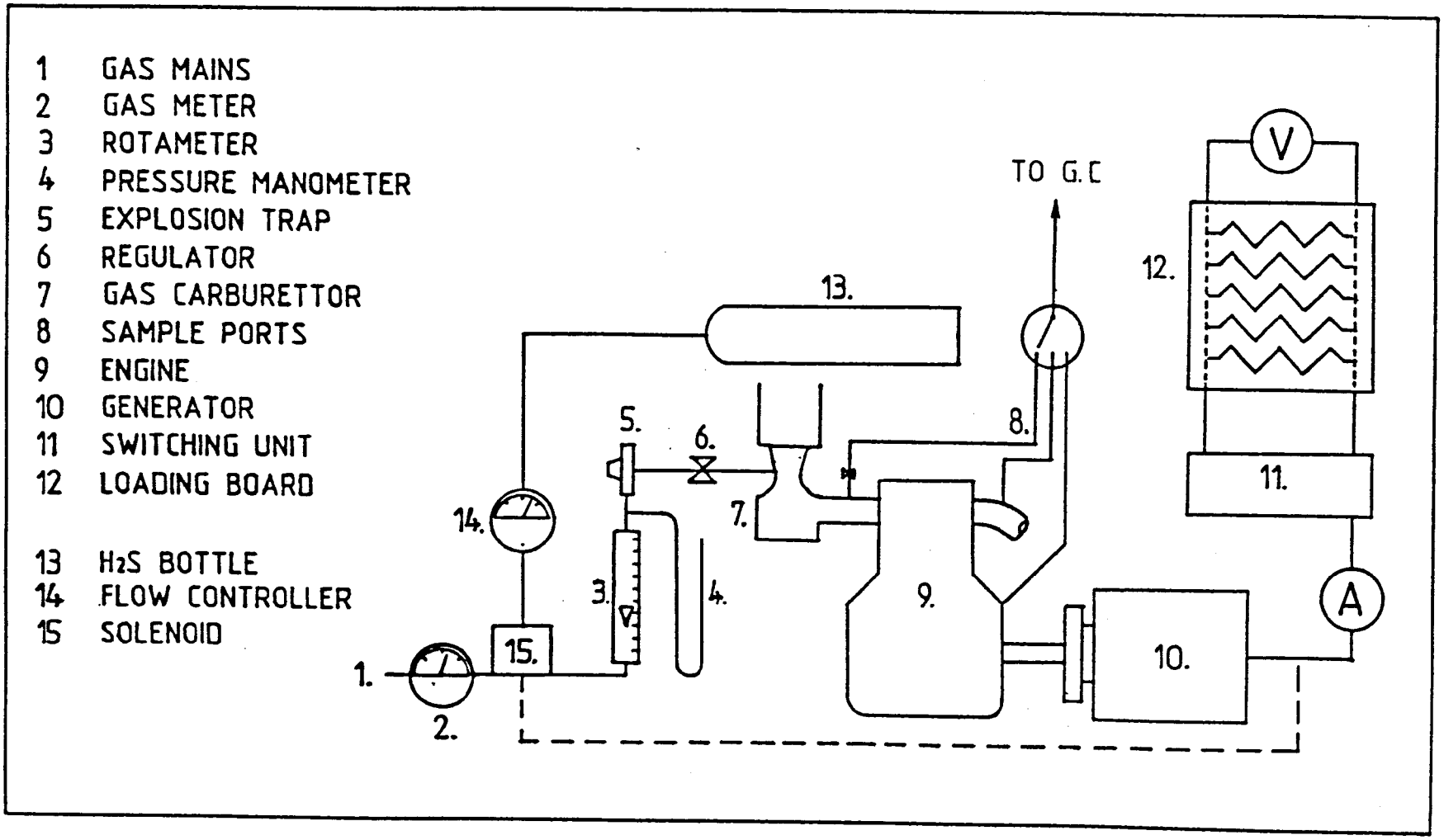

FIG 2.24 DIAGRAM OF THE MODIFIED TEST BED FOR H_2S

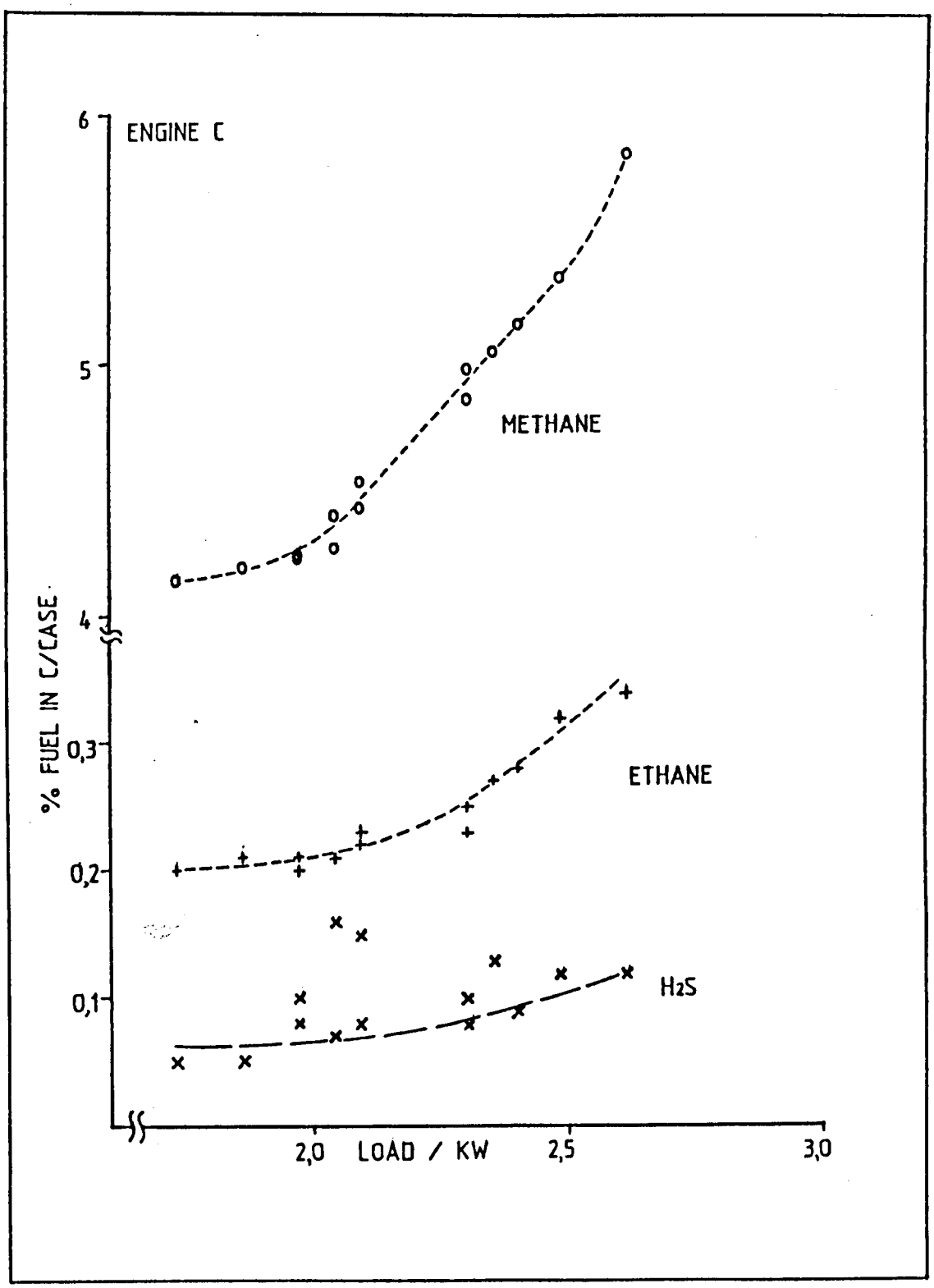

FIG 2.25 GRAPH OF THE BLOWBY GAS FUEL CONTENT

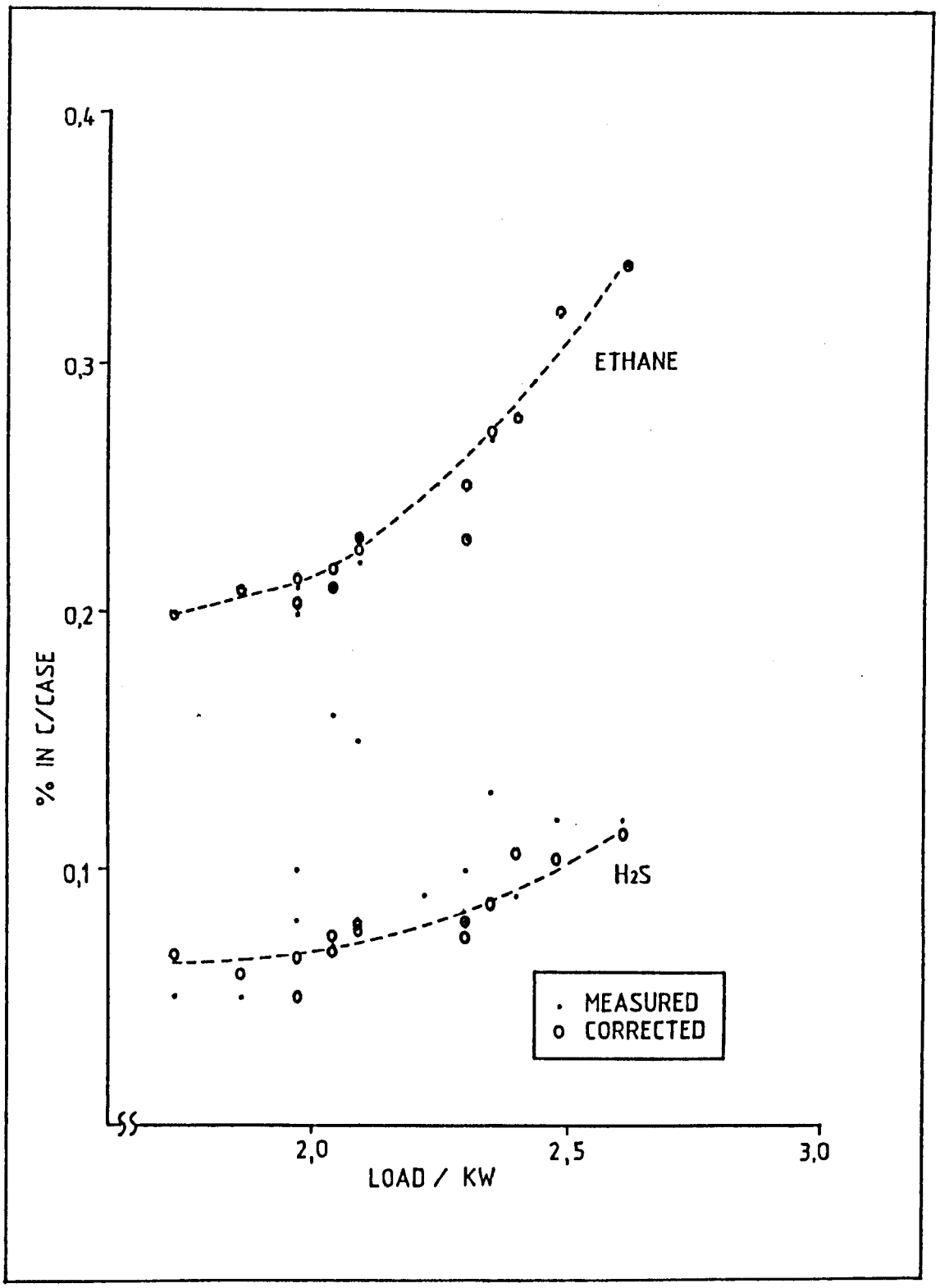

FIG 2.26 GRAPH OF THE BLOWBY CORRECTED TO 0.2% INLET H_2S

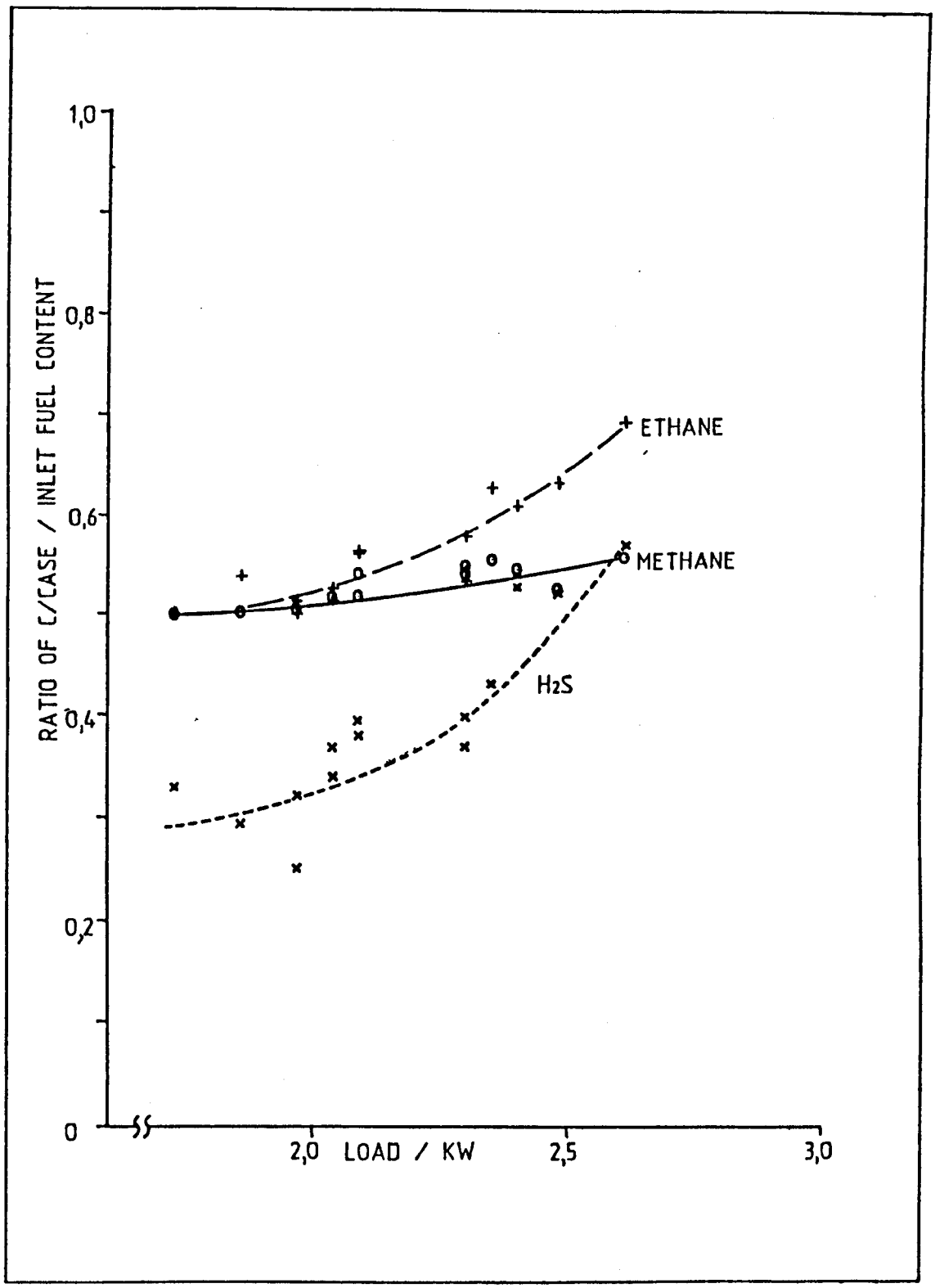

FIG 2.27 GRAPH OF THE INLET TO BLOWBY CONTENT RATIO

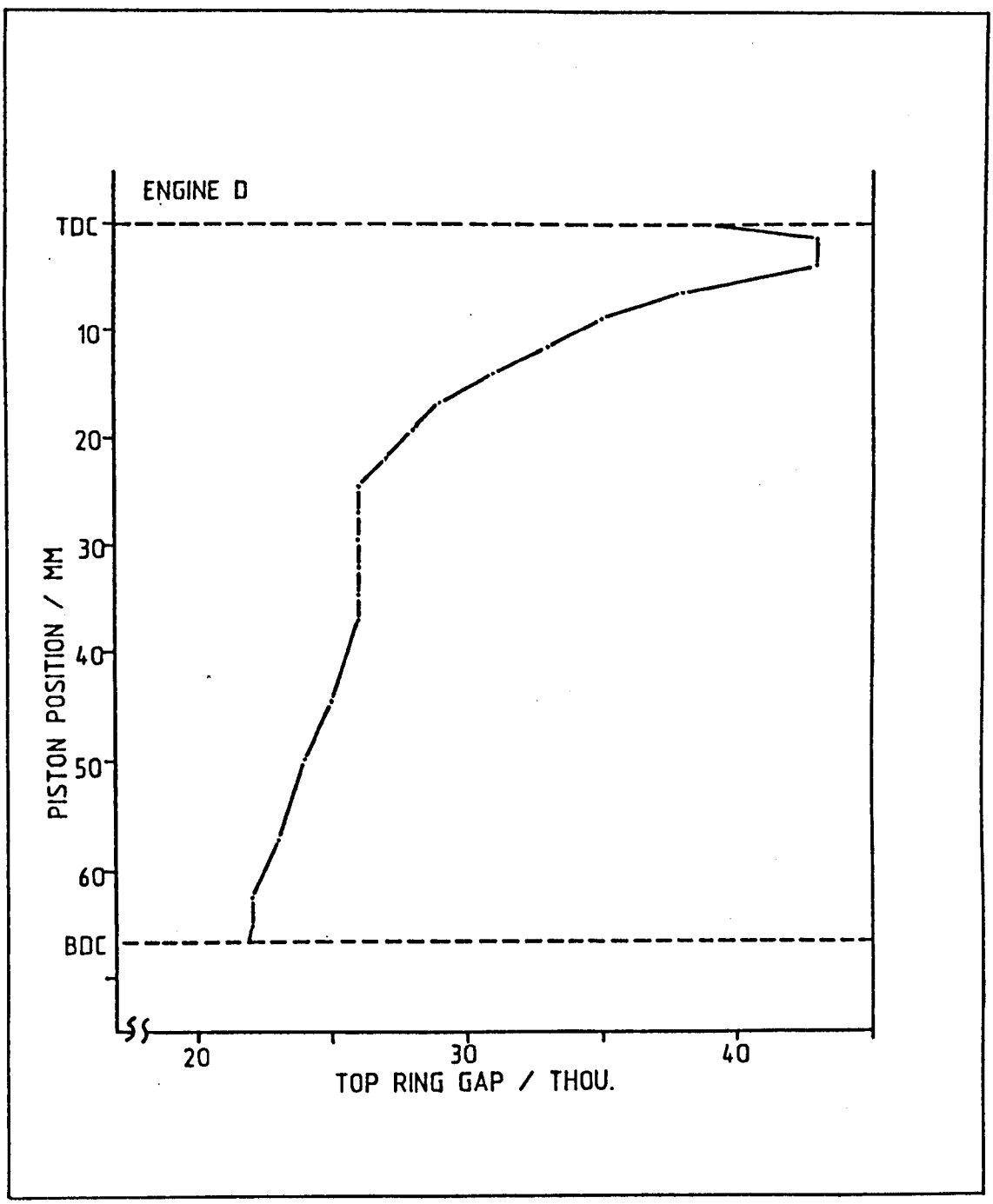

FIG 2.28 GRAPH OF THE PISTON RING GAP FOR ENGINE D

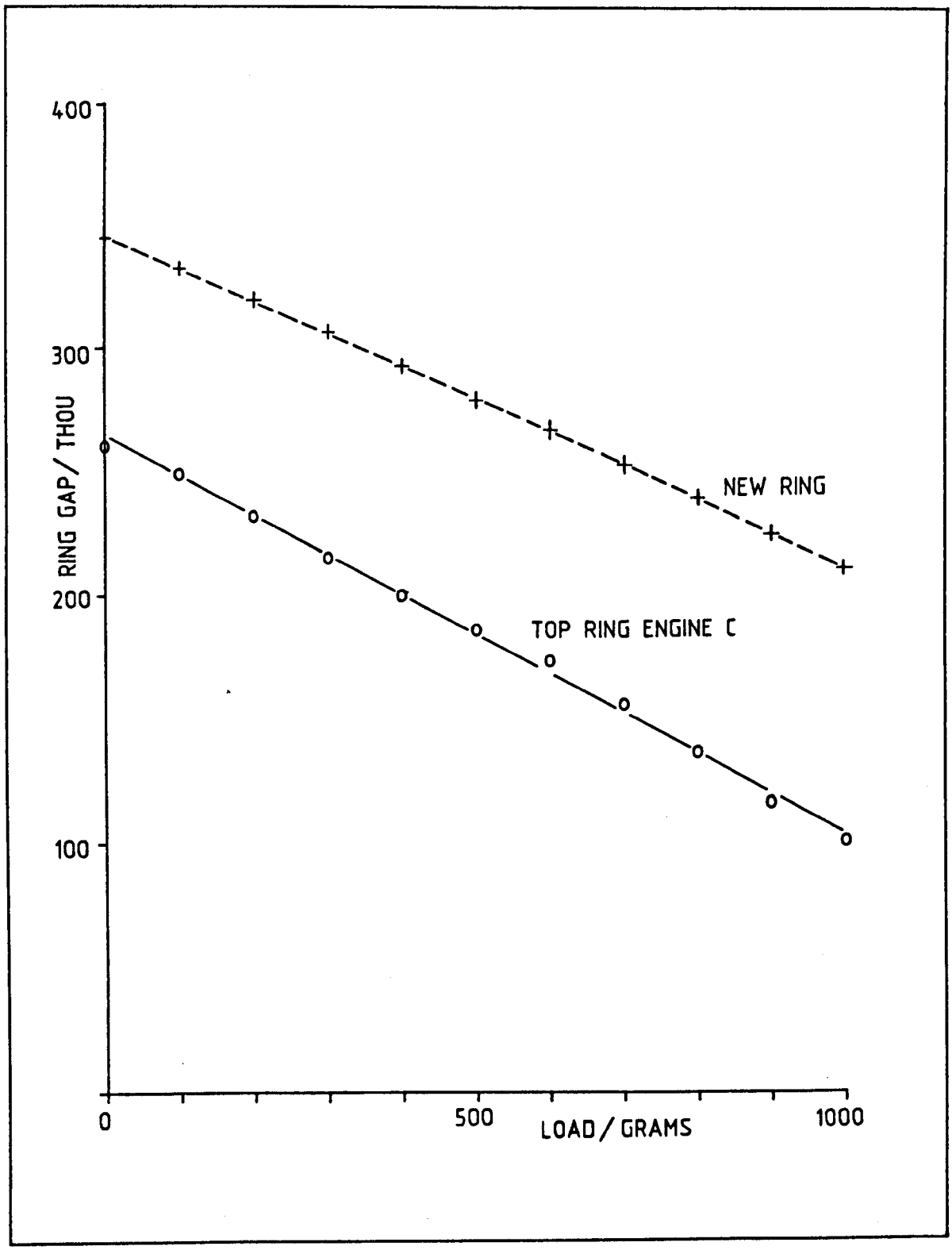

FIG 2.29 GRAPH OF THE CHANGE IN PISTON RING GAP WITH LOAD

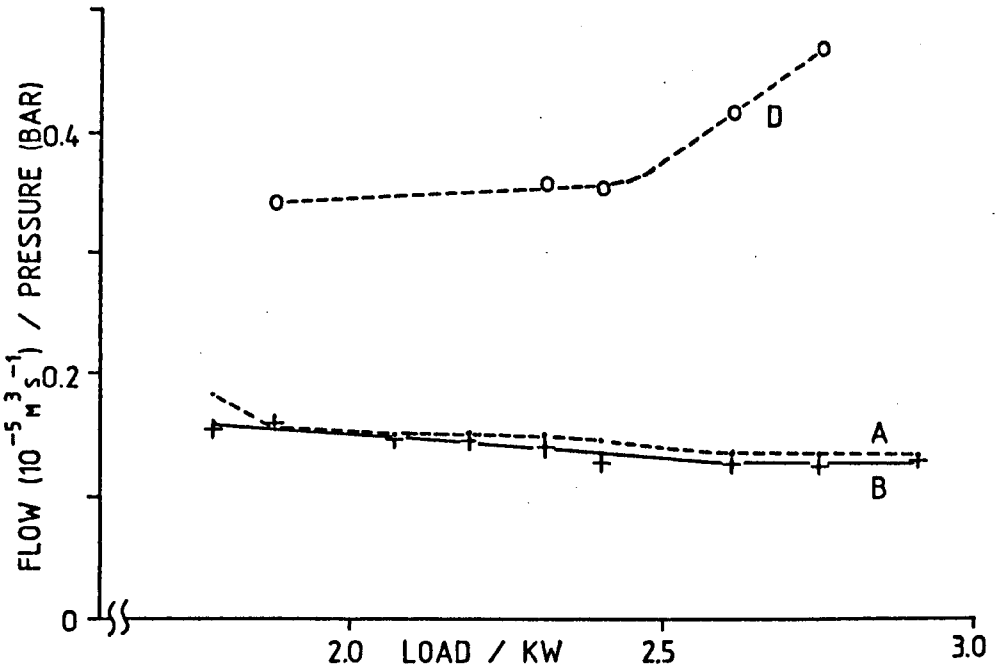

FIG 2.30 GRAPH OF FLOW TO PEAK PRESSURE RATIO

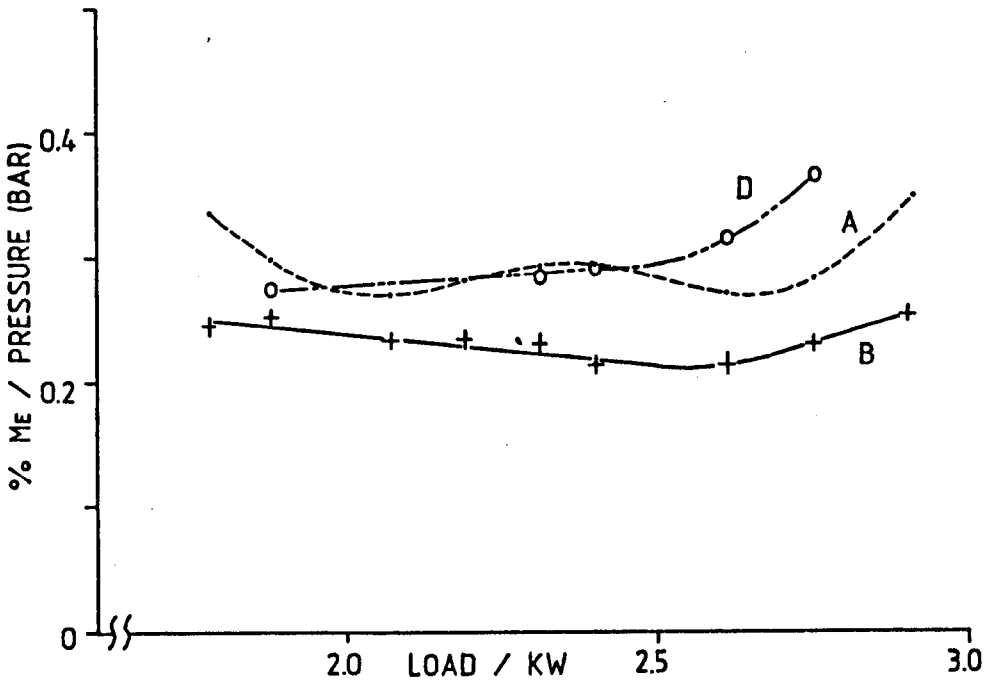

FIG 2.31 GRAPH OF % ME TO PEAK PRESSURE RATIO

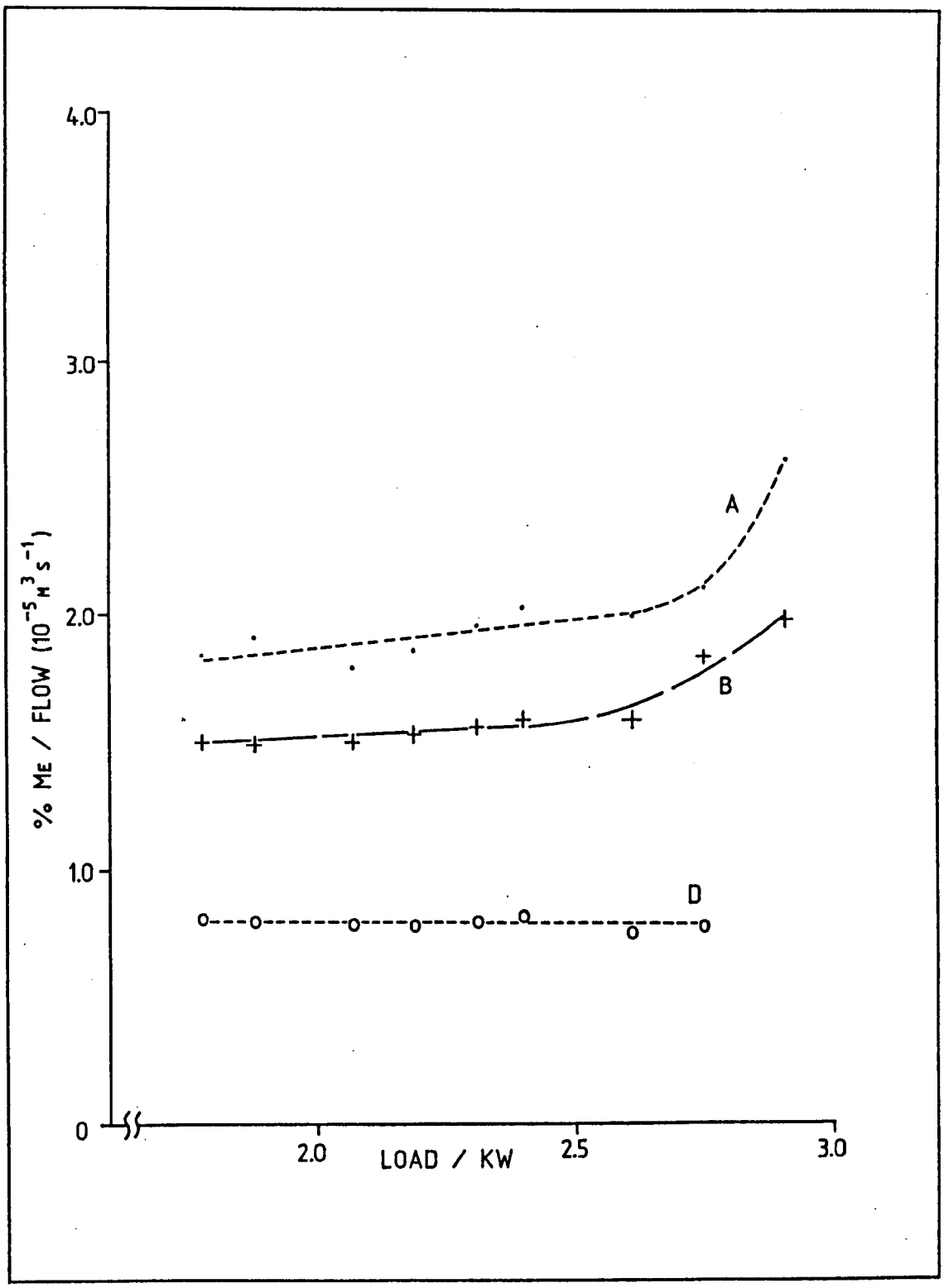

FIG 2.32 GRAPH OF THE METHANE CONTENT TO FLOW RATIO.

Chapter 3. An investigation of the mechanism of blowby.

3.1 Introduction.

The experimental work has shown the quantity and composition of the gases in the crankcase. These could have entered the crankcase by the following mechanisms:

(a) Passage of unburnt and then burnt gas past the piston rings.

(b) Ingress of fuel polluted air through the breather system.

(c) Transport by adsorption and then desorbtion from the lubricating oil.

(d) Retention of the trace gases in the crankcase for a longer period of time than predicted by the bulk flow of gases.

The work detailed in this chapter investigates whether the most likely route (a) can account for the gases in the crankcase. This has been done by an experiment to measure the the amount of gas passing the piston rings for all engine combinations. A series of calculations are used to investigate the blowby flow and composition and are based on the following rationale:

(a) Divide the combustion cycle into discrete increments and, using a calculated position of the flame front, obtain the values of flow and composition for each increment.

(b) Sum the incremental values to obtain the blowby flow and composition across the whole combustion cycle, and analyse the trends in flow and composition with engine load and wear.

(c) Analyse the data from both (a) and (b) above to evaluate the mechanism of blowby, and compare the conclusions with those derived from the experimental work.

In order to construct this analysis, the mechanism of blowby in the engine is simplified, and account must be taken to consider all of the implications of any assumptions made. For the study of blowby, the engine assembly can be considered as a system with two chambers. The combustion chamber is the source of the blowby gases, which pass the piston rings and into the second chamber - the crankcase. The blowby is a function of the interrelationship between cylinder pressure, piston position, and the progression of the combustion process during the combustion cycle. It is important to consider the variables that will affect the piston blowby in a running engine. Once identified, the calculations can be adapted to remove or simplify the variables. These can be identified as:

(a) Engine design. The blowby mechanism is likely to be dependent on the dynamic interaction of the cylinder components, which are different for each engine design.

(b) Operating parameters. The results of the previous chapter show that both the blowby flow and composition vary with engine load. The increase in peak cylinder pressure with increasing load is a major factor of this behaviour. The way in which the engine is used will also affect the contribution from (c) and (d) below.

(c) Lubrication. A combination of engine operating conditions and design parameters will determine the lubrication within the ring pack. The direct effect of the oil layer on blowby is unknown, but it will indirectly affect it through liner wear, ring sticking and piston deposits.

(d) Engine wear. As the engine ages, the cylinder liner becomes worn, and the piston rings lose their ability to follow the deteriorating liner profile as a result of their permenent deformation. The seal offered by the ring pack becomes less effective. This results in an increase in blowby flowrate.

The extent to which these variables can be controlled or eliminated determines the scope and limitations of the calculations. The effect of engine design on blowby formation was too complex a subject for this project, and a set of standard design parameters are difficult to relate to the experimental results obtained from the Villiers engines. In order to provide simple and readily processed input data to compare with the experimental results, the complexities associated with the specific design of the Villiers engine must be eliminated. Compatible with the two chamber concept introduced earlier, the engine design and wear variables were eliminated by using the engine itself as a source of input data. This was achieved by the use of the Static Piston experiment (Section 3.2). Piston blowby occurs when the pressure drop across the piston ring pack is sufficient to overcome the sealing mechanism of the piston rings. The Static Piston experiment is a technique of measuring the relationship between the cylinder pressure and blowby within a given engine assembly, allowing the direct comparison of computed and experimental results. Lubrication was an unknown factor, but was investigated in both Section 3.2 and in Chapter 4. Finally, the operating conditions, of which load is introduced indirectly through the pressure-crank angle diagrams (Section 3.3). Cylinder pressure is an input in the Static Piston Experiment, and also in the flow simulation. Hence, the operation of an internal combustion engine has been broken down into its basic operational unit - the combustion cycle. Data obtained from the engine assembly is used as the basis of the calculations, thereby eliminating the design related variables.

The calculations of the movement of gases between the upper (combustion) chamber and the lower (crankcase) chamber have been achieved by divided up the engine cycle into discrete 2^{o} increments of crank angle. The sectioning of the cycle enables an incremental blowby to be calculated for a series of piston positions throughout the combustion process. The use of data from the pressure-crank angle diagrams and the Static Piston experiment (Section 3.2) yields a pressure-flow relationship for each 2^{o}

incremental piston position. The programme uses the experimental pressure for each 2^{o} increment to generate an incremental flow. After summation throughout the engine cycle, the calculated overall blowby flow is obtained, and this approach is further developed to obtain a result for the crankcase gas composition. This is achieved by calculating the passage of the flame front across the piston crown, and obtaining incremental blowby compositions. These are summed across the engine cycle to derive overall composition.

3.2 The Static Piston Experiment

3.2.1 Experimental

The calculations described in this chapter are based on the pressure, crank-angle and flow measurements obtained by this experiment. The objective was to examine the variation of blowby flowrate with both piston position and pressure, in a way in which the complexities of the combustion process (temperature, motion, change in composition) were neglected.

The flow measurements were taken from a series of tests on each piston/barrel combination. In each experiment, the piston position was fixed, a pressure applied in the cylinder head and the resulting blowby flow was recorded (Fig 3.1, Table 3.1). The bore profiles for these engines have been measured, by the scratch technique (Ref 3.1) and direct surface analysis by Talysurf. The cylinder wear varies with the past history of each engine, but all showed the greatest wear near to the TDC position of the top ring. A decrease in flow was therefore expected by moving the piston away from TDC .

The crankshaft of the C-30 engine extends externally from the rear of the crankcase, and the generator shaft is joined to its end via a 'doughnut' coupling system. The exposed end of the crankshaft provided an ideal location for a clamping bracket. This enabled the crankshaft, con-rod and piston assembly to be positioned and fixed with the minimum disturbance of the internal engine components. For

each engine, a series of experiments was carried out, starting with the piston at the TDC position and then moving it down the cylinder wall. For each experiment, the crankshaft was clamped with the piston at the predetermined position, and then the exact piston crown height was measured using a depth gauge (Fig 3.2). The gauge measured the depth from a specially machined flat plate which was firmly bolted to the top of the engine by the cylinder head bolts. The depth gauge probe was lowered through the pressure transducer orifice (which was directly above the piston) and a reading of the height of the piston crown was taken. This measurement was used to derive the corresponding crank angle (Eqn 3.1). The pressure transducer was then installed into the cylinder head, and compressed air from a gas bottle was admitted through the spark plug hole via pressure tubing and a custom thread adaptor. The cylinder head pressure was controlled by a high pressure gas bottle diaphragm valve, but the pressure readings used in the calculations were those measured from the transducer installed in the cylinder head. The resulting blowby was measured using a rotameter connected to the crankcase breather. The pressure was gradually increased and the change in blowby flow with applied pressure was recorded. The pressure was taken above the maximum value recorded during engine running (Fig 3.6), and then reduced back down to atmospheric conditions. The pressure transducer was then removed, and the piston crown height was checked before the crankshaft was unclamped to set a new piston position. This procedure was repeated for a range of piston positions for engines A, B and D.

3.2.2 Results and Calculations.

The experiment was easy to perform, with the maximum applied pressure being limited by the ability of the clamp to hold the crankshaft in its original position. The measured flowrates for each piston position showed some disparity (maximum 5%) between the pressure rise and the pressure fall section of each test. The values used in the calculations were the average of the two values at each pressure.

The blowby flow readings were taken for a range of pressures up to and beyond those experienced by the engine under running conditions. The results are summarised in Table 3.2. The depth gauge readings of the piston crown were corrected by the subtraction of the reading taken when the piston was at TDC (i.e, the maximum height recorded). This correction gave values of the piston position relative to that at TDC, which are related to the crank angle (θ) by equation 3.1.

$$\cos \theta = x^2 + s^2 - l^2/2sx \qquad (3.1)$$

where l = Con-rod length (127.5 mm)
s = Stroke/2 (33.35 mm)
x = (1 + s) - (height measurement/mm)

There are several experimental details that require discussion. This experiment was conceived as a simple means of imitating the dynamic blowby flow through the piston ring pack. As such there are several differences between this experiment and the conditions experienced by the engine whilst running.

During the initial development of the clamped piston blowby measurement technique, an attempt was made to introduce an oil film onto the cylinder wall, in order to simulate the oil film present in the ring pack during actual running conditions. This involved spreading a small amount of oil onto the cylinder wall and manually motoring the engine (with the cylinder head removed) until the oil had spread evenly and also until no excess was pushed above the top ring at TDC. The engine was then reassembled, and the crankshaft clamped. The Static Piston experiment was then carried out, and it was found on comparison that the oil film made no difference to the blowby flowrate. This experimental observation is consistent with reports from several workers (Refs 3.2, 3.3, 3.4) that piston blowby normally occurs through the piston ring gaps, and under the static piston conditions, any oil in the piston ring gaps is likely to be removed by the blowby gases flowing into the crankcase.

The experimental results shown in Table 3.2 were obtained without any attempt to create an artificial oil layer on the cylinder liner. This can be justified because:

(a) The lack of oil does not alter the static flowrate.

(b) The film consistency would be difficult to quantify between tests, and any oil in the ring gaps would be forced out of the way by the moving gases.

(c) Oil in the top ring zone is highly degraded and is difficult to reproduce (see Chapter 4).

The wear at BDC occurs under similar conditions to that at TDC, because the piston experiences the same change in velocity, similar breakdown in controlled lubrication and breakdown in piston ring as that which occurs at TDC. The amount of wear is not as much as that at TDC, however, because the cylinder pressure and temperature are much reduced at BDC, and the liner is extensively lubricated by splash from the sump. No measurements were taken at BDC, because, pressurisation of the combustion chamber was not possible, as the valves were open at BDC, and no simple method of overriding the valve mechanism could be devised (Figs 2.7 and 2.8). This is unlikely to affect the computer program because:

(a) The blowby flow decreases as the cylinder pressure decreases. This occurs as the piston moves towards BDC on the power stroke.

(b) The blowby flow is likely to be very small after the exhaust valve has opened on the power stroke, because the combustion gases would leave through the exhaust port in preference to the more restrictive route through the piston ring pack.

It should also be noted that these measurements were taken with a cold engine, where none of the engine components had expanded to their normal operating temperatures. Any attempt to heat the engine

was considered impractical, firstly because of the technical difficulty of sustaining the temperatures required, and secondly because it would be unlikely to re-create the temperature distribution that the cylinder components experience (the heat flow, from the heater into the engine block, would be in the reverse direction to that occurring whilst the engine is running).

Likewise, the piston was stationary and it was assumed that the piston rings were forced hard against the cylinder wall by the applied pressure from the combustion chamber. This assumption is vindicated by the consistency of the results with no outlying readings occurring as the result of incomplete piston ring sealing. In order to ensure consistent location of the rings, the piston was always positioned by upward movement prior to position measurement. This procedure was intended to locate the piston rings on the base of the ring grooves. The quality of piston ring seal obtained is one of the major advantages of this technique, as the measured flowrates should be derived only from blowby through the ring gaps with no contribution from ring flutter and independent of the ability of the rings to follow the cylinder wall whilst in motion.

The gas used was compressed air at ambient temperatures. It has a composition which approaches that of the inlet gases, but has a density and viscosity which is different to the hot combustion gases.

3.2.3 Curve fitting of Static Blowby Data.

The results obtained from the Static Piston experiment represent only part of the possible combinations of pressure, crank-angle and blowby flowrate that could be obtained by this technique. A simple curve fit routine has been employed to aid data handling. The measurements are co-ordinate points on a 3-dimensional surface, each engine having its own surface. These surfaces can be mathematically described by their appropriate equations. The curve fit technique can thus be used to generate a simplified source of data for use in the calculations (an equation as opposed to a data matrix).

The equations were derived from the experimental measurements by curve-fitting the data obtained from each engine. The results in Table 3.2 were curve fitted using a short program on the PET microcomputer. The program used an equation of the type:

$$F = P\ (a + bP)\ EXP\ (-\ cA) \qquad (3.2)$$

where F = flowrate (10^{-4} m^3s^{-1})
P = pressure (Absolute Bar)
A = ABS [0 - 360] (degrees)

(a,b,c) are the function coefficients derived from the data supplied.

This equation was used only because it approximated to the expected shape of the 3-Dimensional surface obtained by plotting crank angle and applied pressure against blowby flowrate. The programme uses A as a function of crank angle 0, recognising that the position of the piston is symmetrical about TDC (TDC = 360^{o} in the combustion cycle). The curve fit uses a quadrilateral function of pressure, where the constant in the quadrilateral equals zero because there is no flow at zero pressure. This is multiplied against a negative exponential of the angle derivative, A, reflecting the anticipated reduction in flow away from TDC. A manual check was made of the accuracy of the curve fit routine, using the measurements from each engine. The resulting surfaces are shown in Fig 3.3. The curve fit program explanation and listing appears in Appendix 1.

The resulting equations provide a mathematical relationship between piston position, pressure and static piston flows for each engine. The range of the static piston pressure measurements, and therefore the extrapolated limits of the derived equations, are beyond those measured on the running engines. Hence, each engine has one equation for the pressure-crank angle data obtained in section 3.3 to calculate the incremental blowby curves for all operating conditions.

3.3 Measurement of Pressure-Crank angle diagrams.

3.3.1 Experimental

The next stage of data aquisition was to obtain the input pressure and crank angle information, from which a calculated blowby could be derived. The measurement of pressure-crank angle diagrams is a well established technique (Ref 3.5).

The cylinder head pressure was measured as before (section 3.2), with the pressure transducer positioned directly above the piston. A timing plate was clamped to the crankshaft. This circular steel disc had five notches machined into the outer rim at 10^{o} intervals, which, when picked up by a magnetic probe aligned near to the rim, were used to indicate the exact piston position. The position of the notches in the timing plate were calibrated against the peak pressure recorded as the engine was motored, assuming that this pressure corresponded to TDC. The timing plate could be used to measure both the position of TDC, and also to calibrate the crank angle scale on the X axis of the oscilloscope. The magnetic probe and pressure transducer signals were fed into the two channels of the Gould storage oscilloscope, and the screen display was automatically recorded by the Gould plotter. The oscilloscope produced data which directly related crank angle to cylinder pressure, with the two traces superimposed to allow easy annotation (Fig 3.4, 3.5). These diagrams were produced for engines A, B and D at a wide range of loads (Figs 3.6, 3.7, 3.8).

3.3.2 Calculations

Although the transducer calibration curve gives the linear variation in output voltage with pressure, the pressure-crank angle diagrams have no indication of absolute pressure. This is because the storage oscilloscope displayed the pressure-crank angle output from the transducer, but the position of the Y axis gain had to be adjusted to display the curves, with no measurement of the offset

voltage. It is therefore necessary to adopt a base pressure. It was assumed that the pressure of the system is atmospheric at Inlet Valve Closure (IVC) and the calibrated readings were based on this point. This assumption can be justified by two main factors:

(a) The calculated value for IVC is 227 ^{o}C (see below) which is only 47 ^{o}C beyond BDC. The piston has just passed through BDC where its vertical movement is relatively little (IVC = 8.35 mm above the BDC position), allowing the pressure in the combustion chamber to stabilise.

(b) IVC is the point at which the combustion chamber becomes an isolated system.

The exact angle of IVC was unobtainable from the manufacturers and it was necessary to measure the angle on the test engine. The inlet valve tappet clearance of engine B was set at the recommended 0.006 inch (cold) and, with the cylinder head removed, a dial gauge was positioned to touch the centre of the inlet valve. The engine was positioned beyond IVC on the compression stroke and the crankshaft was rotated backwards until the dial moved, indicating that the valve was moving. The exact position of IVC was determined to better than 0.001 inch of valve lift. The height of the piston crown was measured at this point by using a second depth gauge inserted into the pressure transducer orifice (see Section 3.2.1). This was repeated several times to establish the piston position at IVC. The height of the piston at TDC was also measured, and these values were used in Eqn 3.1 to determine the crank angle at IVC.

The position of IVC was marked onto all the pressure-crank angle diagrams obtained from the storage oscilloscope, and the pressure at this point was assumed to be atmospheric. The transducer calibration curve was used to obtain the pressures at all other points on the graph, and pressure data was taken for points at 2^{o} intervals between 300^{o} and 442^{o} of crank angle. This data was stored on computer disk for subsequent use in the blowby calculation.

It should be noted that great care was taken to ensure that the pressure traces recorded were representative samples. The oscilloscope had a storage facility allowing user comparison of curves from individual firing strokes of the single cylinder engine whilst it was running. There was some variation in the peak pressure values observed between cycles, especially at very low or high loads.

3.4 Calculation of Blowby Flowrate and Composition.

3.4.1 Flowrate Calculation

The Blowby flowrate has been calculated using the variants of equation 3.2 for each engine, obtained from the curve fits from the Static Piston experiment and input data from the pressure-crank angle diagrams. The 3-dimensional surfaces from Section 3.3 (Fig 3.3) have been used to give flow increments for every 2^{o} of crank angle of the combustion cycle. The purpose of obtaining a blowby simuation in incremental form is that it allows analysis of the blowby process both during the combustion cycle itself, and also in summarized form to compare with measured flowrates.

The program listing appears in Appendix 1. It is presented together with a line-by-line description of the program flow. The same program calculates both the blowby flow and the blowby composition, using common input data and calculation subroutines. A glossary of symbols is also included.

Equation 3.2 can be used to generate blowby flow increments for any combination of combustion cylinder pressure, and crank angle. Using the form of the equation specific to each engine (with variables from Table 3.3), each 2^{o} incremental point from a pressure-crank angle diagram can be used to generate the corresponding incremental flow as a solution of equation 3.2. By solving the equation for all points on the pressure-crank angle diagram, the blowby flow increments for the power stroke are generated. This is equivalent

to tracing across the surface of Fig 3.3. The values of blowby flow, pressure and crank angle are stored in arrays, to be displayed using the PD4 plotter (see Appendix 1). In order to analyse the blowby flow change during the combustion cycle, the flow is plotted against crank angle. Typical blowby increment curves, derived from this technique, are shown in Figs 3.9, 3.10, and 3.11. As expected, these curves show a rapid increase in blowby flowrate as the piston approaches the TDC position, corresponding with high cylinder pressures and high bore wear.

An overall flowrate is derived by the summation of the increments, subsequently divided by the cycle time (Eqn 3.3). Such a summation assumes that the blowby occurring outside the region 300^{o} to 442^{o} on the compression stroke is negligible. Fig 3.12 shows the variation in computed crankcase flowrate with load for the three engines, and compares them with the experimental flowrates measured in the work in Chapter 2 (Fig 2.15).

$$\text{Blowby flow } (m^3s^{-1}) = [\sum(\text{flow increments})] \times [N/120] \qquad (3.3)$$

Several observations can be drawn from these derived flowrates. The Static Piston experiment, from which these flowrates were originated, can be considered to be a measure of piston ring blowby through the piston ring gaps. As such, it is only a component of the dynamic blowby mechanism. The magnitude of the calculated flowrates obtained are close to those measured. For engine B (the low wear engine), the agreement is very good, both the trend and magnitude of the computed curve (within 10^{-5} m^3s^{-1}) confirm that the blowby mechanism for this engine is through the piston ring gaps only. For engines A (new) the values are three times, and for D (worn) the values are approximately twice those measured. Engine A has a similar curve shape for the computed and measured blowby flow, whereas engine D has a computed curve that does not reflect the large increase in measured flowrate observed at higher loads (Fig 3.12). The result for engine A also shows that the mechanism of blowby is through the ring gaps only. The result for Engine D shows

that there are two mechanisms, ring gap blowby at low loads, and an additional mechanism at high loads.

The curves show that the Static Piston experiment is a reasonable approximation of blowby flow when compared with a running engine. The difference can be examined in terms of the limitations of both the experiment and the calculation. Physically, the difference between the Static Piston experiment and the running engine has been summarised in Section 3.2.2. For any given increment in the cycle, the effect of engine motion has been minimised by the division of the combustion process into such small components. However, the effect of lubrication on the attitude of the piston ring throughout the cycle may be important. Any such effect must be slight, because the order of magnitude of the blowby flow has been calculated for all of the engines.

The important feature of the blowby flow results is the shape of the curves in Fig 3.12, and their analysis during the combustion cycle itself in Fig 3.9, 3.10 and 3.11. The computed crankcase flowrates show a gentle increase with increasing load. This corresponds to the difference in areas between the blowby increment curves, which in turn are due to the differences in cylinder pressures experienced at these loads (Figs 3.6, 3.7, 3.8). As Figs 3.9, 3.10 and 3.11 show, the areas under the increment curves only diverge significantly near to TDC, and it is at this point in the combustion cycle that any difference in blowby flowrate is determined. For engines A and B, the shape of the calculated curve closely resembles that of the measured curve. This suggests that for an unworn engine, the mechanism of blowby is only through the piston ring gap, throughout the load range. However, for engine D, Fig 3.12 clearly shows that, with increasing load and cylinder pressure, the blowby through the ring gaps, as represented by the calculated results, increases slightly, whilst in practice the measured flowrate increases substantially. This feature can be explained in two ways. There are only five blowby increment curves for engine D, which give calculated blowby results with more apparent scatter than those for

engines A and B. The derived points could be insufficient to provide a clear picture of the overall curve. However, as already indicated, mathematically, the difference between the calculated flowrates for any given engine, is proportional to the difference in the area under the pressure-crank angle curves obtained from that engine at around TDC. The divergence required to provide the measured curve shape has not been seen in practice. Therefore, it is unlikely that a pure combustion pressure effect, as calculated from the Static Piston data, can explain the high flowrate at the high loads on engine D. This indicates that an additional mechanism (piston ring seal breakdown) is supplementing the ring gap blowby at higher loads. In comparing the curves from the different engines, it is clear that the supplementary mechanism occurs under different loads for differing states of engine wear. For the newer engines, the measured blowby curves are similar to the computed curves. For engine D there is some similarity at lower load with a transition point followed by deviation of the measured curve from the computed curve shape as the load increases.

It is important to note that both the experimental results from Chapter 2 and the calculation of blowby flow indicate that there is more than one mechanism of blowby occurring in the engines at higher loads. In the calculation of blowby composition, such a complexity must be taken into account.

3.4.2 Calculation of Blowby Composition

In order to extend the calculations to derive blowby composition, several assumptions have to be made. The crankcase gas is formed from both burnt and unburnt fuel mixture as discussed in Section 2.5. The composition of the blowby entering the crankcase during the combustion cycle, is obtained by dividing the combustion chamber into two sections based on the position of the flame front, with unburnt charge in front of the flame, and combustion products behind the flame. In this approach, the flame front is considered to be a transitional item with finite width, which moves rapidly across the

combustion chamber. As the Villiers engine is a side valve design with an offset spark plug situated in the cylinder head directly above the two valves, the flame front will approach the cylinder bore and travel across the piston crown from one side. The program can be greatly simplified by using a cylindrical combustion chamber with the "ignition point" (I) at the top of the cylinder wall. The calculation of the combustion process is thereby confined to a cylindrical chamber. This simplification can be justified on the basis that the important region in blowby gas formation is the piston and top ring zone, and not the remote areas of the side valve head.

The composition of each of the blowby increments is derived from an extension of the flowrate calculations in Section 3.4.1. The blowby increment curves (Figs 3.9, 3.10, 3.11) are divided into pre- and post- combustion curves based on the relative position of the flame front. This divides the piston crown, and the ring pack directly below it, into two sections, giving the two component compositions to the overall blowby. The assumptions used here are that:

(a) The flame front passing across the piston crown is spherical with its centre at the ignition point (I), and travels with turbulent velocity which is assumed to be constant (the correction for the flame propagation prior to speed stabilisation is given in (b) below). The flame velocity was measured experimentally.

(b) The flame propagation delay (pre-turbulent combustion) and time for the flame to travel from the spark (real position) to point I (imaginary position) are accounted for by a delay in the combustion program ignition (See Fig 3.13).

(c) Combustion is assumed to be completed within the flame front which has a negligible depth. This assumption is made for the convenience of calculating the exact division of the piston crown by the flame front. In practice, the resolution of the

flame position is compromised by the 2^{o} of crank angle between each calculation.

(d) The inlet and exhaust gas compositions measured in the manifolds are taken to be equivalent to the gas mixture present in the combustion chamber before and after the flame front respectively (See Figs 2.13, 2.14). These are referred to as pre- and post-combustion gases within the combustion chamber.

(e) There is no correction for a quench zone component, all gases passing through the ring pack are derived from pre- or post-combustion gases as defined in (d) above.

(f) The pressure either side of the flame front is equal, and that both pre- and post-combustion gases have the same ability to pass the piston ring pack.

(g) The location of the top ring gap is not important in the determination of overall composition. Tests were conducted to discover the mobility of the rings around their grooves, and it was found that the orientation of the rings was completely random after running. The composition results assume complete mobility of the top ring, and hence there is no correction for ring gap position.

The calculations advance the flame front position for each increment during the combustion cycle. It was therefore necessary to measure the flame speed inside the combustion chamber. This was measured using ionization gaps installed into the cylinder head, the output from which were fed into the Gould oscilloscope (Fig 3.14). The flame front contains high temperature ions and free radicals, which allow current to pass across the ionization gaps. The separation of the ionization peaks (as time on the oscilloscope's X axis) combined with the measured separation of the ionization probes gave the flame speed of 36 ms^{-1} over a range of loads up to 2 kW.

The mathematical basis is that of a simplified cylindrical combustion chamber with an ignition source (I) at the top of the cylinder liner sidewall (Fig 3.13). The flame front progress is calculated for each 2^{o} of crank angle, corresponding to the pressure-crank angle diagrams and the blowby increment simulation. The object in the calculation is to divide the blowby up into two component parts from either side of the flame front, corresponding to the amount of burnt and unburnt combustion mixture passing by the ring pack. The program achieves this by:

(a) Testing to see if the flame front has reached the piston crown directly below the ignition point (I) (Fig 3.13). If this has not occurred then all the blowby will be unburnt gas.

The ignition point is a fixed distance from the real ignition source - the spark plug. At an assumed constant flame speed, the flame will reach the top of the cylinder at the same point in the combustion cycle, independent of load. After this delay, flame initiation occurs from point I, with the flame travelling radially away from I into the cylinder bore. The increase in flame radius per 2^{o} increment is constant (Eqn 3.4) and the total flame radius will be the sum of all increments (Eqn 3.5).

Flame radius from ignition point (I).

$$\text{Radial increase per increment } (FR_i) = (36 \times 60)/(3000 \times 180) \qquad (3.4)$$

where Engine speed = 3000 rpm
Flame speed = 36 $m^3 s^{-1}$

$$\text{Flame Radius (FR)} = \sum_{i}^{o} (FR_i) \qquad (3.5)$$

As the flame front expands towards the piston crown, the piston moves upwards, compressing the unburnt gas mixture. The position of the piston for any crank angle can be calculated using equation 3.1 (see Fig 3.2) as the solution to the quadratic (Eqn 3.7). This

piston crown position is relative to the crankshaft centreline, and can be used to derive the distance between the piston crown and the top of the cylinder bore (Eqn 3.8).

Piston crown position

For any crank angle θ, from the cosine rule

$$2sx\cos\theta = x^2 + s^2 - L^2 \qquad \text{(From 3.1)}$$

Rearranging $$0 = x^2 - 2s\cos\theta x + (s^2 - L^2) \qquad (3.6)$$

Solving quadratic $$x = s\cos\theta \pm \sqrt{s^2(\cos^2\theta - 1) + L^2} \qquad (3.7)$$

Dist to top of stroke $= (L + s) - x$

Dist to top of bore $= (L + s) - x + j = IX$

$$IX = L + s(1 - \cos 0) - \sqrt{L^2 + s^2(\cos^2\theta - 1)} + j \qquad (3.8)$$

where θ = crank angle
s = stroke/2
L = con rod length
j = distance between TDC and top of bore (3 mm)

The flame front will reach the piston crown initially at the point (X) directly below the ignition point (I). Until IX = FR, all the blowby is assumed to be unburnt fuel mixture (see Fig 3.13).

(b) Calculating the flame front's progress across the piston crown, thereby dividing the piston circumference into two parts. This corresponds to the fractions of burnt and unburnt gases combining to form the blowby.

As the flame spreads across the piston crown, it engulfs an area which can be represented mathematically as part of the base of a cone (Fig 3.13). At any stage in the combustion cycle, the engulfed volume is considered to contain burnt gases and the remainder is, as yet unburnt. From simple geometry,

At any stage $FR = IY = IA = IB$ (3.9)

Also $XY = \sqrt{(FR)^2 - (IX)^2}$ (3.10)

And $XY = XA = XB$ (3.11)

Therefore $\sin \phi = \dfrac{\sqrt{(FR)^2 - (IX)^2}}{2CB}$ (3.12)

Fraction engulfed $= 4\phi/360$ (3.13)

Fraction unburnt $= (360 - 4\phi)/360$ (3.14)

For each 2^{o} increment, the piston circumference is divided up in this manner until the flame front has engulfed the whole piston crown.

(c) Testing to see if the flame front has traversed the piston crown to the point directly opposite the point of initial flame contact, after which, all the blowby is assumed to be burnt gas.

The piston crown is completely engulfed when the flame radius has reached the point diagonally opposite to the ignition point (I). This occurs when the base of the cone is equal to the piston diameter.

Piston is engulfed when $2CX = \sqrt{(FR)^2 - (IX)^2}$ (3.15)

The resultant two fractions, obtained for each blowby increment from the flowrate simulation in Section 3.4.1, are used to divide up the

blowby in that increment. The composition of the blowby for each 2^{o} increment is determined by multiplying the corresponding fraction with the composition of the pre- and post-combustion gases. The composition of the crankcase gas is the sum of the composition of all the increments. This calculation uses the measured compositions of the inlet and exhaust gas samples from Figs 2.13 and 2.14 to represent the pre- and post-combustion elements of the summation.

This approach allows an examination of both the composition of the blowby across a typical combustion cycle (Fig 3.15, 3.16, 3.17) and the summarized compositions (Fig 3.18). As expected, in the early stages prior to and for some time after ignition, the blowby gas is all unburnt fuel mixture, because the flame front has not reached the piston crown. Within the region of the power stroke between 340^{o} and 410^{o} the flame front crosses the piston crown, and the blowby gas is a combination of pre- and post-combustion mixture. Beyond 410^{o} the blowby gas is all post-combustion mixture.

The computer program stores the fraction of burnt and unburnt gas from each increment, and sums the fractions over the whole combustion cycle. The product of this calculation is the overall fraction of gas flowing through the ring pack from either side of the flame front (equations 3.16, 3.17). The post-combustion fraction CF(E) is then adjusted to remove the effect of the water vapour, which is present in the ring pack as a gas, but which is condensed from the crankcase gases prior to analysis. The correction is derived from the stoichiometric combustion as given by equation 2.9. The correction is given in equation 3.18, and then the composition of the crankcase gas is derived from equation 3.19 by the summation of these increments. The inlet and exhaust gas compositions used in this calculation are shown in Fig 2.13 and 2.14. The resulting blowby composition curve is shown in Fig 3.18.

$$(F(I)) \;/\; (F(I) + F(E)) = CF(I) \qquad (3.16)$$

$$(F(E)) \;/\; (F(I) + F(E)) = CF(E) \qquad (3.17)$$

$$CF(E)\ \text{corrected} = CF(E) * 0.810 \qquad (3.18)$$

$$CF(I) \times \text{Inlet comp} + CF(E) \times \text{Exh comp} = \text{Blowby comp} \qquad (3.19)$$

where F(I) = Pre combustion incremental fraction
F(E) = Post combustion incremental fraction
CF(I) = Total cycle pre combustion fraction
CF(E) = Total cycle post combustion fraction

Equation 3.19 can be applied to any gas present in both the inlet and exhaust gas samples. The result of this calculation gives a methane content of the blowby which is very close to that measured at low load. However, as the load increases the measured methane content rises rapidly, but the calculated content varies little with load. This result parallels that of blowby flowrate, where the measured results diverge from the calculated results. This discrepancy can be explained in a similar manner for both parameters. In order for the calculations to generate a wide change in composition with load, the incremental fractions must be significantly different. As Figs 3.15, 3.16, and 3.17 show, this is not the case because the way in which the flame front crosses the piston is similar for all loads and the blowby flow increment curves are similar for all loads.

3.5 Discussion of the computed results.

The measurement of blowby flowrate in Chapter 2 identified three proposed mechanisms of piston blowby.

(a) Blowby through the piston ring gaps.

(b) Blowby around the piston rings as they move away from the sealing surface on the piston groove as the piston passes through TDC.

(c) Blowby between the piston ring outer face and the cylinder liner as a result of the breakdown of the piston ring seal.

The possibility of any indirect technique of gas transport, such as that of gases dissolved in the oil, will not significantly contribute towards the quantity and composition of blowby measured for each engine.

The Static Piston experiment was devised to measure piston ring gap blowby, with the major assumptions that the applied pressure was sufficient to cause the piston ring to seal and that the properties of compressed air would parallel those of the blowby gases. As such this technique examined the mechanism which is considered in the literature to be the major source of piston ring blowby.

The flow and composition results derived from the calculations yield good agreement in magnitude. However, the trend of both parameters across the load range is not representative of the increase measured in practice. In the analysis of this feature, it is important to recognise the limitations of the calculations in its initial form, and to evaluate the information gained from these results.

As discussed in section 3.4.1 the blowby flow calculations yielded blowby flow results close to those measured, the approximation being particularly good for engine B. However, the change in flowrate with load for engine D is not calculated with confidence. The proposed explanation for this discrepancy is based on the nature of the pressure dependence of the calculation. A comparison of the computed curve shapes in Fig 3.12, and the measured results displayed in Fig 2.30 show good agreement. Both indicate that blowby flowrate is proportional to cylinder pressure, except for engine D at high loads.

The calculated flowrate is derived from equation 3.2 (Fig 3.3). Throughout the combustion cycle, the increase in flowrate with load for any given increment is dependent on the increase in pressure with load. In summing the increments across the combustion cycle, the overall blowby flowrate is dependent on the area under the pressure-crank angle curves. As a comparison of the pressure curves in Figs 3.6, 3.7 and 3.8, and the flowrate curves in Figs 3.9, 3.10 and 3.11 show, the difference in areas under all the curves, which increase with load, is not large enough to provide the measured increase in flowrate. The conclusions that can be reached are:

(a) The mechanism of blowby as measured by the Static Piston experiment (blowby through piston ring gaps) can be used to approximate the dynamic flowrate for all the engines, but only provides the trend with load for low wear engines.

(b) The blowby through the ring gaps for any engine varies with cylinder pressure across the load range.

(c) The blowby in low wear engines occurs through the piston ring gaps, and not as a result of ring seal breakdown.

(d) There must be another mechanism of blowby occurring at high wear and/or high load. The proposed mechanism is piston ring seal breakdown.

The extension of the calculations to introduce piston ring seal breakdown must involve a consideration of both the potential mechanisms of piston ring seal failure, the mechanisms of gas transfer within the ring pack, and also the conclusions drawn from the initial derivation of blowby composition.

In proposing a rationale for piston ring seal breakdown, it is important to understand the sealing mechanism. There are two main types of piston ring, compression and oil control. The Villiers engine has three identical compression rings and one oil control

ring. The top compression ring is the most important ring in the sealing of the ring pack because it is the ring directly in contact with the pressure from the combustion chamber.

The piston ring is radially compressed to ensure that there is always an outwards force by the piston ring onto the liner surface. The ring is held in a piston groove which is slightly oversized, but which prevents excessive twisting of the piston ring during vertical motion of the piston and ring assembly. The ring experiences forces in the direction of piston travel related to the movement of the piston, and also due to the difference between the combustion chamber pressure and the pressure below the ring sealing face.

During the compression stroke, the piston is moving towards the combustion chamber, compressing the inlet fuel mixture. The piston ring is firmly seated onto the base of the groove, and the combination of the outward force from the ring itself, and the high pressure of the gases above and behind it, force the ring onto the cylinder wall (Fig 3.19). Friction and wear as a result of ring to liner contact is prevented because the ring running face is lubricated and supported by hydrodynamic oil lubrication (see section 4.1.2 and Fig 4.1). The combustion chamber pressure is the major sealing force, because it is the pressure drop across the piston ring that holds the ring onto the base of the groove. In high speed engines, the cycle time is very short, allowing only a small amount of blowby through the piston ring gaps per cycle. As a result, there is a large pressure drop across the top ring, with a relatively small drop across the rest of the ring pack.

As the piston approaches and passes through TDC, the movement of the piston slows rapidly, and reverses direction. The ring experiences a decrease in upward force imparted by the base of the piston groove, and an increase in friction with the cylinder liner as the lubrication begins to break down. These combine to upset the seal between the ring and the base of the groove. As the piston passes through TDC, the seal can be broken momentarily if the pressure from

the combustion chamber is insufficient to hold the ring onto the groove base. This breakdown normally occurs only on the exhaust stroke, where the combustion chamber pressure is low. On the compression and power strokes, the combustion chamber pressure is high and ring flutter is less likely. Beyond TDC on the power stroke, any ring flutter will cease as the seal is rapidly reinstated by the combustion chamber pressure.

This sealing mechanism is further complicated if lubrication is poor (boundary conditions or worse), or if piston grooves or cylinder liner is worn. These combine to reduce the effectiveness of the seal at both the groove base and the liner wall. Under these conditions, the pressure of the gases above the ring cannot maintain the seal integrity, and blowby occurs, particularly as the piston approaches TDC.

From this analysis of piston ring seal breakdown, there are two major failure modes:

(a) Ring flutter as the piston passes through TDC. This feature is usually prevented from occurring during the power stroke by the correct design of the engine. The duration of the loss of the seal and the quantity of blowby passing through the ring pack is related to the combustion chamber pressure and engine wear. This mechanism is only likely to contribute a small constant amount of blowby across the load range, because during the exhaust stroke the combustion chamber pressure is low and the frequency of the breakdown is dependent on the motion of the piston.

(b) Ring seal breakdown as a result of component fatigue and wear. This is likely to occur near to TDC at high pressures. This mode includes ring flutter on the power stroke, induced by excessive wear which becomes indistinguishable from general seal breakdown. The blowby is related to the combustion chamber pressure and the condition of the components involved.

Fig 3.18 shows that the derived composition of the blowby gas is relatively constant across the load range for all of the engines. This result has been obtained by a straight forward division of the blowby into pre- and post-combustion gases, and its derivation from a pressure-flow relationship. Several factors must be taken into account when considering a more complex approach.

The region around the top ring is likely to contain quench gases, and as the flame front crosses the piston crown, it will be quenched as it approaches the ring crevice. Therefore, no matter how the blowby passes the ring pack, quench zone gas is likely to pass into the crankcase followed by the gas from the bulk volume of the combustion chamber.

The flame front passing across the piston crown has been simulated as being of negligible width, spherical and travelling at constant velocity corresponding to well established turbulent combustion. No attempt has been made to include any effect of mixture turbulence near the flame front.

There has been no attempt to investigate the complex nature of the combustion process, or the mixture distribution within the combustion chamber. The fuel is a gas at STP, and with no atomisation required, the mixture distribution should be very good. However, the calculation of blowby composition is based on the measurements of mixture content in the inlet and exhaust manifolds. The corresponding pre- and post-combustion gases within the combustion chamber must be compared with the measured gases.

The major physical differences between the gases inside and outside the engine are those of temperature and pressure. Of these, only the combustion product, water, will be significantly affected. In the combustion chamber, the water is a gas, only condensing in cooler parts of the exhaust system, or within the crankcase. The water passing through the piston rings is derived from the post-combustion gases. In the analysis of the inlet, exhaust, and

crankcase gases, water is eliminated (a dry analysis). The correction of the calculated blowby to include the condensation of the water gives the composition of the calculated crankcase gas. This has been carried out to give the results shown in Fig 3.18. A further correction could be included to compensate for the difference between the the viscosity and density of the ambient air used in the Static Piston experiment, and that of the combustion gases within the combustion chamber. This would require the interactive feedback of the predicted composition of the blowby gases into the calculation routine.

The computer calculation is based on data obtained from the engine assembly. In comparing the computed and actual results, the following conclusions can be drawn.

(a) Both results indicate that the blowby flowrate through the piston rings is approximately constant across the load range. This blowby mechanism occurs for newer engines, and worn engines at low loads.

(b) The blowby flowrate for worn engines at higher loads includes an additional mechanism not operating at low loads.

(c) The fuel content of blowby does not occur as a simple division of the combustion chamber gases by the flame front. At higher loads the fuel content rises, indicating that larger amounts of unburnt mixture and quench zone gases are passing through the ring pack early in the combustion cycle.

The calculations are limited by the Static Piston experiment, which was designed to imitate the blowby flow in a working engine assembly. This method has produced results which confirm the postulated mechanism of blowby formation proposed in the discussion of the experimental data. An extension of the calculation routine, to include more detailed analysis of the behaviour of the gases at the ring pack, is required to further evaluate the mechanism.

References Chapter 3.

3.1 HASSAAN, H.A "An investigation into the absolute life of an Internal Combustion Engine". PhD Thesis, Leicester Polytechnic, 1983.

3.2 PAYNE J Q, SIGWORTH H W "The composition and nature of blowby and exhaust gases from passenger car engines." Proc 2nd Nat Air Poll Symp 1952 Vol 2 pp 62 - 70.

3.3 BENNET P A et al, "Reduction of air pollution by control of emission from automotive crankcases." SAE Transactions, Vol 68, pp 514 - 536.

3.4 Department of Industry Report TRD 162, Piston Ring Design 1974.

3.5 TAYLOR C.F "The Internal combustion engine in theory and practice." 2nd Ed MIT Press 1983 pp 114 - 119.

Figures Chapter 3

Tables Chapter 3

Table 3.1 Equipment used for Static Piston Experiment

Parameter	Equipment Used
Applied Pressure	Southern Instruments T 500 pressure transducer with readout unit. Voltage display by Hewlett Packard D.V.M.
Flowrate	Marconi X series and S 45 Rotameters.

Table 3.3 Static Piston Coefficients.

Engine	a	b	c
A	0.50797	-0.00965	0.00009
B	0.35010	-0.0065	0.0151
D	1.43155	-0.00612	0.02823

ENGINE A			ENGINE B			ENGINE D		
ANGLE	P	FLOW	ANGLE	P	FLOW	ANGLE	P	FLOW
360.0	6.16	2.56	360.0	4.85	1.74	360.0	7.17	7.76
	8.68	3.40		6.71	2.06		10.74	13.18
	11.38	4.15		8.33	2.31		14.40	18.39
	14.02	4.80		10.07	2.63		18.09	23.16
	16.62	5.58		11.97	2.99		21.76	27.29
	19.22	6.14		13.76	3.27		25.46	30.97
372.7	6.01	2.5		15.49	3.53	375.9	10.68	7.76
	8.69	3.38		17.14	3.79		14.46	10.58
	11.29	4.11		20.66	4.34		18.06	12.96
	13.96	4.81		24.18	4.83		21.77	14.70
	16.51	5.46	383.8	10.7	1.95		25.46	16.22
	19.10	6.11		12.62	2.11	386.2	10.35	5.59
383.6	4.97	1.98		14.37	2.29		14.03	8.41
	6.2	2.34		16.25	2.44		17.74	10.14
	8.75	3.15		18.24	2.68		21.30	11.66
	11.39	3.85		21.8	2.89		25.21	13.18
	14.05	4.55		25.61	3.09	399.5	3.31	1.61
	16.55	5.20	397.9	12.24	1.85		4.85	2.00
	19.17	5.88		14.01	1.98		6.57	2.44
391.5	4.64	1.95		15.83	2.13		8.28	3.02
	6.16	2.31		17.58	2.26		9.78	3.46
	8.78	3.12		19.65	2.42		11.51	3.85
	11.32	3.8	408.9	13.44	1.85		13.23	4.26
	13.97	4.47				404.4	4.9	2.05
	16.52	5.15					6.68	2.16
	19.09	5.82					8.29	2.63
397.8	4.93	1.95					10.05	3.15
	6.23	2.39					11.71	3.51
	8.75	3.17					13.35	3.90
	11.31	3.85				409.8	4.76	2.18
	14.06	4.68					6.44	2.21
409.0	4.93	2.08					8.21	2.78
	6.14	2.37					9.95	3.22
	7.41	2.81					11.49	3.61
	8.75	3.3					13.10	3.93
	10.07	3.72						
	11.31	4.00						
438.6	4.92	2.03						
	6.14	2.42						
	7.39	2.89						
	8.66	3.28						

Angle: Deg A.T.D.C
Pressure: Absolute Bar
Flow: 10-4 m3 s-1

Table 3.2 Static Piston experimental results

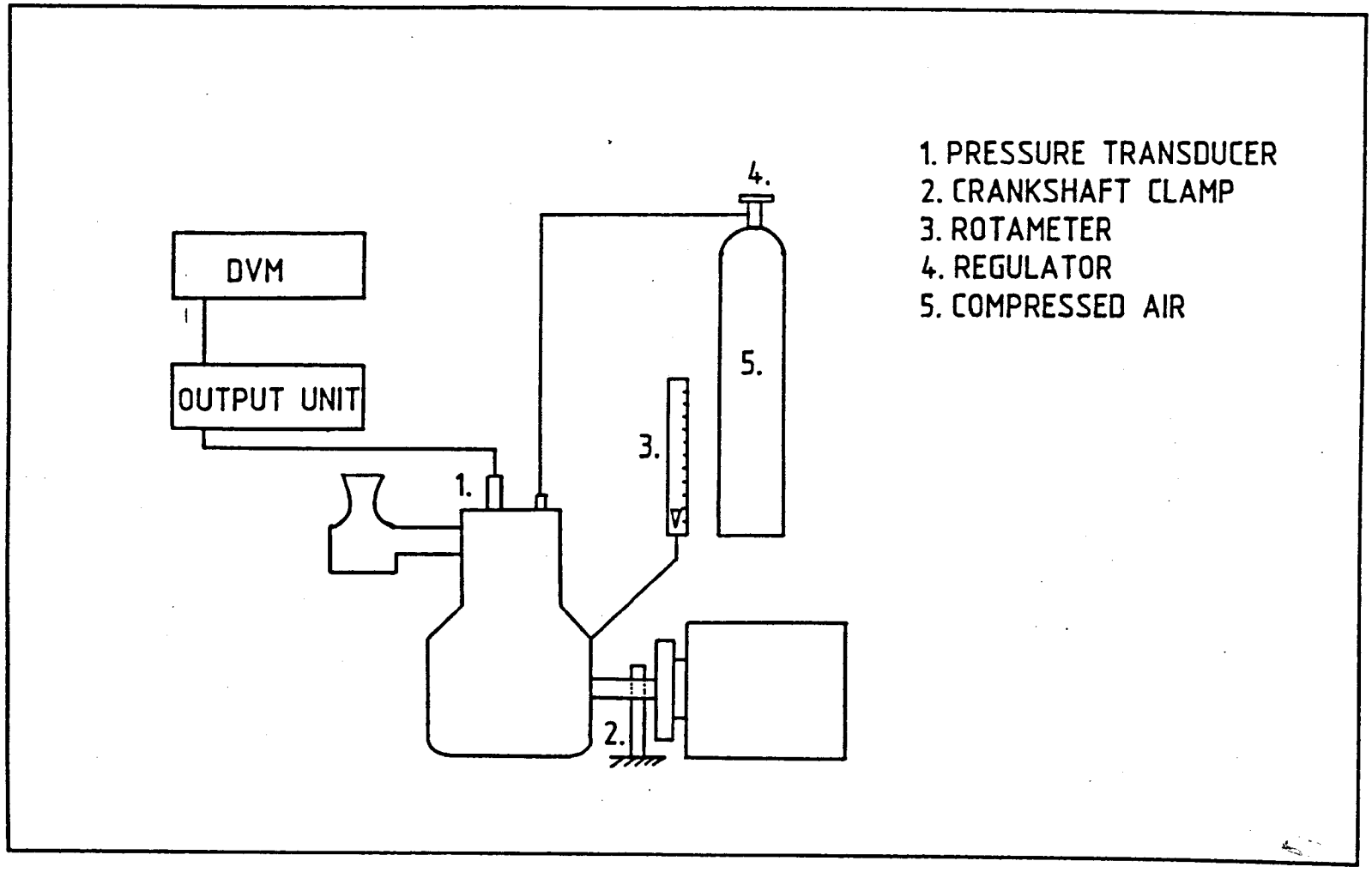

FIG 3.1 DIAGRAM OF THE STATIC PISTON FLOW APPARATUS

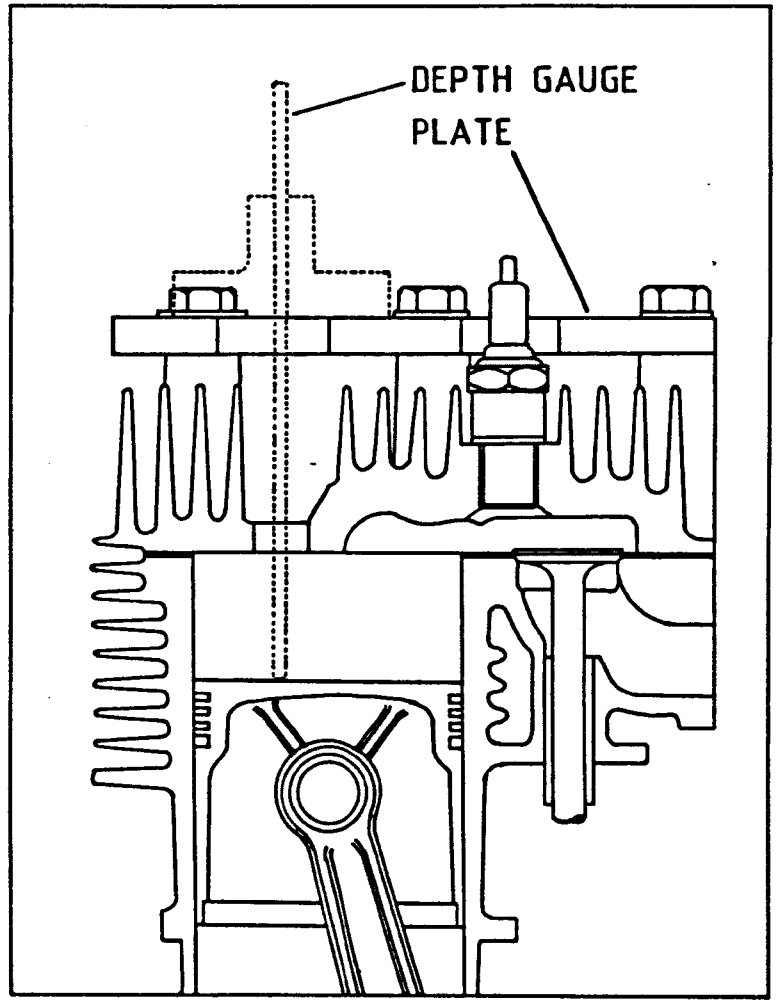

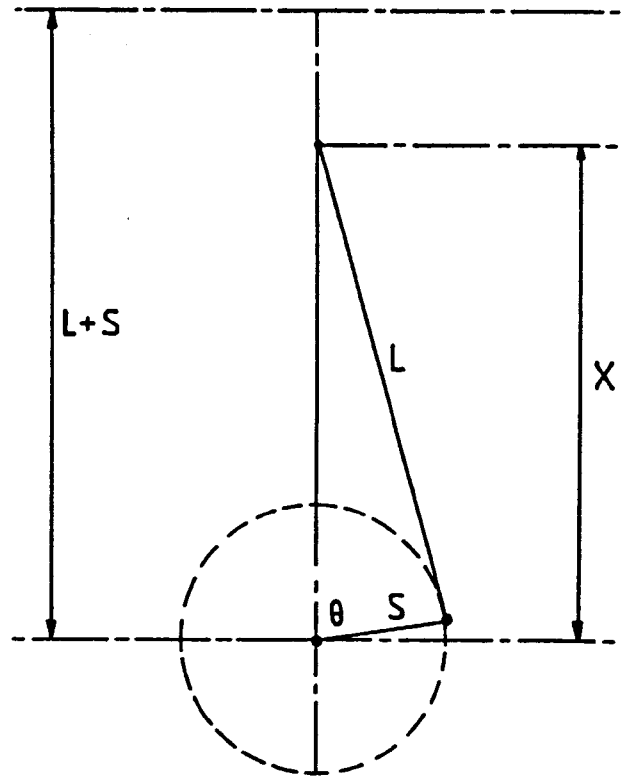

$$\cos\theta = X^2 + S^2 - L^2/2SX$$

FIG 3.2 DIAGRAM OF PISTON POSITION MEASUREMENT

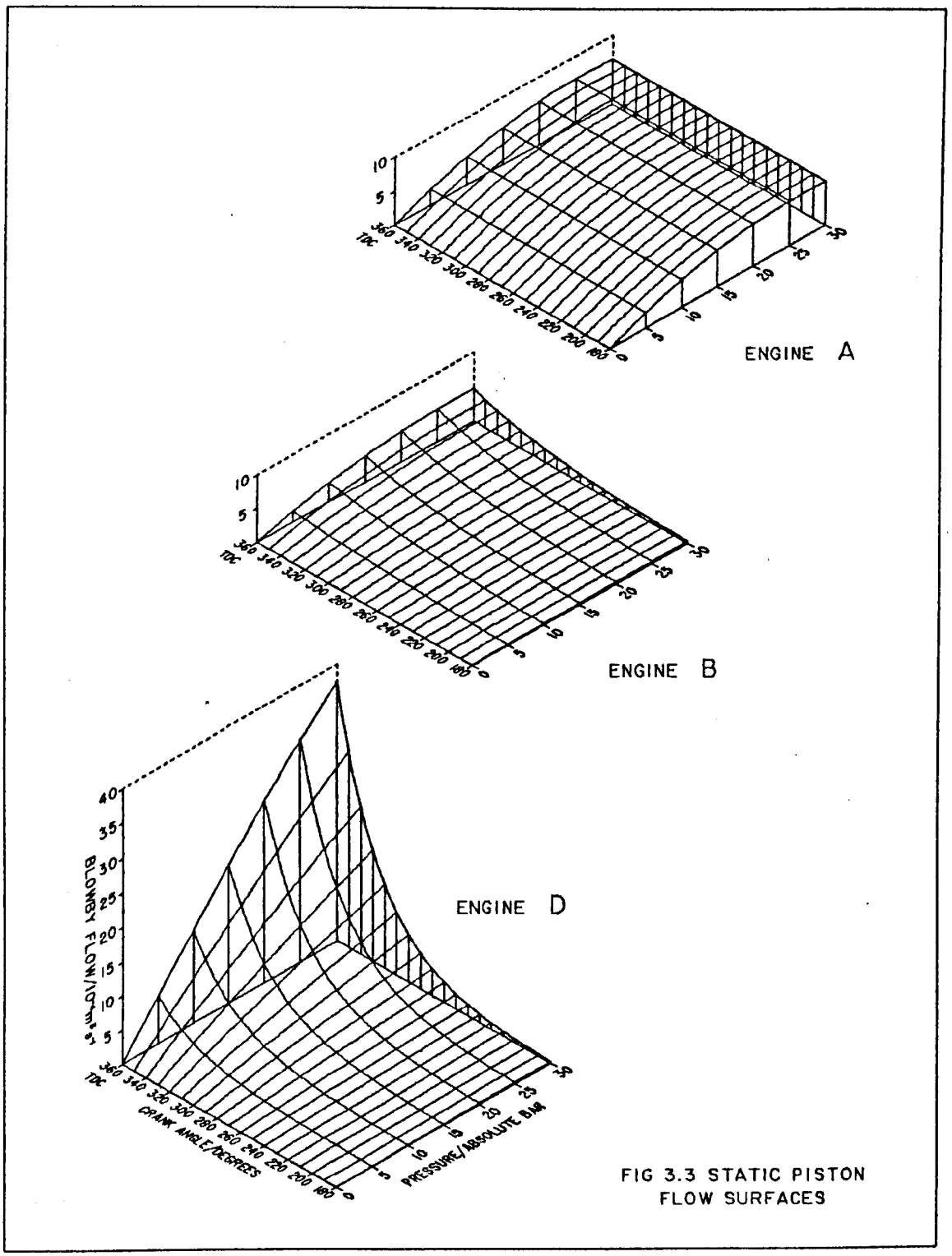

FIG 3.3 STATIC PISTON FLOW SURFACES

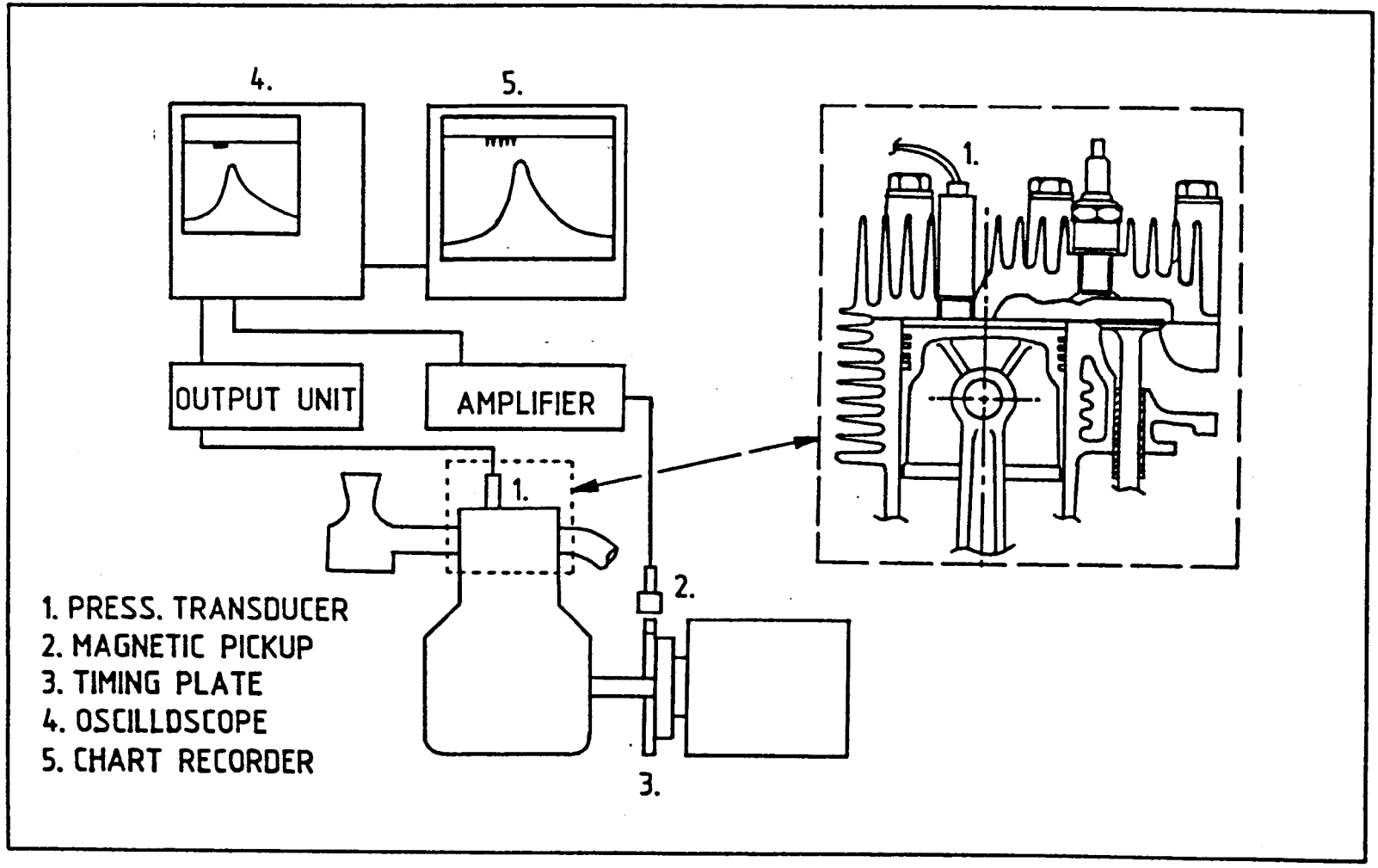

FIG 3.4 DIAGRAM OF THE PRESSURE - CRANK ANGLE APPARATUS

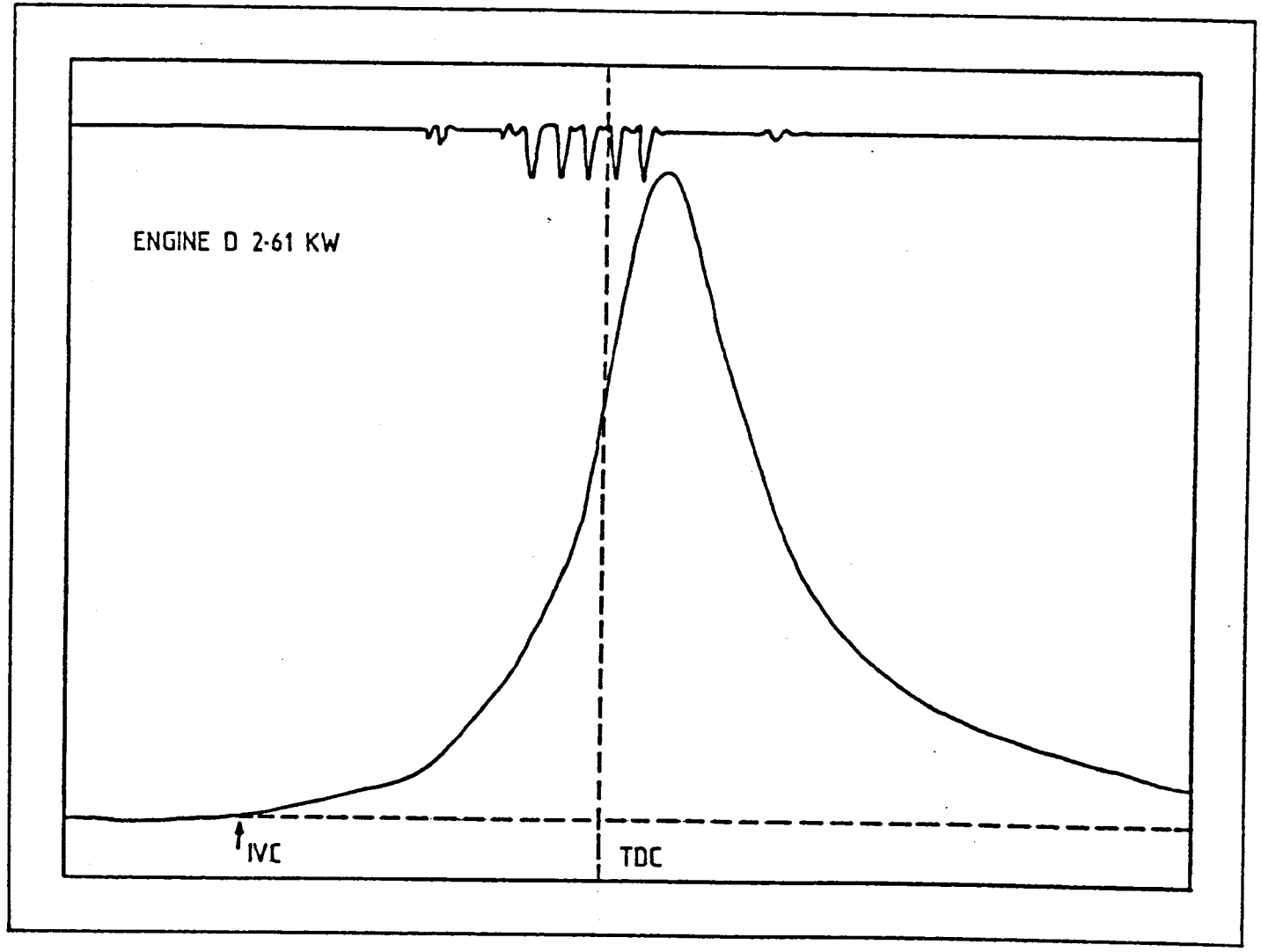

FIG 3.5 DIAGRAM OF OSCILLOSCOPE DISPLAY

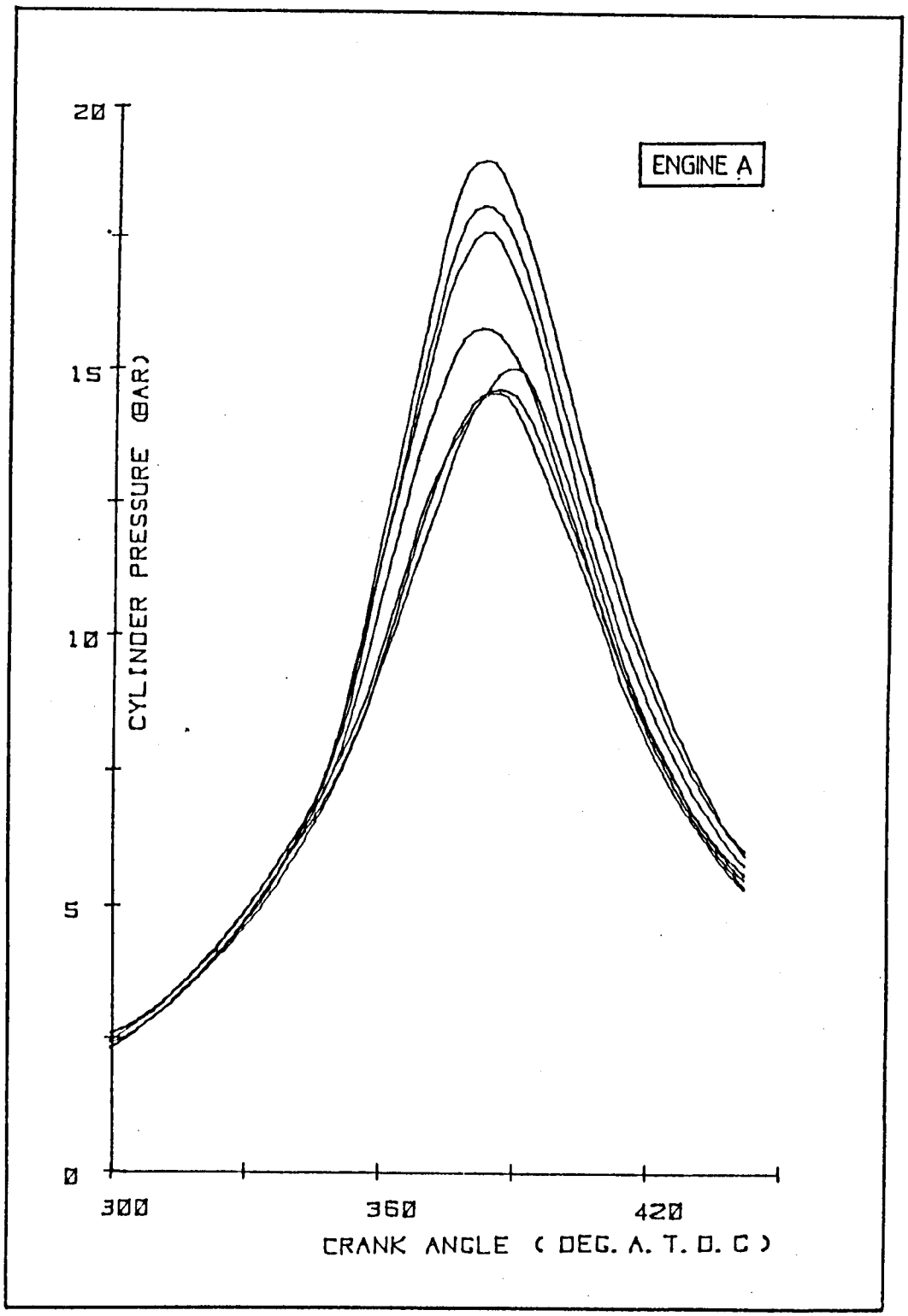

FIG 3.6 PRESSURE - CRANK ANGLE CURVES FOR ENGINE A

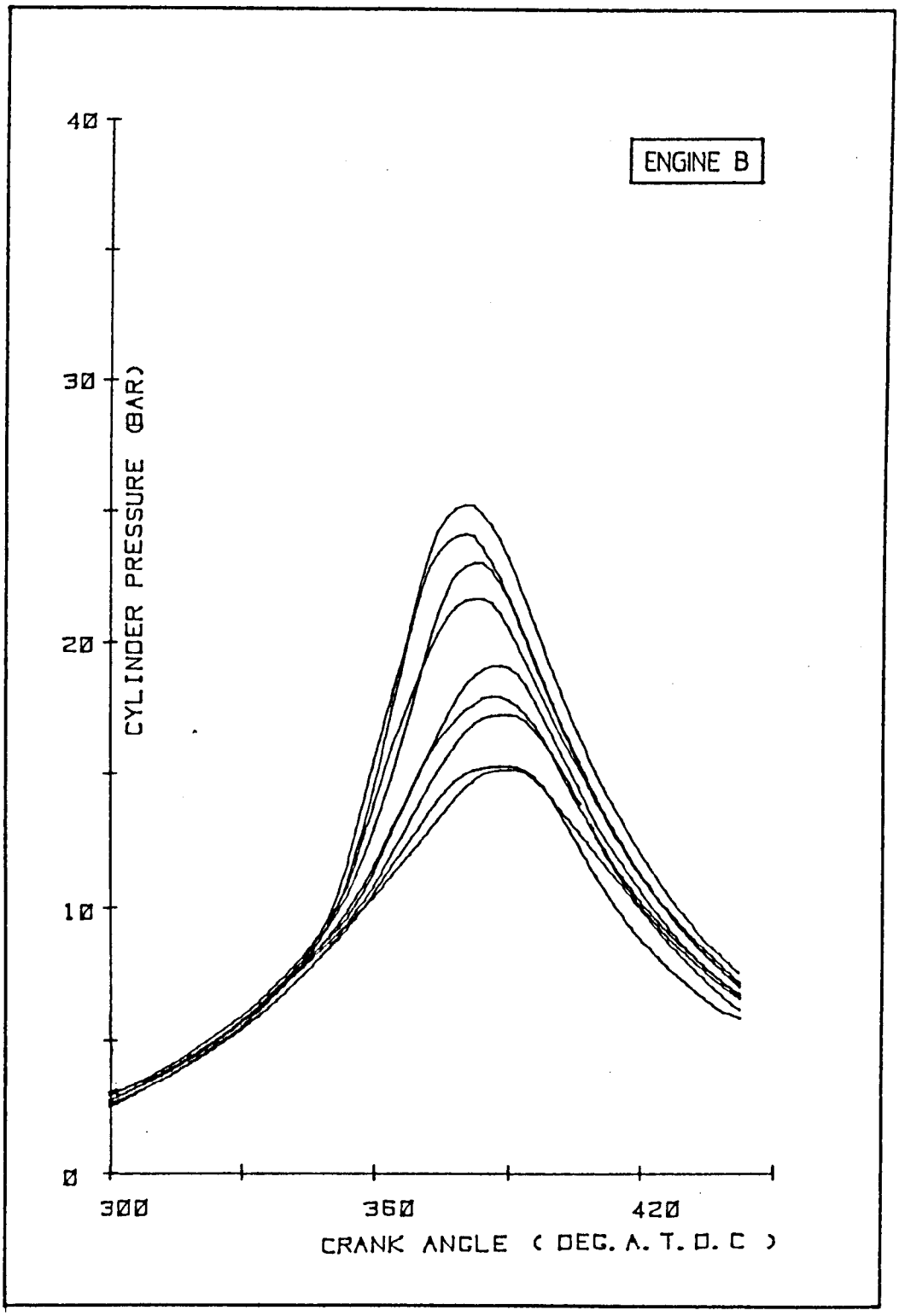

FIG 3.7 PRESSURE - CRANK ANGLE CURVES FOR ENGINE B

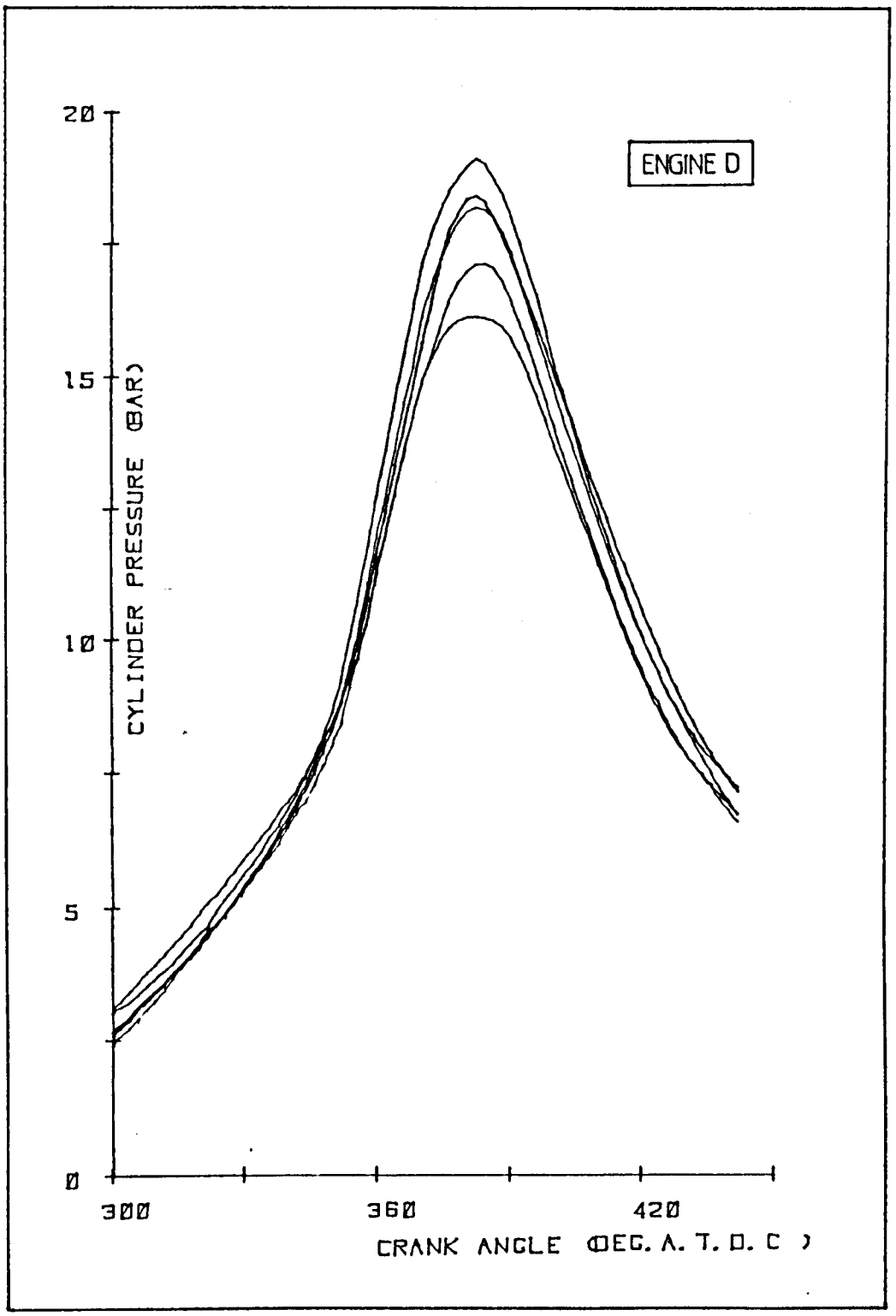

FIG 3.8 PRESSURE - CRANK ANGLE CURVES FOR ENGINE D

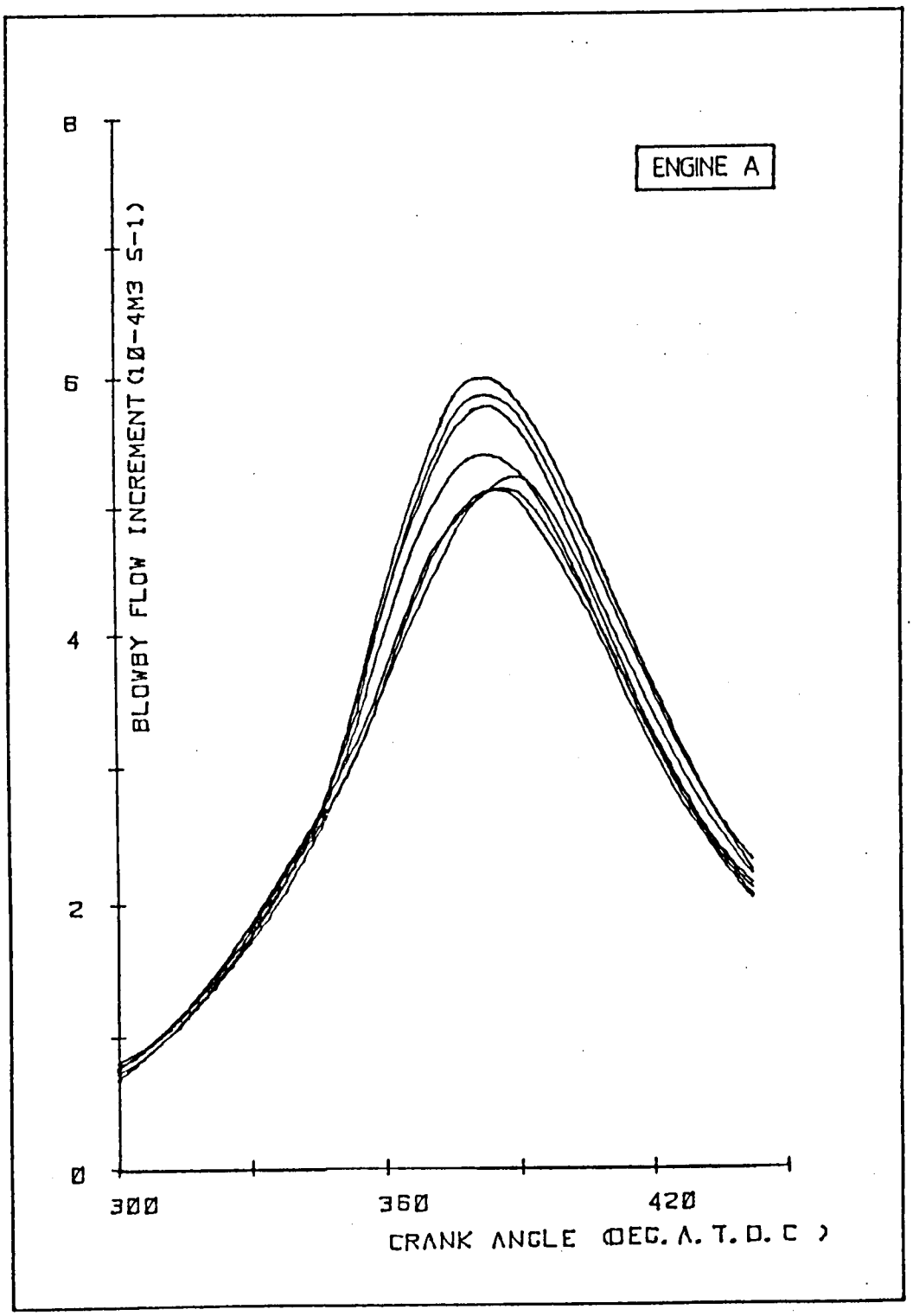

FIG 3.9 BLOWBY INCREMENT CURVES FOR ENGINE A

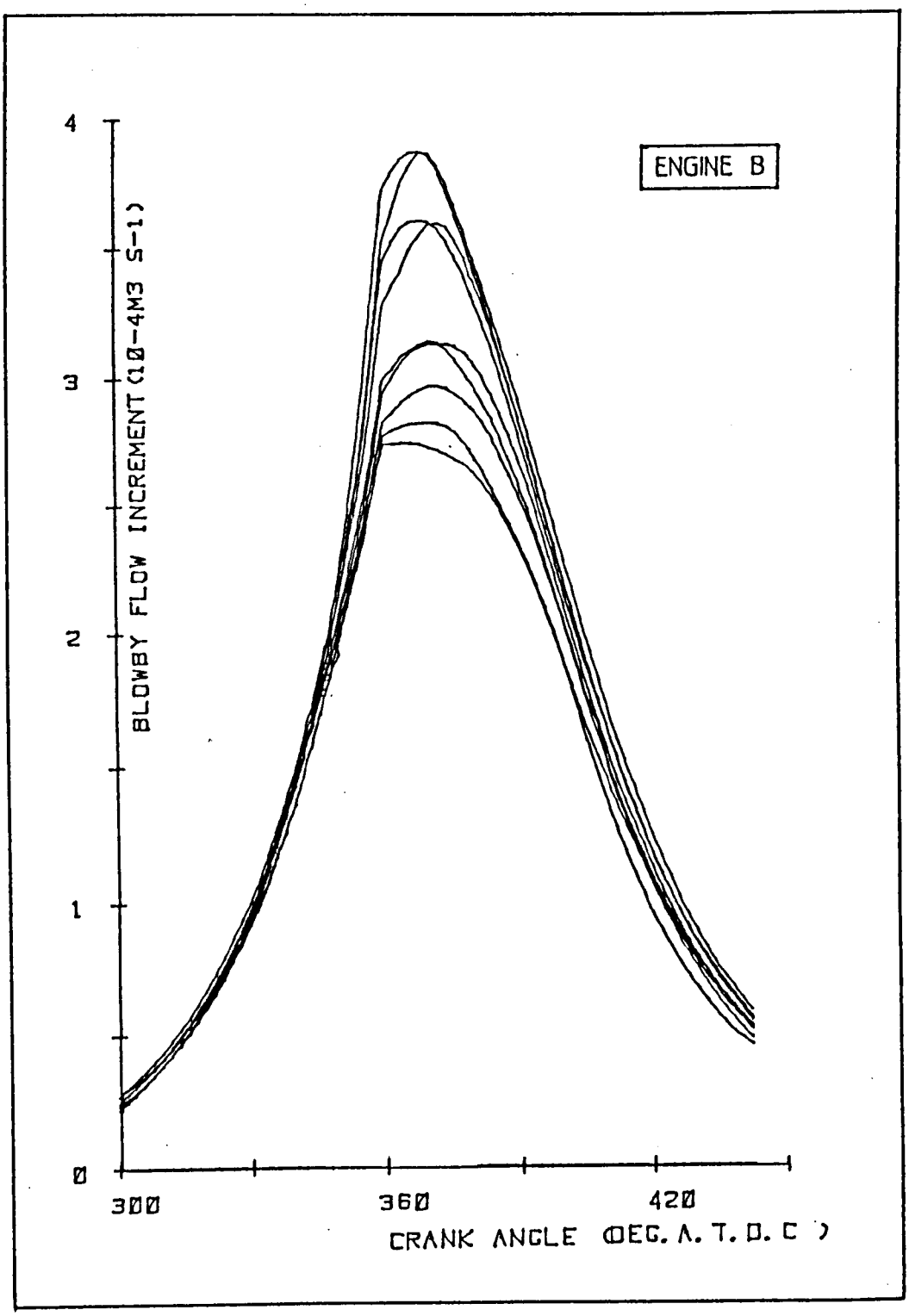

FIG 3.10 BLOWBY INCREMENT CURVES FOR ENGINE B

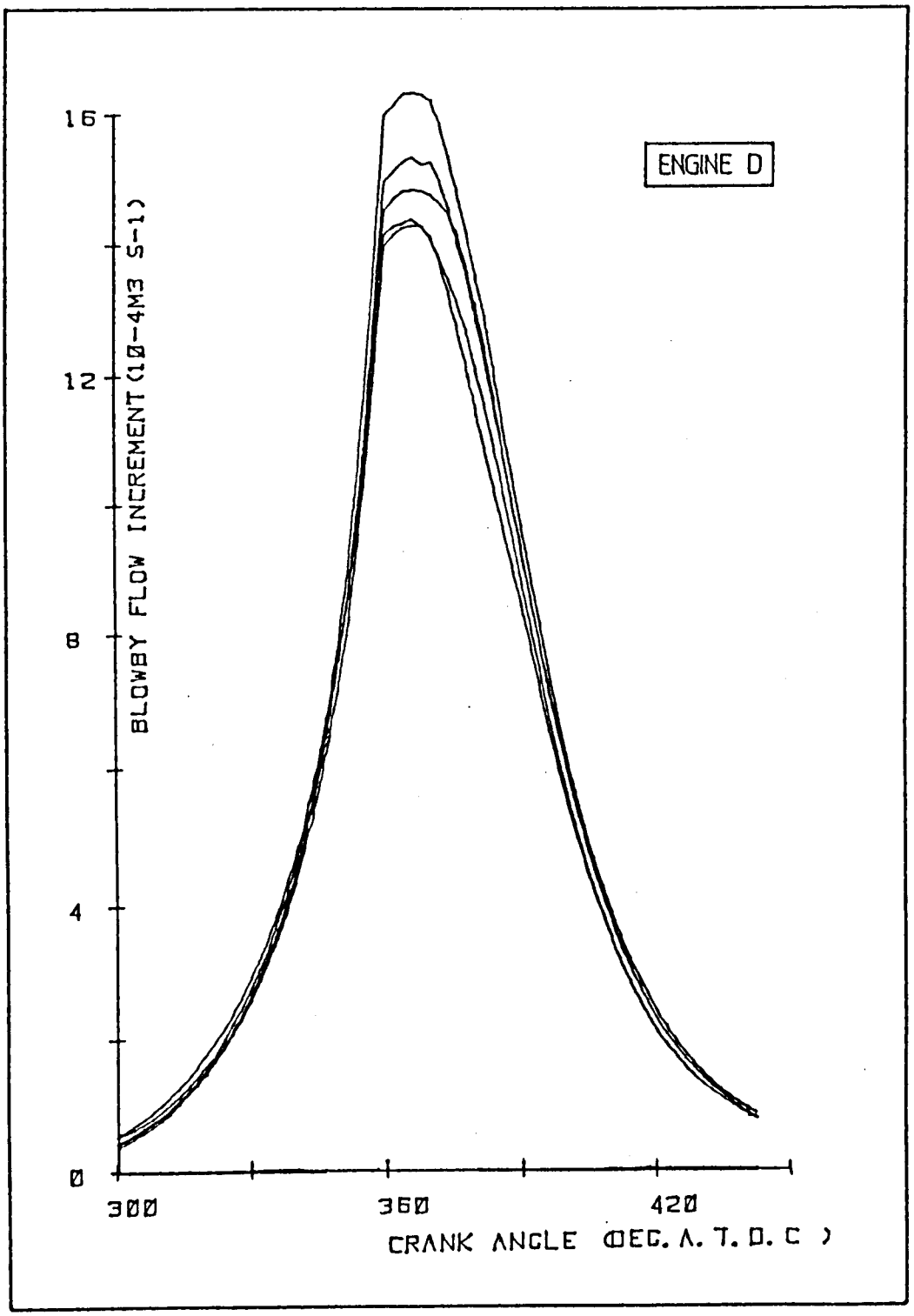

FIG 3.11 BLOWBY INCREMENT CURVES FOR ENGINE D

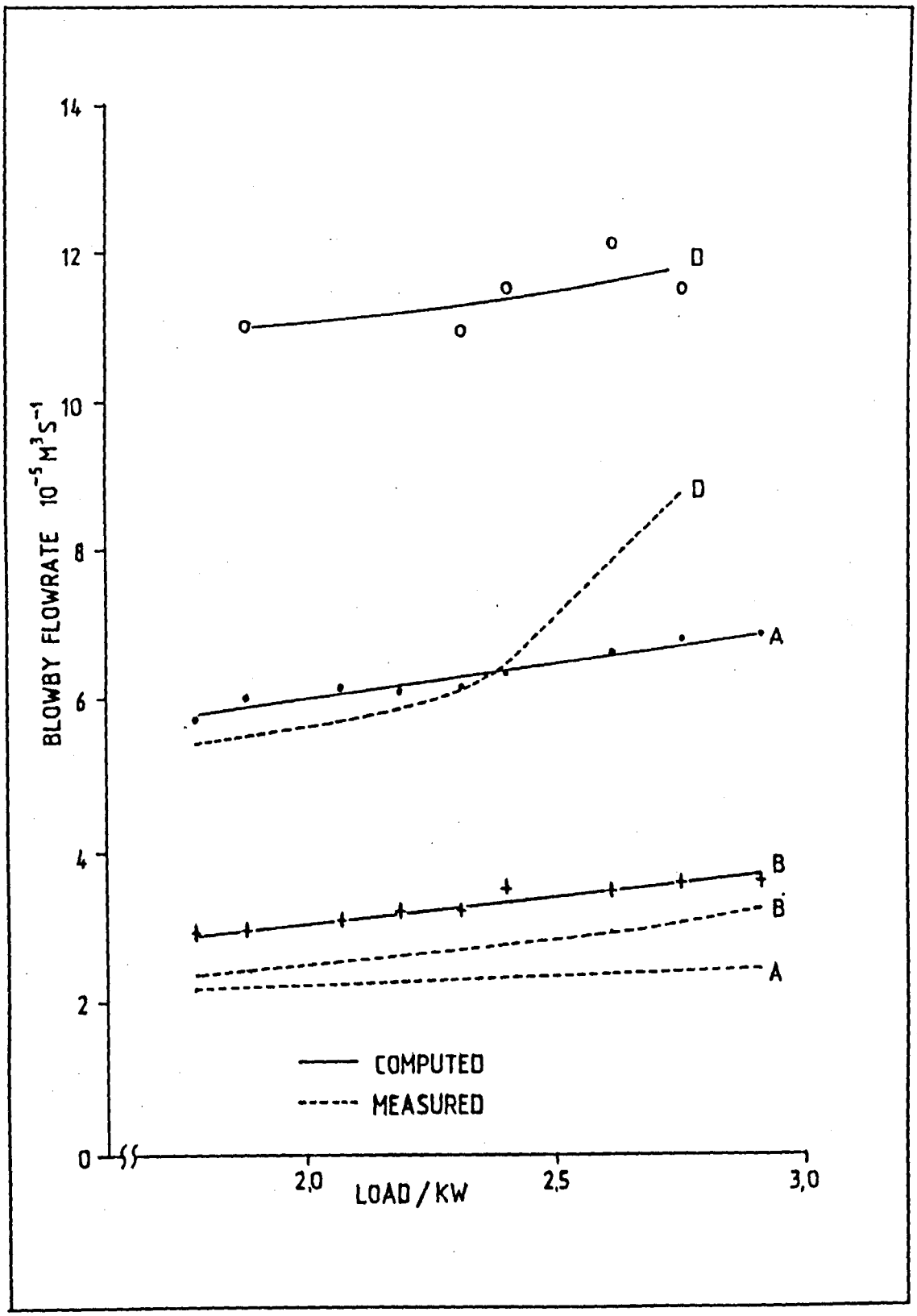

FIG 3.12 GRAPH OF COMPUTED AND MEASURED BLOWBY FLOW

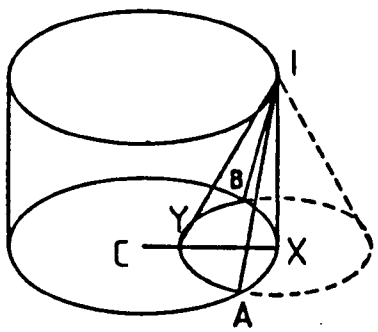

SPHERICAL FLAME WITH RADIUS IY ENGULFS PISTON CROWN AS PART AREA OF CONE BASE

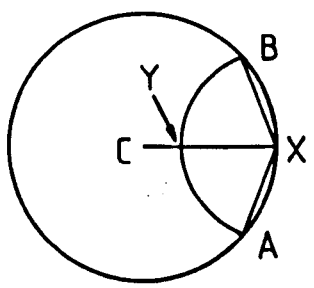

ANGLE OF COVERAGE 4Ø IS CALCULATED FROM ENGULFMENT RADIUS

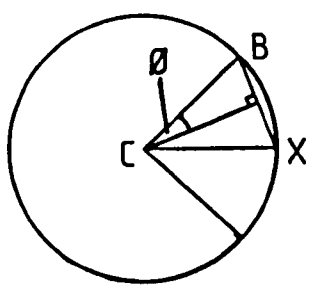

FIG 3.13 MATHEMATICAL BASIS OF FLAME FRONT POSITION.

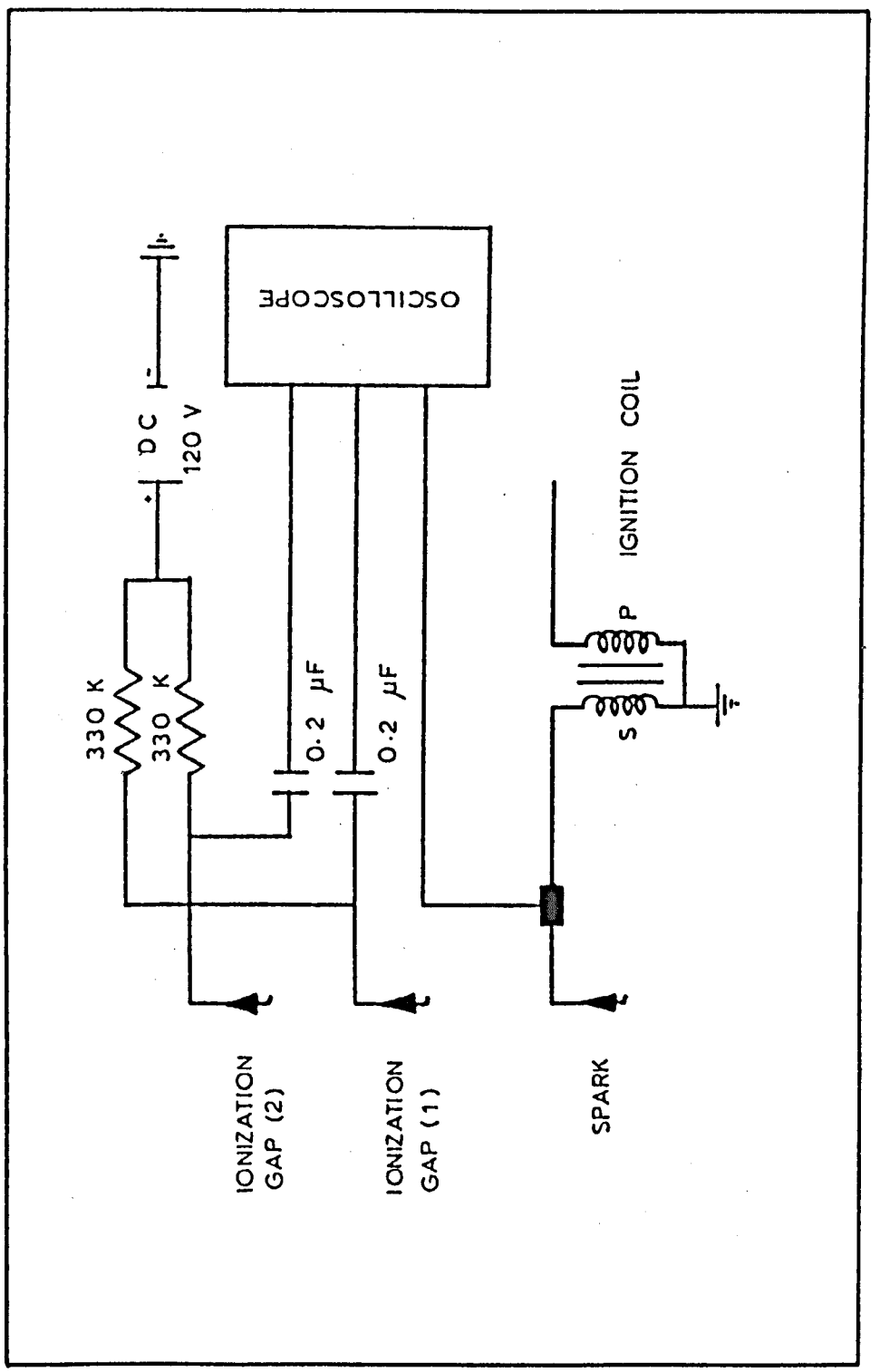

FIG 3.14 DIAGRAM OF FLAME SPEED MEASUREMENT APPARATUS

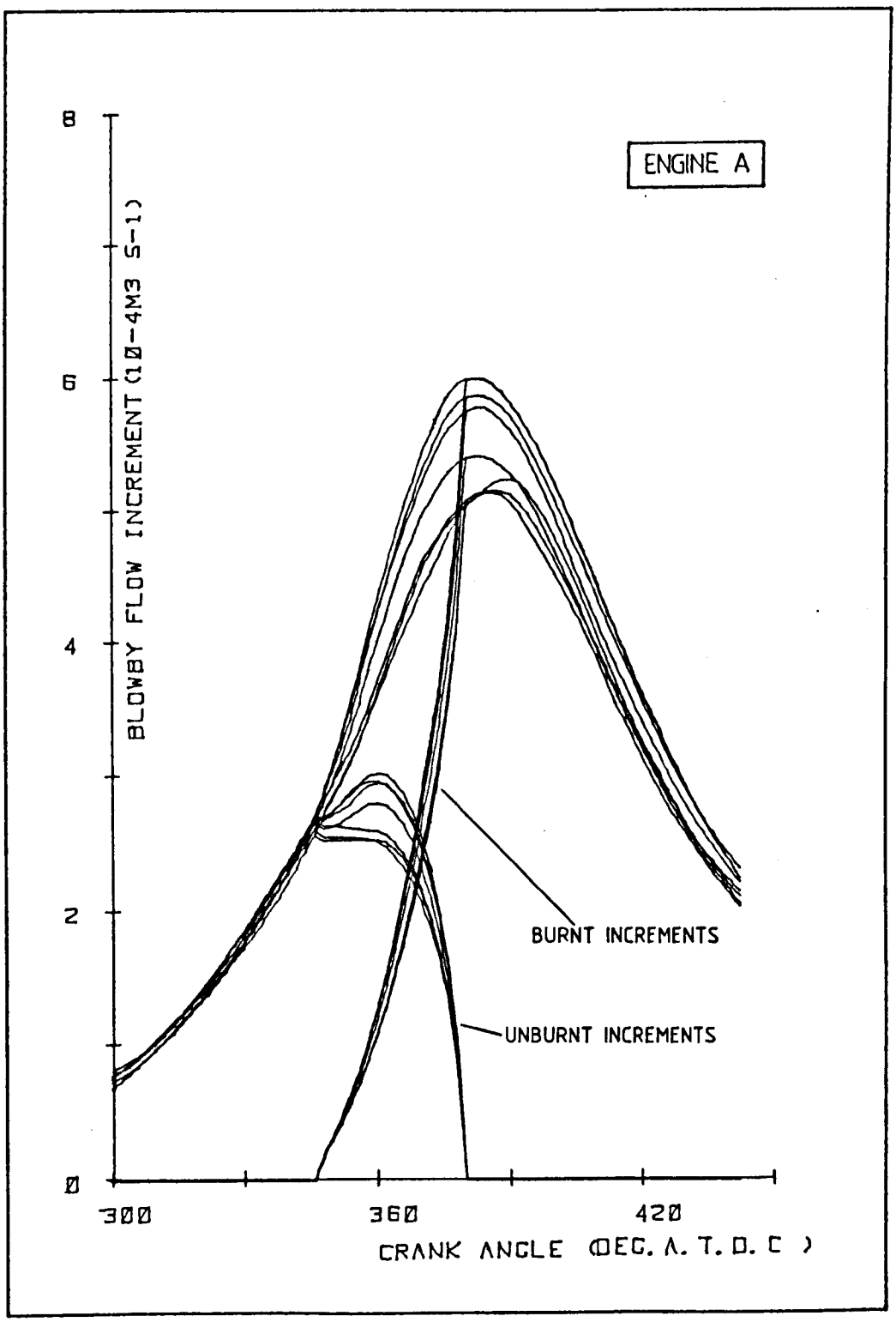

FIG 3.15 COMPOSITION INCREMENT CURVES FOR ENGINE A

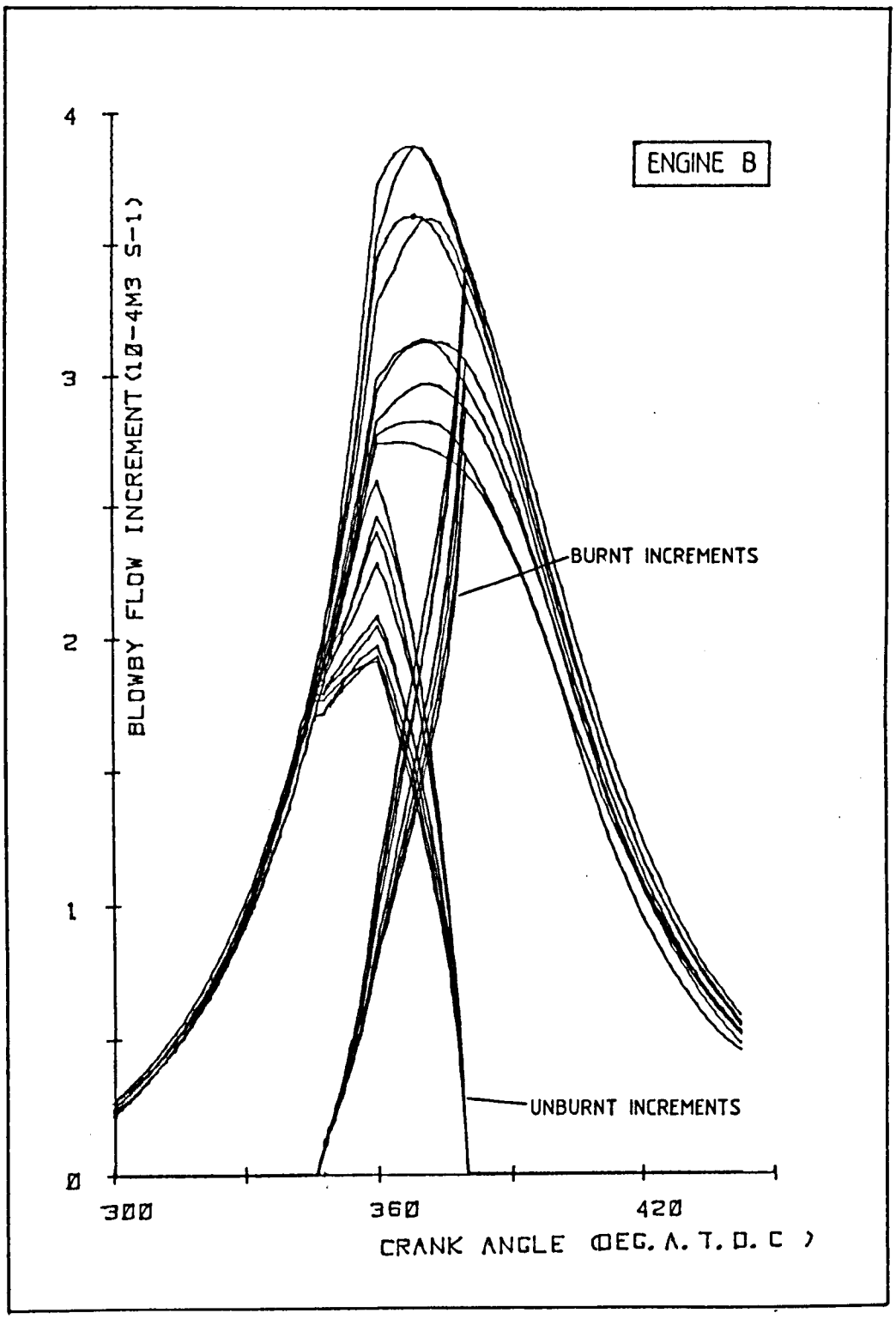

FIG 3.16 COMPOSITION INCREMENT CURVES FOR ENGINE B

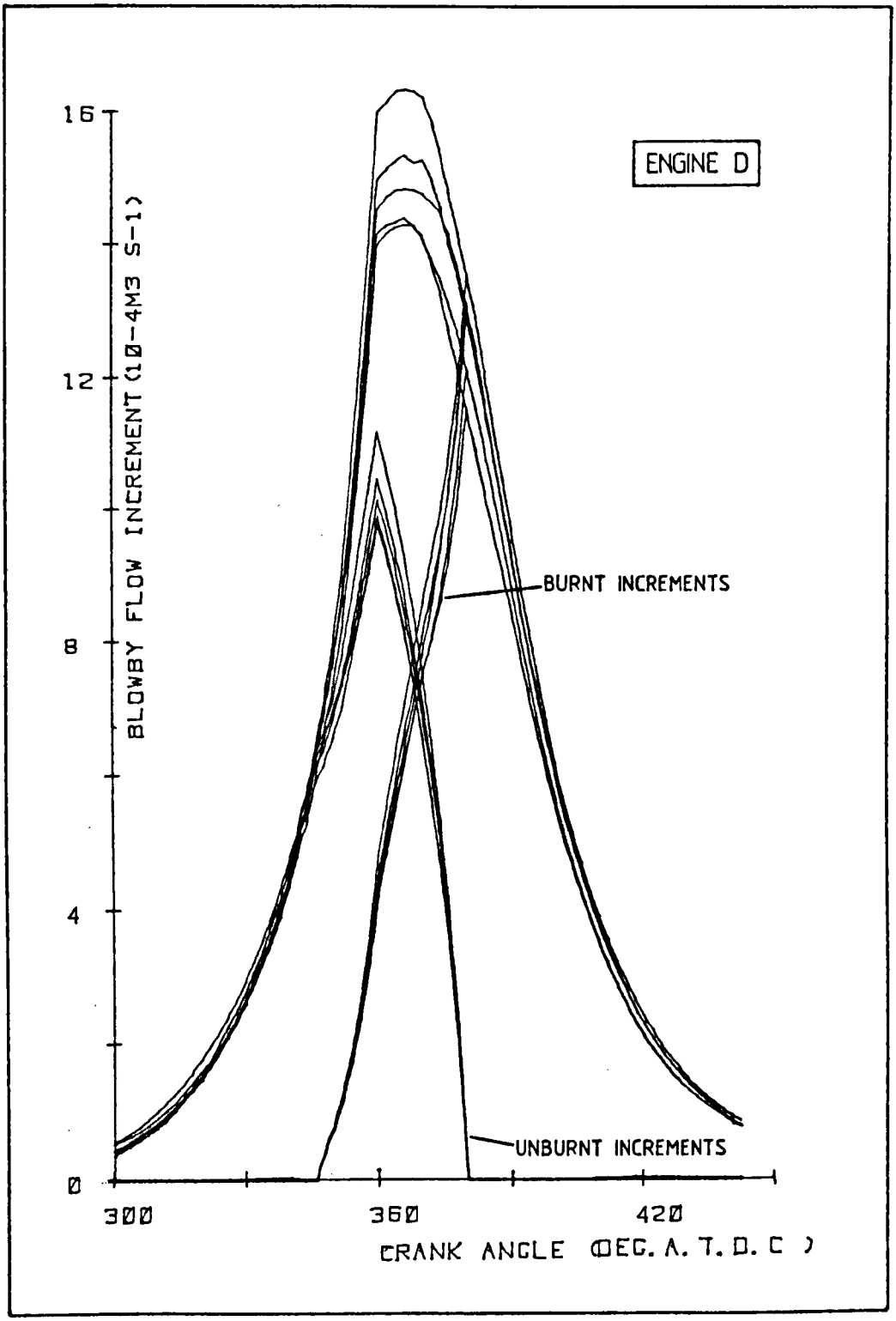

FIG 3.17 COMPOSITION INCREMENT CURVES FOR ENGINE D

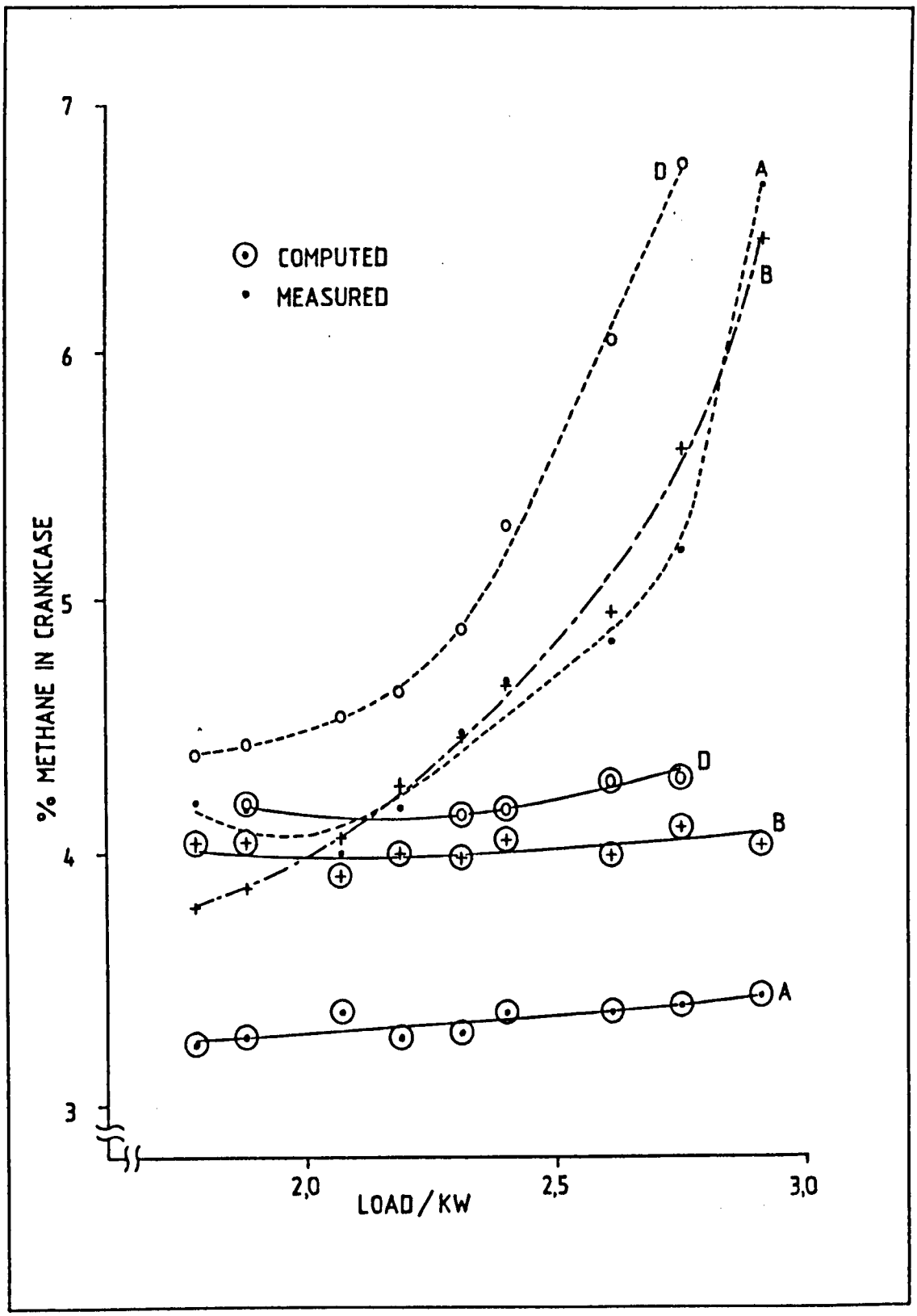

FIG 3.18 GRAPH OF COMPUTED AND MEASURED COMPOSITION

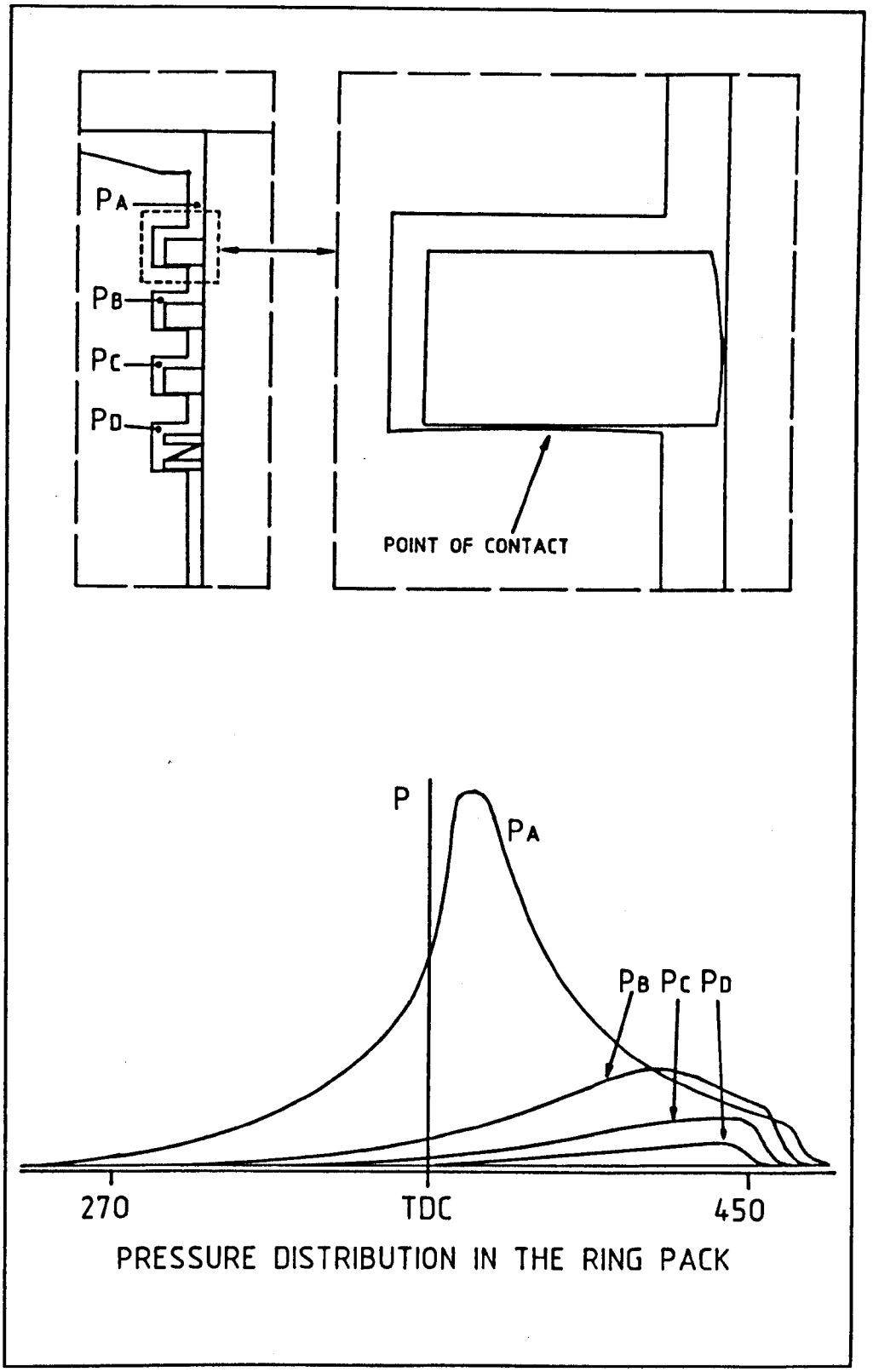

FIG 3.19 DIAGRAM OF COMPRESSION RING SEALING

Chapter 4 The Investigation of Oil in the Top Ring Zone.

4.1 Introduction

4.1.1 Lubricating oils and crankcase gas.

Blowby occurs as a result of the differential pressure between the combustion chamber and the crankcase, by passing through the piston ring pack. It is in this region that the oil is performing its most demanding task - the maintenance of lubricated contact between the piston rings and the cylinder liner. The oil is working under conditions of rapid motion, changes in both velocity and direction of the piston assembly, leading to high shear rates, temperatures and pressures, and the encroachment of hot blowby gases. Poor lubrication and high wear lead to excessive blowby, and so the quality of the oil's performance indirectly affects the nature of crankcase gas formation. The interaction between blowby and the oil on the cylinder liner is therefore very important, as it can reduce the effectiveness of the cylinder liner lubrication.

This section of the research project investigated the nature of the lubrication oil in the cylinder bore, at the point where the top compression ring is at the limit of its travel (TDC). This region has the maximum wear of the cylinder liner. As a prerequisite to details of the research, the nature of the oil used is introduced.

Modern automotive multigrade lubricating oils are formulated from a blend of base oils and specific additives which, as a total package, are designed to cope with the demands of modern high performance engines. The additives complement the properties of the base oils to provide lubrication under a wide range of conditions. The oil has to perform the following main tasks:

(a) Lubrication of moving surfaces. The oil must prevent damaging contact between paired surfaces, ensuring good separation under a wide range of temperature and load conditions.

(b) Retain its chemical integrity whilst inhibiting chemical attack on the engine. The engine requires protection from both combustion and oil degradation products, and the oil package must resist degradation under conditions of high temperatures, pressures and agitation.

(c) Cooling of high load areas. The engine bearings rely on oil as the primary coolant - a fresh supply of oil is provided directly to the region of highest load, cooling all the bearing surfaces. Secondary systems such as water cooling only affect the general temperature of the engine assembly.

(d) Resist thermal degradation and fractionation. The start up temperature can be $-30^{o}C$ or lower in cold climates, with associated sludging problems. The normal sump temperature is 80 to $95^{o}C$ with cylinder liner temperatures of up to $200^{o}C$, and accompanying exposure to hot combustion gases of approximately $900^{o}C$.

The modern multigrade engine oil contains a base oil mixture derived directly from the distillates of a blend of crude oils. The performance of the base oil has shortcomings in several areas, notably the temperature-viscosity and extreme temperature characteristics. The use of additives improves performance in these areas, and extends the range of other areas. The additive package in an oil formulation consists of several chemicals, many of which enhance the properties of the base oil in more than one way. However, the single most important role of any additive is that it is compatible with both the base oil and the other additives present in the package. The properties of the additives fall into one or several of the following classifications:

Detergent/Dispersants are designed to prevent the contamination of metal surfaces by oil impurities and breakdown products (e.g. carbon). This is achieved by surface adsorption onto the engine internals, thereby creating a non-polar hydrocarbon layer above the

metal surface; and also by adsorption onto the impurities, enabling them to remain in suspension within the oil matrix. This process is similar to the action of detergents in aqueous solutions.

They fall into two major chemical groups; organic metal salts, with a hydrocarbon molecule associated with a metal anion via a polar group in its structure; or ashless polymeric compounds with varying degrees of polar activity. These additives are selected for their ability to:

- Hold contaminants in suspension.
- Coat engine internals.
- Resist foaming or sludging.

Corrosion Inhibitors prevent corrosion of the engine, which can occur as the result of acid attack by combustion products dissolved in the oil. These additives usually have an anti-oxidant ability. They have two main modes of action - adsorption onto the metal surfaces to form a protective layer against chemical attack, and chemical reaction within the oil matrix to neutralise corrodant molecules. The latter function often includes the use of hydroxides and carbonates of calcium, magnesium or barium to eliminate acid molecules, or organic sulphur, nitrogen and phosphorous molecules to eliminate free radical attack. These additives are selected for their ability to:

- Resist the promotion of the oxidation of oil and additives.
- Remain in suspension both before and after reacting.
- Control the pH of the oil over a large temperature/life range.
- Be effective, without yielding a high ash content in the oil (alkali metal salts).

Antioxidants are added to discourage oxidation of the base oil and additive package - which leads to an increase in viscosity, sludging and acidity - by oxygen (from the crankcase, blowby gases and dissolved in the oil) and also by oxidising impurities. They also complement the corrosion inhibitors, in that they prevent oxidation of the alloys within the engine. All antioxidant additives possess a

degree of corrosion inhibition, and vice versa. This category includes the dithiophosphates and hindered phenols. The mechanism of chemical reaction in solution is usually complex. These additives are selected for their ability to:

- Inhibit peroxide free radical oxidation reactions.
- Complement the corrosion inhibitors and overbase additives.

Viscosity Index Improvers are designed to maintain constant viscosity throughout the service temperature range. They are polymers, commonly methacrylates, whose molecular structure uncoils in response to input of thermal energy into the bonds with increasing oil temperature, thus counteracting the coincident thinning of the base oil. At the high temperatures developed locally at loaded surfaces within the engine, VI improvers undergo transient viscosity reduction under sheer stress, as a result of the elongated molecules becoming aligned with the oil flow. This reduces friction and allows the rapid removal of heat. VI improvers are selected for their ability to:

- Complement the base oil's temperature/viscosity properties.
- Withstand chain scission under extreme loads and temperatures.
- Withstand oxidation.
- Remain in suspension under all conditions.

Pour-Point Depressants prevent low temperature sludging and waxing , thus assisting the start up and cold running of the engine. This is achieved by adsorption on the surface of organic precipitates, or preventative co-crystalisation with wax molecules. Modern pour-point additives are polymer methacrylates and also have dual VI roles.

Extreme Pressure additives assist in the lubrication of moving surfaces as the properties of the base oil tend towards breakdown under peak load conditions. Their mode of action is via adsorption/reaction with the loaded surfaces to give a surface layer with a low shear strength, this effect is accelerated with increasing temperature (i.e increasing resistance to load).

4.1.2 The Mechanism of Cylinder Liner Lubrication

Engine oil plays an important part in the operation of the piston and piston rings by lubricating the cylinder liner wall. A properly lubricated cylinder wall is vital to reduce the wear of both piston, piston rings and liner. The oil film reduces friction between the piston assembly and the cylinder wall, thereby reducing power loss. However, the amount of oil supplied must be carefully controlled. Too much oil results in an increase in consumption, as the excess oil is flushed into the combustion chamber and subsequently burnt. This is also undesirable as it increases combustion chamber deposits, increases exhaust hydrocarbon emissions and provides carbon deposits which can clog the piston rings and piston land leading to piston scuffing. Too little oil leads to breakdown of the oil film, the increase in friction and temperature leads to excess wear and scuffing of the piston assembly and the cylinder liner, and eventually to complete siezure.

Cylinder liner lubrication is dependent on the operation of the piston rings. The oil reaches the cylinder wall by a combination of direct splashing of the sump by moving engine components, and also indirect oiling as a result of the small end oil feed or oil used to cool piston crowns. The mechanism for individual engines varies depending on the design of the lubrication system. Once the oil has reached the cylinder wall, it is then spread over the travel of the piston by the action of the piston rings.

The main mechanism of oil film formation is that of hydrodynamic wedge action which occurs as a result of the sliding velocity of the piston rings combined with a ring running face profile which generates a hydrodynamic wedge (Fig 4.1). Careful design of the piston ring outer profile promotes hydrodynamic lubrication in the mid-stroke region of piston travel, where the sliding velocity of the piston is sufficient to force the oil to separate the ring and liner surfaces. The oil supplied to the cylinder wall is evenly distributed by this action, whilst any excess oil is returned to the sump via the oil control ring

and oil drain holes in the piston wall. Towards the limits of the piston travel, the sliding velocity decreases thereby reducing the oil film thickness. However, at this stage in the cycle, the piston ring expands towards the liner as the hydrodynamic pressure decreases. The oil trapped between the piston ring and the cylinder wall is compressed, and therefore pressure is developed. This squeeze effect delays the collapse of the oil film and the expansion of the piston ring to touch the cylinder wall as the piston approaches, reaches, and passes TDC. A well designed piston ring pack will ensure that the combination of hydrodynamic and squeeze effect mechanisms will lubricate the cylinder wall throughout the whole combustion cycle.

The oil film formed by the action of the piston rings is not necessarily continuous, nor is it always even. Considerable work has been done to establish the nature of the oil film layer.

Early research concentrated on friction and establishing the mode of lubrication. The electrical resistance of the oil film was measured in running engines (Fig 4.2) giving a qualitative measurement of the film thickness (Ref 4.1). This shows the breakdown of the oil film towards TDC, corresponding to the loss of full hydrodynamic action. The early theoretical studies concentrated on the piston ring profile for ideal operation, and this has been extended to cover the combined operation of the whole ring pack. Recent work has included the role of the oil control ring in limiting the supply of oil to the compression rings, and the extent that full hydrodynamic operation has been reduced in modern engines as a result of attempts to reduce oil consumption (Ref 4.2). The hydrodynamic lubrication mechanism controls the movement of the oil within the ring pack once supplied by the oil control ring (Refs 4.3, 4.4).

Wear of the cylinder liner and the piston ring running face occurs throughout the life of the engine. During the running in period, the formation of the oil film is incomplete as a result of the mechanical "bedding in" of the cylinder components. This includes the complementary smoothing of both piston ring and liner surfaces,

between which the hydrodynamic oil film is eventually fully generated. Throughout the remainder of the engine's life wear occurs mainly at the dead centre positions, corresponding to the breakdown of the hydrodynamic oil film and direct piston ring contact with the cylinder wall. This process is encouraged with engine age, as the piston rings lose their springiness as a result of thermal effects, and fatigue due to their confinement within the cylinder. Hence, as the engine ages, weaker piston rings find it difficult to follow an increasingly worn cylinder profile. The ability of the rings to generate the oil film decreases correspondingly, and blowby, oil consumption and further wear occur as a result.

The wear of the piston rings and cylinder are the major cause of the increasing blowby with increasing engine age. The wear of the cylinder wall near to the TDC position of the top ring compromises its ability to seal. High speed engines rely mainly on the top ring to control blowby, because the pressure drop across the top ring is large. This is because the pressure above the top ring is maintained by the fast cycle time. In slower engines there is more time within each cycle for the blowby gases to pass through the ring pack, and the pressure drop across the top ring is smaller. In high speed engines, it is important that the top ring provides an adequate seal, with the other compression rings playing a lesser role. The performance of the top ring in the region of TDC determines the quantity of blowby to reach the other compression rings.

The conditions that the top ring, and any oil film lubricating and supporting it, undergo at TDC are severe because the combustion process creates an agressive atmosphere of hot gas at high pressure. This, combined with the high temperature of the upper cylinder liner and piston crown provides a hostile environment for the lubricating oil. The composition of the oil film within this region is largely unknown, but it has been proposed that a standing ring of oil forms above the limit of travel of the top ring. This oil will be subjected to the agressive, hot combustion products, and forms the major component of the oil film lubricating the top ring at the limit of its

travel (Ref 4.5). The quality of the top ring oil controls the lubrication, wear, and therefore blowby of the engine. The supply of fresh oil to this region is a compromise between adequate lubrication and reducing oil consumption. Modern engine designs use tighter control of lubrication by the oil control ring to reduce oil consumption (Ref 4.4). This will also reduce the circulation of oil to and from the top ring zone. Oil is transported to this region by the top ring on the upward stroke of the piston. Once exposed to the combustion gases it will be partly removed by burning or evaporation. The remainder will eventually recirculate back down the cylinder wall and return to the sump.

Recent research by Richard (Ref 4.5) has considered the nature and retention time of the top ring oil in a Petter AVB engine. The top ring oil was extracted during normal running from a capillary hole in the cylinder wall. The non-volatile magnesium content of both the sump and top ring samples was used to establish the amount of oil that was recycled from the top ring zone. This indicated that the majority of the oil was lost, with only 42% returned to the sump on average.

4.2 Experimental.

The technique adopted by Richard (Ref 4.5) was considered ideal for the investigation of the nature of the oil lubricating the piston rings in the Villiers engines used in this work. The simple design of the air cooled single cylinder engine allowed easy modification and access to the top ring zone of the cylinder liner. The natural gas fuel was also favourable, because there was no possibility of fuel contamination of the oil samples (this is a problem with diesel engines).

The object of this experiment was to analyse the top ring oil, with the aim of examining the lubrication of the compression ring as it passes through TDC. The oil found in this region is subjected to the severest conditions, which also corresponds to the greatest wear.

A sample hole was carefully drilled in the cylinder wall of engine A at the point opposite the limit of travel of the top ring (Fig 4.3). This engine was chosen because of its relatively unworn components which allowed good development of hydrodynamic lubrication with minimal blowby. This combination was likely to produce the best oil samples with the minimum of impurities such as carbon. The actual height of the hole was selected to to ensure that oil from the upper edge of the top ring was sampled. The hole was positioned on the thrust side of the cylinder bore, perpendicular to the crankshaft axis.

The 1 mm sample hole in the liner had no restriction device and the oil passed through a brass fitting inserted into the cylinder block. The fitting located a 10 cm length of 4 mm internal diameter copper tube which carried the sample to the collecting vessel. The length of copper pipe was made as short as possible to prevent the oil from burning onto its interior wall.

The initial work attempted to establish an adequate trap to collect the oil sample. The trap had to de-mist a fast flowing gas whilst cooling and trapping the oil. The initial runs showed that the main problem appeared to be that the flow of gas was fast enough to force the oil vapour through the system before it had condensed onto the inner surface of the sample vessel. This led to a loss of sample vapour. The first trap was not very efficient, collecting only a trace of oil in one hour's running. The technique of collecting a sample of top ring oil was re-examined. The important components for a successful trap were considered to be:

(a) Water cooling of the container. This ensured the rapid cooling of the oil vapour from the hot gases passing through the sample trap. The continuous flow of hot gases from the engine, combined with direct heat transfer from the cylinder head through the collecting tube, rapidly warmed the collecting vessel, thereby hindering the condensation of the oil. The cooling of the container also reduced the chance of any thermal degradation of the sample.

(b) A relatively large volume condensation trap. This would contain a large amount of the condensation medium described in (c) and would allow a longer vapour contact time as a result of the drop in gas velocity. Better heat dissipation would also be expected.

(c) A condensing medium within the trap to collect the cooling oil vapour. The drop in gas velocity as a result of the sample mixture expanding into the condensation trap was not sufficient alone to allow the oil vapour to condense. Impingement plates were also not adequate. It was deemed necessary to pack the condensation trap with as much condensation medium as possible. The ideal properties for the condensing material included a high surface area with good thermal conductivity and chemical inertness. Various materials were tried, including glass and wire wool, lead shot, carbon fibre matting and glass beads.

(d) Positioning the trap as near to the engine as possible. The sample probe was not cooled and the connecting pipe between the engine and the cooler sample container was kept as short as possible to prevent the oil vapour from burning onto its inner wall. Ideally, the collecting pipe should be water-cooled from its connection to the cylinder head. However, with the air cooled Villiers engine this was not possible without extensive modifications to the engine assembly.

The first successful trap (Fig 4.4 left-hand diagram) collected oil with natural gas as a fuel. The gases passed through a brass silencer fitting into the trap packed with steel wool. These runs were at a load of 2 kW over a one hour period with frequent changes of the cooling water in the cooling bath to ensure that the condensation trap was kept at the lowest possible temperature. The second series of experiments were run using a collecting system which had been improved to the later version (Fig 4.4 right-hand diagram) with continuous cooling water.

4.3 Results and Discussion.

The engine was run for 1 hour periods, with at least 1 hour shutdown between sampling runs. This was because the extent of the oil extraction was difficult to assess, and until the calculations were completed, no apparent rate of oil removal could be determined and compared against the estimated rate of oil supply to the top ring. The oil used for these tests was a proprietary 20W/50 multigrade oil, as used for all the experimentation on blowby.

Unlike the reported oil from the Petter AVB (Ref 4.5), the traps used in this work collected a mixture of oil and water. The presence of water can be explained by both the quality of the condensation process by the water cooling of the collection system, and the large amount of water in the combustion products because of the high hydrogen content of the fuel (CH_4) when compared with diesel. The sample also contained carbon, flushed out of the combustion chamber by the sampling process. These samples required working up before analysis. The procedure devised was:

(a) Gentle water evaporation at 50°C overnight in a dark oven. The low temperature was designed to slowly remove the water without chemically degrading the oil sample.

(b) Extraction in n-pentane. This was chosen because of its non-polar solvent potential, and also its low boiling point (36 °C).

(c) Centrifuging of pentane insolubles from the extract. These consisted mostly of carbon, and some oil breakdown products.

(d) Evaporation of the pentane to leave an oil sample. This was carried out at room temperature in a dark, well ventilated enclosure.

In all cases, the product oil sample was a dark brown viscous liquid, of great subjective difference to the corresponding sump sample. The oil had been subjected to a fundamental change in its properties by its residence in the top ring zone. Several samples were collected for analysis, the extraction rate was approximately 0.5g per hour of running. The oil samples were analysed by the following techniques to give the results presented in Table 4.1.

Total Base Number (TBN). This is a measure of the base content of the oil formulation. It is defined as the quantity of mineral acid (expressed as the equivalent number of milligrams of Potassium Hydroxide) required to neutralize the base content of one gram of oil. The analysis technique (IP 177, Ref 4.6) is a titration of an oil sample by HCl, using suitable solvents. The end point is determined potentiometrically.

The results show that the TBN of the sump oil has reduced slightly, indicating that there has been some reaction between acids from the combustion process and the oil. However, there is a dramatic difference between the sump oil and the top ring oil. The top ring oil has suffered from severe deterioration of its alkali reserve.

Total Acid Number (TAN). This is a measure of the acid content of the oil, as a result of the acids introduced by combustion products. It is defined as the number of milligrams of Potassium Hydroxide required to neutralize the acids in one gram of oil. The analysis technique (IP 177 Ref 4.6) is similar to that for TBN, using KOH titrant.

The results show that the TAN of both the new and the sump oil is zero, indicating that there is no free acid present within the oil. The top ring oil has a high TAN however. This also coincides with a very low TBN, and the top ring oil has an excess of free acid which is potentially corrosive.

Viscosity Index Improver (VII) mean molecular weight. This was determined by gel permeation chromatography (GPC), which compares the

molecular weight of standard chemicals to that of the sample by their relative position within the chromatographic column.

The results show that the VII content of the oil formulation has decreased by 5% in 40 hours within the sump, but that its presence in the top ring oil is reduced to 50%.

Simulated distillation by gas chromatography. This involves the distillation and analysis of the oil sample by a temperature programmed GC. The analysis is presented as a weight within each temperature band.

The results show that the lighter fractions of the oil, which appear early in the distillation have been removed from the top ring oil.

Oxidation onset by PDSC. This involves the forced oxidation of the oil sample within a calorimeter. The exothermic reaction associated with the oxidation of the oil only occurs after the anti-oxidant additives have been exhausted.

The results show that the top ring oil has zero oxidation stability and is very poor when compared to both the sump oil and new oil. This indicates that the antioxidant additives have been completely consumed in the top ring oil.

Oxidation by IR spectroscopy. This involves analysis of the sample to determine the extent of carbonyl species present.

The results show that no oxidation (as measured by the formation of carbonyl bonds) has occurred in any of the samples.

The oil in the top ring zone is subjected to the high temperatures and pressures experienced by the combustion chamber. There will be a tendency for the oil to burn, a phenomenon reduced by engine designers by limiting the quantity of oil reaching the top ring zone, usually by modifications to the performance of the oil control ring. However, a

certain amount of oil reaches the top ring zone, in its role of lubricating the top ring. Not all of this oil is burnt, but it is otherwise modified by the conditions in this region. The oil is also subjected to chemical attack from the combustion gases, under the favourable conditions of high temperature and pressure. The oil sampled in this work was collected from the region at the top of the top ring at TDC. The oil in this region can be considered to be semi-permanent, forming a ring around the cylinder liner (Ref 4.7). Its properties are controlled by a combination of the conditions at the top ring zone as it is partially consumed, replaced by fresh oil or returned to the sump.

The TBN and TAN results show that the alkali reserve of the oil formulation has been almost totally neutralized, and that a quantity of free acid is present in the oil. The acids will be partially neutralized by fresh sump oil supplied by the lubrication mechanism, but inevitably some must be transported into the sump. The free acid present in the top ring oil must be considered as a serious corrodant.

The oil has experienced thermal degradation which will alter the viscosity in two opposing ways. The lighter fractions of the oil will be preferentially evaporated by the high temperatures involved. This will tend to increase the viscosity of the top ring oil. This is illustrated by the GC distillation results. The longer polymer molecules present in the oil will undergo chain scission. This will tend to reduce the viscosity of the oil. As the analysis of the VII improvers shows, the content of polymer additive has been greatly reduced by its residence at the top of the cylinder bore.

The two results examining the oxidation of the oil indicate that there is no remaining anti-oxidant additive in the top ring oil. However, no carbonyl oxidation is present. This suggests that the lack of anti-oxidant is due to thermal degradation rather than chemical reaction.

The oil sampled by this technique is subject to a dynamic transport system and is partially returned to the sump by the action of the piston rings. By comparing the measurements for top ring and new oil, it is possible to determine the degree to which top ring oil has been returned to the sump. This can be expressed as a percentage as shown in equation 4.1, using the results given in table 4.1. For the TBN results the top ring oil content in the sump (x) is:

$$(1.36x + 7.5\ (100 - x))\ /\ 100 = 6.95 \qquad (4.1)$$

$$x = 8.79\%$$

Similarly for VII analysis $x = 10.00\%$

and for distillation profile $x = 13.70\%$

These calculated results show good agreement for differing aspects of the oil formulation. The calculations above assume that the top ring zone is a region of significantly high chemical and thermal activity when compared with the sump, and that therefore all sump oil deterioration occurs as a result of the transport of top ring oil back into the sump. This assumption is clearly valid, as illustrated by the degradation of the top ring oil. However, antioxidant activity does occur within the sump, and oxidation life of 14 mins is a combination of both top ring and sump based reactions. By using a value of x = 10% for the PDSC, an expected oxidation life of 20.7 mins (cf 14 mins) is derived. The difference can be explained by the continuing activity of antioxidants within the sump.

Section 4.1.2 outlined the basis of hydrodynamic piston ring lubrication. The oil control ring provides sufficient lubrication to allow hydrodynamic and squeeze mechanisms to support the piston rings, without excessive oil being burnt in the combustion chamber. However, the oil supply to the upper part of the cylinder liner, beyond the travel of the oil control ring, is governed by the way in which the compression rings distribute the oil film supplied. In order to

reduce consumption, the supply of oil is kept at a minimum, yielding conditions where full hydrodynamic lubrication is compromised. As the top ring approaches TDC, the deceleration results in the oil film above the ring being thrown onto the upper liner. This replenishes any oil lost at the top of the stroke due to evaporation, and provides a layer of oil above the normal travel of the piston ring (Ref 4.1). This ring of oil has been noted in photographic studies (Ref 4.7). The oil sampled in this work is formed as a result of this mechanism. The oil within this region is subjected to the severest conditions.

The combustion chamber temperatures are hot enough to induce both evaporation and thermal cracking. In a high speed four stroke engine the exposure time for evaporation is short relative to oil replenishment by the piston on the unloaded exhaust stroke.

All the results given in Table 4.1 indicate that the top ring oil has been subjected to severe thermal degradation, the only result highlighting a chemical change is associated with the TBN/TAN. The lack of chemical degradation can be explained by the quenching of the combustion within the combustion chamber, hence the top ring oil is untouched by the flame front.

References Chapter 4

4.1 Department of Industry Report TRD 162, Piston and Ring Design 1974.

4.2 RUDDY B.L, DOWSON D, ECONOMOU P.N "A theoretical analysis of the Twin Land type of Oil Control ring" J Mech Eng Sci, Vol 23, 1981, pp51 -62

4.3 PARKER D.A, ADAMS D.R, "Friction losses in the reciprocating internal combustion engine" in Tribology - Key to the efficient engine. MEP 1982 pp31 - 39

4.4 McGEEHAN J.A "A survey of the mechanical design factors affecting engine oil consumption." SAE 790864.

4.5 RICHARD G.P "Lubricant properties in the Diesel engine piston ring zone." presented at the 9th LEEDS-LYON Symposium on Tribology, Leeds University 1982.

4.6 IP177 Institute of Petroleum standards Part I 39th Ed. 1980.

4.7 GREEN A.B "Photographic recording of Dynamic Oil Film characteristics in a Piston Cylinder Simulation rig." I.Mech E conference on Photography in Engineering, London 1969.

Figures Chapter 4.

Tables Chapter 4.

Sample	TBN	TAN	% VII content	% Remaining by dist.	Oxidation onset PDSC	Oxidation by IR
New 20W/50	7.5	0	100%	100%	23 mins	None
Sump oil	6.95	0	95%	90%	14 mins	None
Top ring oil	1.36	5.78	50%	27%	0 mins	None

Table 4.1 Comparison of the properties of Top ring oil.

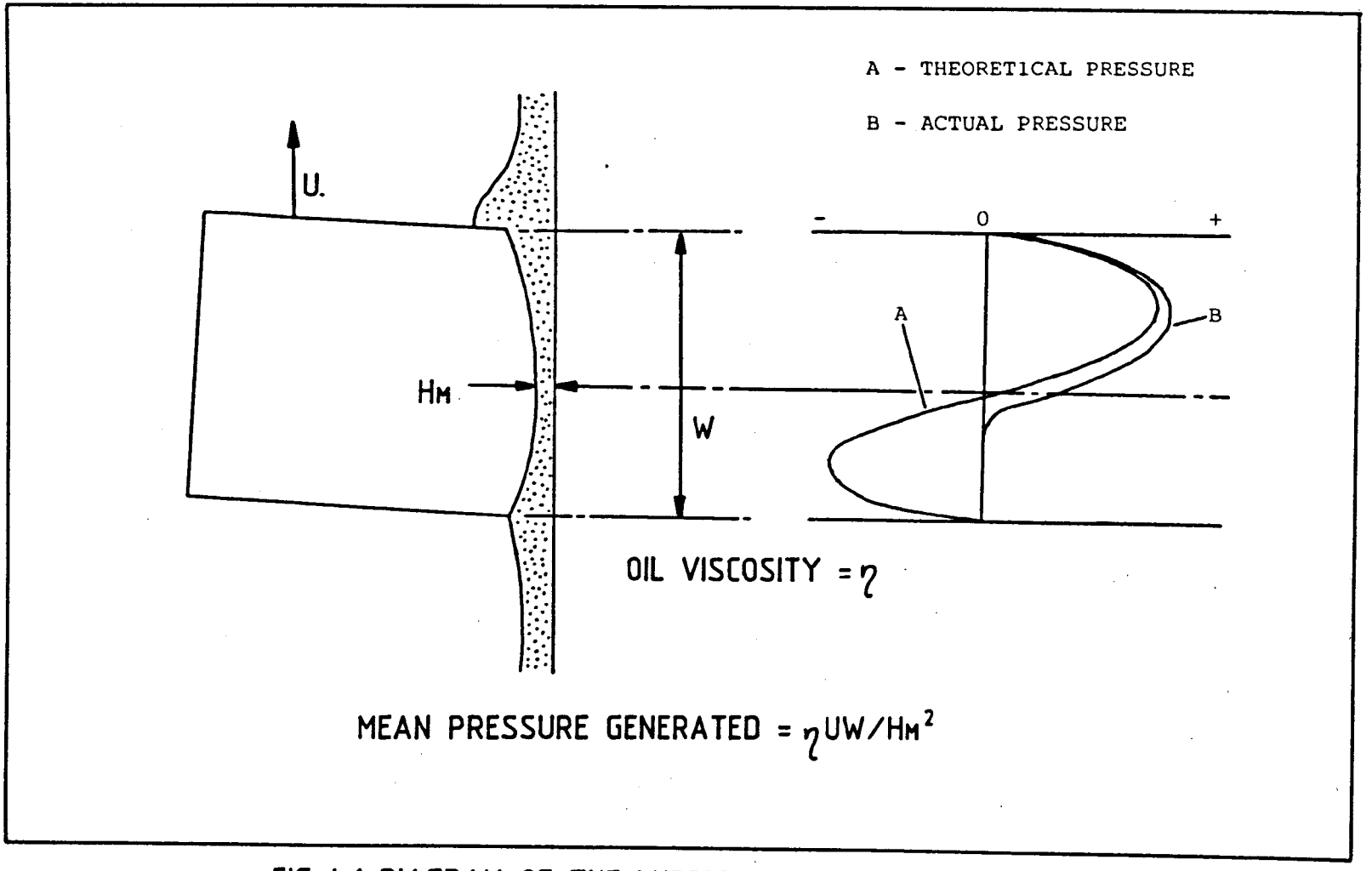

FIG 4.1 DIAGRAM OF THE LUBRICATION OF A PISTON RING

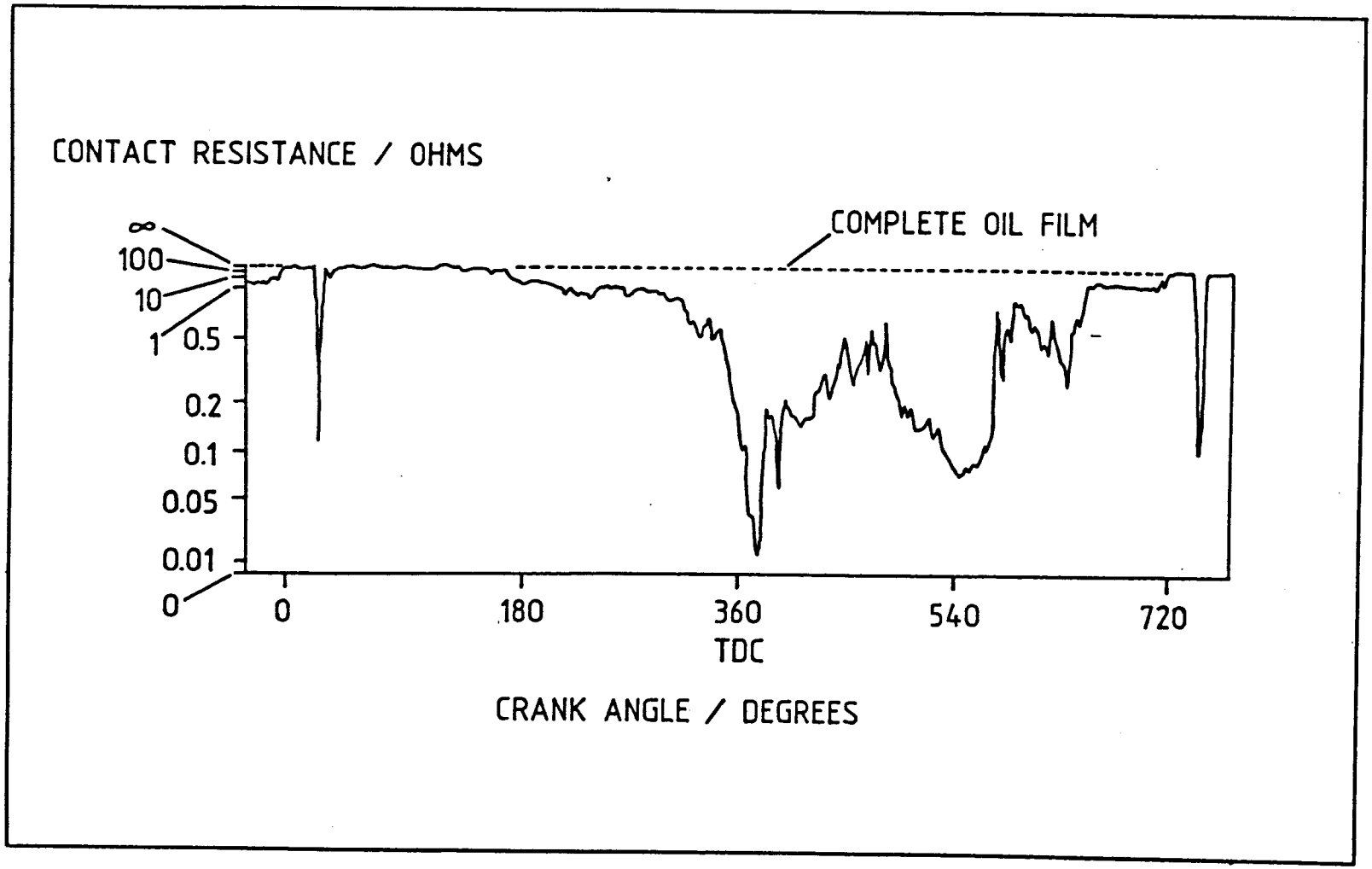

FIG 4.2 RESISTANCE TRACE BETWEEN TOP RING AND LINER

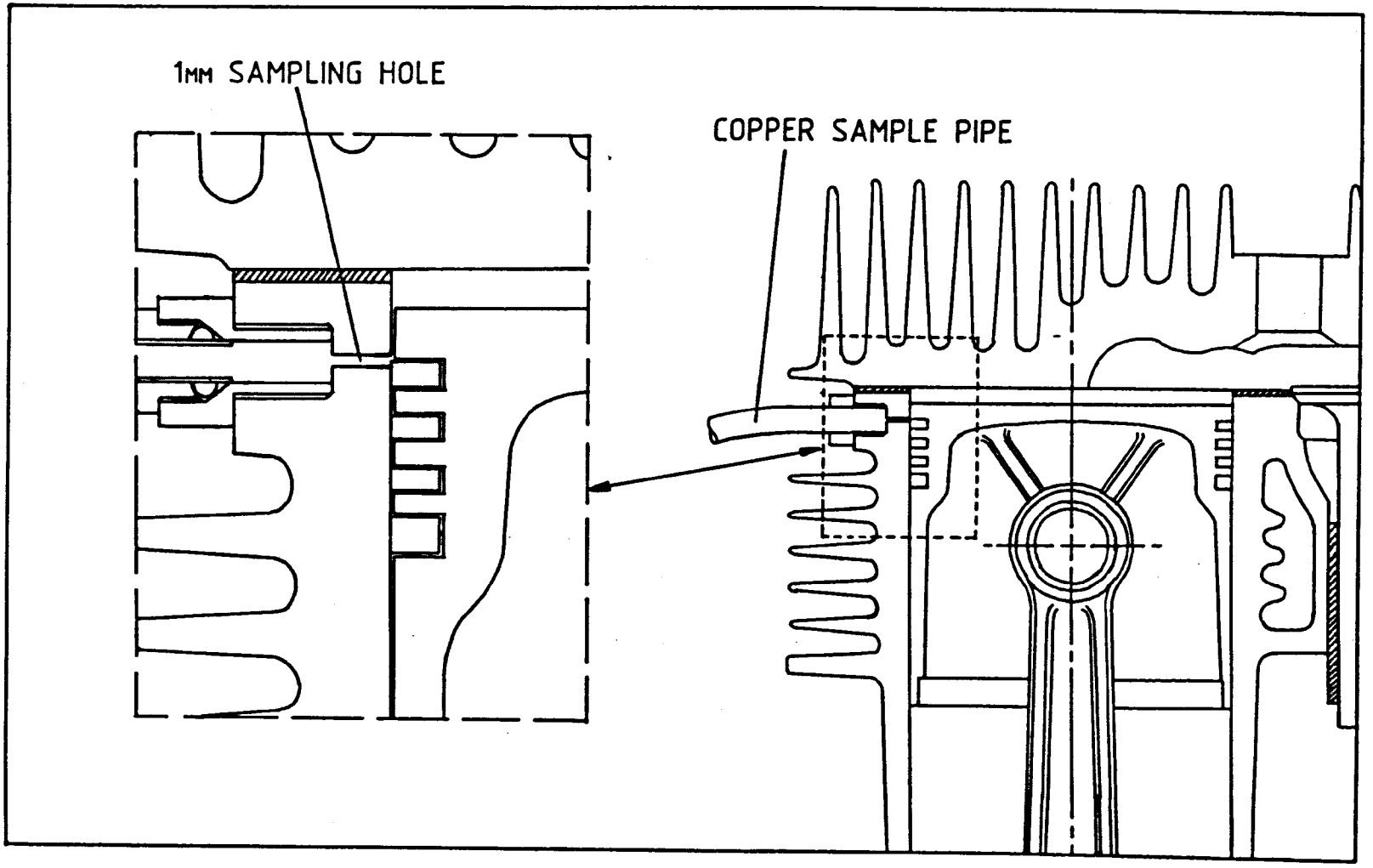

FIG 4.3 SAMPLE HOLE POSITION WITH PISTON AT TDC.

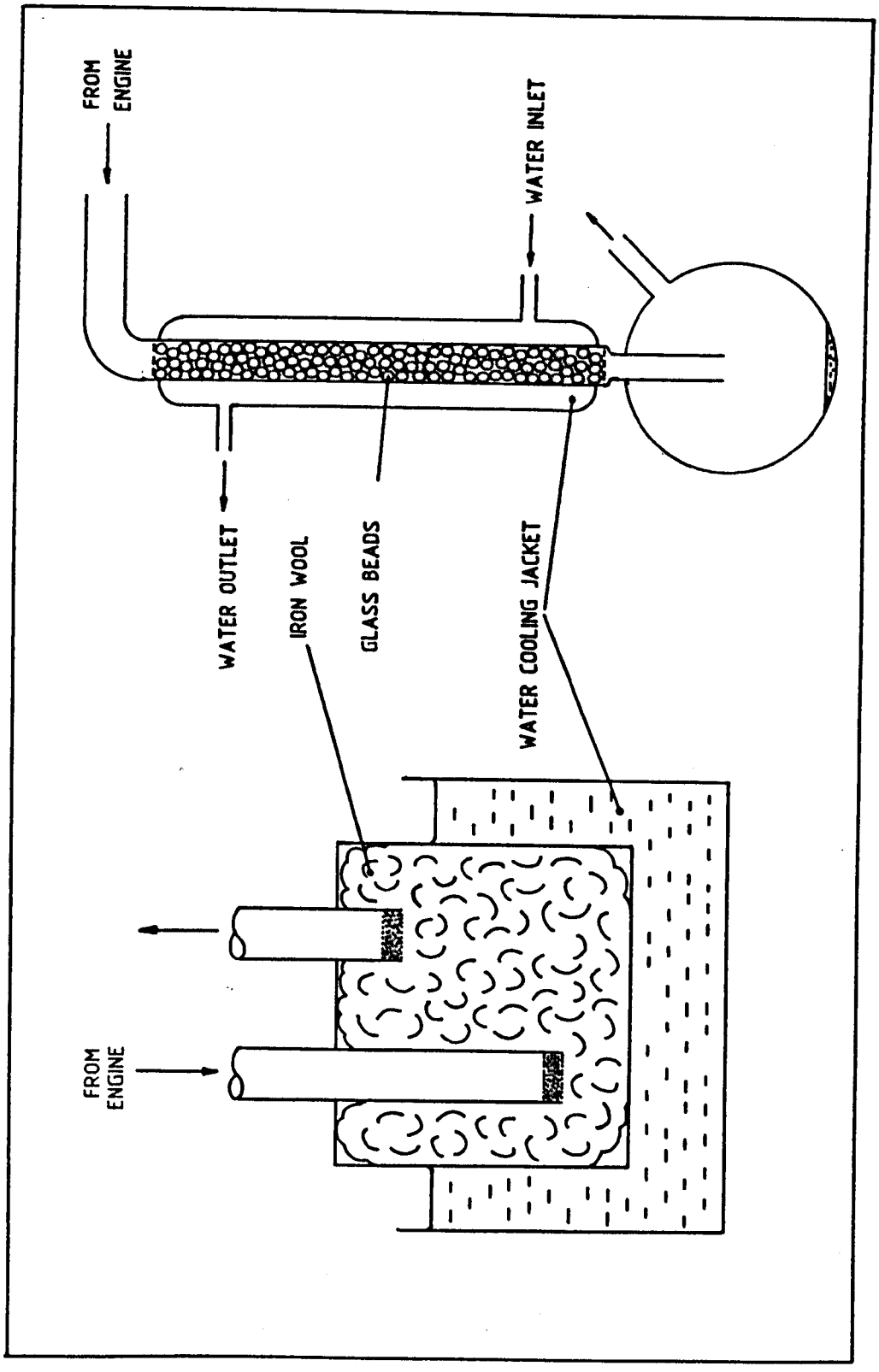

FIG 4.4 DIAGRAM OF THE TWO TYPES OF OIL TRAP

Chapter 5 Discussion.

5.1 Conclusions from the study of blowby gas.

The literature on crankcase gas, engine emissions and piston ring operation reviewed during the course of this work has revealed that several authors have commented that crankcase gas contains a large amount of fuel (Ref 5.1, 5.2, 5.3). Very little investigation of the nature of crankcase gas formation has been done, mainly due to the adopted automotive technique of crankcase gas recirculation. Indeed, the major problem with both open (air bleed into crankcase) and closed recirculation systems is the oil mist from the engine condensing in the induction system, or other cool areas in the engine. However, the adoption of more stringent emission legislations in the automotive industry is likely to encourage more research into crankcase hydrocarbons. This is because crankcase ventilation, unlike cold start fuelling or evaporative emissions, does not readily lend itself to computer control.

The experimental engine work used a single cylinder Villiers C-30 engine to quantify the composition of the crankcase gas obtained from engines of various age and wear conditions. The crankcase system on this engine is simple, with no recirculation of the gases, and a straightforward breather. This type of crankcase ventilation is common on generator engines. The main conclusions that can be drawn from this part of the work are:

(a) The fitting of a new piston and rings in a badly worn engine reduces blowby, but not down to the level of a new engine assembly. In this respect it is important that both the piston and the rings are replaced. New rings in worn piston grooves would not seal effectively. The partial reduction in blowby can be attributed to a better seal by the piston rings, with the measured blowby passing mainly through the piston ring gaps.

(b) Blowby flowrate increases with load at a rate which is greater for worn engines, particularly at higher loads (Fig 2.15). The lack of rapid flow increase with load for the newer engines, despite the increase in combustion chamber pressure indicates that the blowby process is limited by the quality of piston ring seal. The older engines show breakdown of this seal leading to much greater flowrates.

(c) The fuel content of blowby increases with load, despite the increase in inlet fuel composition with load. This feature is common to all of the engines used, and the fuel content of the worn engines is higher than that measured for newer engines. The magnitude of this difference is not large, but when combined with the higher blowby flowrate, yields a greater loss of unburnt fuel gas. The trend of fuel blowby was similar for all fuel gases considered.

(d) The CO_2 content of the blowby showed no conclusive trends, but its mechanism appears to be independent of the fuel gas blowby. The concentration of CO_2 in the crankcase remained within the 1% to 2% range for all engines at all loads. The increase in CH_4 content with load did not appear to influence the CO_2 content.

The calculations confirmed that the mechanism of crankcase blowby is through the piston ring gaps at low load and/or low wear, with another mechanism, piston ring seal breakdown, present under conditions of heavy load and poor liner condition. The experimental and calculated results have also shown that the fuel content of the crankcase occurs as a result of more than one mechanism. The Static Piston experiment is limited in that the blowby environment has been greatly simplified in order to provide the basis for a simple series of calculations to compare with the experimental data. A far more detailed treatment is required to further investigate the blowby mechanism, including corrections for the gases present and a sophisticated model of the combustion process.

5.2 The use of small engines in the Biogas Industry.

The purpose of using internal combustion engines in the Biogas Industry is to utilise the fuel produced from the digester to produce high grade energy. Other applications, such as irrigation pumping may be considered. This work has shown that although the large scale digester engine is successful, the small engine has yet to be fully developed. In analysing this observation the following conclusions can be reached which outline the present status of the technology.

(a) Most small biogas engines are derived from generator and/or automotive designs, and therefore some design compromises are present. The low demand for this application results in engines (converted for natural gas) remaining largely undeveloped and unmodified by the engine manufacturers and suppliers. The use of a Biogas engine is tailored to the needs of the site concerned, concerted development has been hampered by this and by the alterations in the electricity tariffs.

(b) Severe corrosion of copper based bearings is present in all engines where the fuel gas has not been scrubbed. This is shown in Figs 2.1 to 2.6 as the systematic removal of the bearing surface, which at Retford, resulted in the complete disintegration and disappearance of the bearing. Other engine wear problems, notably piston scuffing, have been reported.

(c) The need for the small biogas engine has yet to be fully justified, with high comparitive capital and maintenance costs making the production of electricity in this manner uneconomic in the current financial climate. The Biogas industry must look for a more viable use for their energy source.

In order to identify the future for this sector of the alternative energy industry, the motivation for the production and utilisation of Biogas must be considered.

There are two types of use for anaerobic digestion, the treatment of an obnoxious pollutant, and the use of a material to produce a useful fuel Biogas. Small digester owners in the former category will view the Biogas as a by-product which they will endeavour to use in a profitable manner. However, the viability of their project will be related to the turnover of the digestion process itself, and therefore the production and quality of the Biogas may suffer. Certainly the concept of utilising prototype engine technology to dispose of the Biogas will not appeal, because of the potential maintenance costs and risk of system failure. A simple use for the gas such as space (or digester) heating will be regarded favourably. This category of user is typically:

- A small sewage farm.
- An industrial site with a pollutant requiring safe disposal.

The second type of user has installed a digester specifically to produce gas at a long term profit. Under this approach, the economic utilisation of the gas is of great importance. This category is typically:

- A Third World farmer, who requires the biogas for cooking and heating.
- A European farmer who adopts intensive farming practices.
- A small sewage farm.

The main recommendation for the Biogas industry is that engines running on untreated Biogas should be altered to allow the use of Aluminium-Tin based bearings and to avoid excessive H_2S blowby. This approach is easier to implement than the alternative, the provision of force fed lubrication. Such modifications could be implemented during the conversion for natural gas fuelling, and marketed as an option by engine suppliers.

5.3 Conclusions from the study of top ring oil.

The experimental work into collecting top ring oil has yielded very interesting results. The oil was a viscous liquid, which had been severely degraded by the action of heat from the combustion chamber. There were no signs of chemical degradation, and in particular, no signs of oxidisation.

The longer chain polymer molecules had been pyrolysed by the hot gases from the combustion chamber, chain scission had reduced their VII characteristics. This decreases the ability of the oil to cool the highest stress areas at the surface of the piston rings. The evaporation of the lighter fractions of the oil is likely to counter any deterioration in the viscosity of the oil at the top ring zone. However, the loss of VII additive is also important as the top ring oil returns to the sump.

The combination of the loss of anti-oxidant and the high acid TAN content presents a serious corrosion threat. The implication is that the cylinder bore wear experienced at the top of the stroke could be directly related to the corrosive lubricant present. The combination of high temperatures and pressures are ideal for the corrosion of the cylinder liner.

There are other consequences related to the thermal breakdown of the additive package. The oil will have reduced dispersant/detergent abilities, which leads to piston ring clogging problems and impurities trapped in the ring zone. It is difficult to assess the performance of the top ring oil, faced with the task of lubricating the top compression ring, with such a degraded additive package.

The top ring oil recirculates back into the sump. The control of this process is governed by the supply of oil to the compression rings. The design of future engines, and oil formulations may be able to improve both the quality of oil in this area, and also enhance the life of the cylinder liner. The transport mechanism

requires careful study to highlight the optimum method of oil supply. The behavior of the oil additive package, particularly with engine life, should be studied to identify those additives at greatest risk, and those with the greatest resistance.

5.4 Recommendations and Further Work.

Sections 5.1 and 5.3 have summarised the experimental results and the implications for the use of small engines in the Biogas industry are outlined in sectio 5.2. This project has raised several areas of future interest. The main recommendations are:

(a) Further work is required to discover more about the chemistry of the top ring oil. The drastic change in the properties of the oil in this region imply that the piston ring and the cylinder liner are being lubricated by an organic mixture of high corrosion potential, and depleted additive protection.

(b) An improved technique for measuring TAN and TBN was under investigation at Leicester Polytechnic. The need for a more accurate and consistent analysis technique was highlighted by the difficulty in analysing the top ring oil samples.

(c) An investigation into blowby diversion, as first proposed by Quillan et al (Ref 5.4) may prove successful. This paper investigated the possibility of collecting the blowby prior to its entry into the crankcase. The basic engine modifications required for such a proposal may be possible with a low volume Biogas engine.

(d) A more coordinated approach to Biogas engine modification and utilisation is required. The future of the small engine in the Biogas industry relies on the commercial implementation of engine modifications, which will improve the reliability of Biogas generator systems.

References Chapter 5

5.1 PAYNE J.Q, SIGWORTH H.W "The composition and nature of blowby and exhaust gases from passenger car engines." Proc 2nd Nat Air Poll Symp 1952 Vol 2 pp 62 - 70.

5.2 BENNETT P.A et al., "Reduction of air pollution by control of emission from automotive crankcases." SAE Transactions, Vol 68, pp 514 -536.

5.3 HASS G.C, SCANLIN J.R "The contreol of crankcase hydrocarbon losses." In Vehicle Emissions Part II (Progress in Technology Vol 12) SAE 1968 pp 429 - 433.

5.4 QUILLAN R.D et al "Cleaner crankcases with Blowby Diversion." in Vehicle Emissions Part II (Progress in Technology Vol 12) SAE 1968 pp 434 - 450.

Appendix 1. Computer listings.

Computer program to curve fit Static Blowby data.

Program flow explanation.
Program listing.

Computer simulation of blowby.

Program flow explanation.
Glossary of symbols.
Program listing.

Computer Program to curve fit Static Blowby Data.

Lines	Function
10 - 30	Defines FN(BB), a function of pressure (P) and crank angle (A).
40 - 70	User input of data points, into arrays (A), (P) and (BB).
80	Creates matrices for data handling of function parameters (C), blowby derivatives (D), and curve fit residuals (R).
90	Provides start parameters for the curve fit routine.
100	Starts a loop which is executed for each experimental point.
110	Calculates the residual blowby (Measured blowby - Calculated blowby using FN(BB)).
130 - 170	Calculates the blowby derivatives with respect to the equation variables, using the central differences technique, then closes loops.
180 - 200	Calculates the least squares solution to the derivatives, which are used as corrections to the numbers originally generated in line 90.
210 - 240	Checks that the change from the curve fit is still significant enough to continue.
250	Increments the previous estimates.
260	Repeats curve fit routine if no solution is yet found.
270 - 280	Prints solution if the curve fit is complete.

Computer listing for curve fit program.

```
10  DEFFNBB(P,A);P1,A1:P1=P-1;A1=ABS(A-360)
20  FNBB=P1*(C(1,1)+C((2,1)*P1+C(3,1)*A1)*EXP(-C(4,1)+A1)
30  FNEND
40  INPUT"NO OF POINTS TO BE ENTERED";N
50  DIMA(N),P(N),BB(N,1):PRINT"INPUT ANGLE,PRESS AND BLOWBY"
60  FORI=1TON:PRINT"POINT";I,:INPUTA(I),P(I),BB(I)
70  NEXTI
80  MATC=ZER(4,1):MATD=ZER(N,4):MATR=ZER(N,1)
90  C(1,1)=BB(1,1)/(P(1)-1);C(4,1)=LOG(C(1,1)*(P(N)-1)/BB(N,1))
    /(A(M)-360)
100 FORI=1TON
110 R(I,1)=BB(I,1)-FNBB(P(I),A(I))
120 FORJ=1TO4
130 C(J,1)=C(J,1)+1E-6
140 (I,J)=FNBB(P(I),A(I))
150 C(J,1)=C(J,1)-2E-6
160 D(I,J)=(D(I,J)-FNBB(P(I),A(I)))*500
170 C(J,1)=C(J,1)+1E-6:NEXTJ:NEXTI
180 MATT=TRN(D)
190 MATE=T*D
200 MATDC=INV(E)*T*R:MATPRINTDC
210 Q=0
220 FORI=1TO4
230 IFABS(DC(I,1))>1E-4THENQ=1
240 NEXTI
250 MATC=C+DC
260 IFQ=1THEN100
270 PRINT"COEFFICIENTS"
280 MATPRINTC
```

Computer program to simulate piston ring blowby.

The blowby program is written in BASIC and is menu driven allowing the input, manipulation and display of pressure and blowby information. It is designed to run on a PET 32k microcomputer fitted with the JJ Instruments PD4 plotter software chip. The program is specific to the Villiers C30 engine, but can be used to create new data files for extending blowby work. All new files should have four characters, representing engine type and load (e.g engine A at 2.24 kW = A224).

Lines	Function
180-200	Routine to activate JJ instruments PD4 plotter chip.
210-220	Defines major data handing arrays and program constants.
230-320	Main menu display. Uses OP as the input to initiate program flow.
330-340	Initialises the main program subroutines, based on the main menu alternatives and includes a failsafe return.
350-370	Soft break of program.
380-545	Pressure data input menu including failsafe input protection. Counter PX returned to zero.
550-640	Input routines for pressure data for tape, disk, and manual entry into array P(I).
650-670	Examines pressure array P(I) and establishes the maximum pressure PX.
680-760	Examines the pressure data input string RN$ to determine which engine is involved. Allocates the calculation

coefficients A1, A2, A3 corresponding to that engine (see equation 3.2 and Table 3.2).

770 Registers that pressure data is present K(0) = 1, and zeros blowby calculation flag K(1) = 0. Returns to the main menu via line 340.

780-790 First of two routines associated with the plotting menu. Line 780 checks that pressure data has been entered (Option 3 on main menu).

800 Checks that blowby has been calculated (Option 4 on main menu).

810-900 Plotting menu display. Uses PP as the input to continue program flow.

910-930 Initialises plotting routines, or returns to main menu.

940-980 Start of the plotting routine. All commands prefixed by an exclamation mark (e.g !HO, !MA) are unique to the plotter and are used by the plotter chip located in the computer board extension socket.

990 Sets flag K(4) to 1 to initiate partition curve plotting only. Moves to blowby plotting routine.

1000 Sets flag K(3) to 1 to initiate axis plotting.

1010-1020 Checks for pressure data and blowby calculation prior to blowby plot.

1030 Sets scaling counter MX to max flow counter FX and then moves to scaling subroutine at 1830.

1040-1070 Selects blowby plotting routine based on flags K(3) and

K(4). Returns to plotting menu after completion.

1080 Sets constants and print string A$ for blowby axis plot routine.

1090-1130 Pressure plotting routine. 1090 sets flag K(3) for axes, 1100 checks K(0) for pressure data, 1110 sets scaling counter MX to a function of max pressure counter PX and then moves to scaling subroutine at 1830. Returns to plotting menu after completion.

1140 Sets constants and print string A$ for pressure axis plot routine.

1150-1190 Draws X and Y axes.

1200-1230 Labels Y axis.

1240-1270 Labels X axis.

1280-1320 Numbers X axis.

1330-1390 Numbers Y axis using scaling factor II generated from scaling subroutine.

1400-1470 Plots blowby increment curve using values from F(I) and scaling factor II.

1480-1550 Plots unburnt fraction using values from FI(I).

1560-1630 Plots burnt fraction using values from FE(I).

1640-1700 Plots pressure curve using values from P(I).

1710-1770 Labels graph with engine and load.

1780-1930 Scaling subroutine uses MX as a counter derived from the data to be plotted. The calculation allows for out of range faults and user adjustment of scales for graph superimposition.

1940-1997 Blowby calculation subroutine. Initially checks for pressure data using flag K(0) and if the calculation has already been done K(1).

2000-2010 Sets calculation variables to zero and opens calculation loop using loop counter I.

2020 Establishes crank angle DA using loop counter I and generates DB (TDC = 360 and the piston position is symmetrical about TDC). Pressure is corrected to actual from absolute.

2030 Blowby increment generated from equation 3.2 and stored as a whole number in array F(I).

2040 Incremental volume calculated and stored in V(I). Accumulated volume stored in V2.

2050 Maximum incremental flow counter is compared.

2060 If the flame has not reached the ignition point (see Fig 3.13) then F(I) is all unburnt (= FI(I)). Program moves to 2160.

2070 Updates flame radius RF using flame speed of 36 m^3s^{-1}.

2080 Converts crank angle DA into radians and calculates piston height H from TDC using equation 3.1. H is then modified by 3mm because this is the distance between the piston crown and the top of the cylinder bore at TDC.

2090 Checks to see if the flame radius RF has reached the piston height H.

2100 Calculates the distance that the flame has crossed the piston crown.

2110 Checks to see if the flame has completely engulfed the piston.

2120-2140 Calculates the amount of piston covered by the flame front as an angle BA.

2150 Divides the blowby into burnt and unburnt fractions.

2160 Calculates volume fractions and updates volume accumulator V3.

2170 Restores P(I) and continues calculation loop from 2010.

2180 Sets flag K(1) on completion of calculation. Increases counter FX to whole number.

2190-2260 Calculates overall blowby flowrate and displays results on the screen. Returns to menu on completion.

2270 Checks flag K(0) for pressure data.

2280-2330 Displays pressure output menu.

2340-2420 Transmits pressure data P(I) to storage medium.

Glossary of symbols

A	Spacing constant in X axis plot.
AA	Crank angle in radians.
AI	Scaling constant for Y axis numbering.
A$	String used in coefficient determination and plotting routines.
A1, A2, A3	Coefficients from equation 3.2 used in calculations.
B	Spacing constant in X axis plot.
BA	Ratio of piston crown coverage.
BR	Radius of flame front across piston crown.
C	Spacing constant in Y axis plot.
C$	String used to number axes.
D	Spacing constant in Y axis plot.
DA	Crank angle for increment.
DB	Angle away from TDC.
DC	Start angle for plotting calculations (300^{o}).
DI	Increment of crank angle (2^{o}).
FX	Counter for maximum flow.
F(I)	Array for flow increments.
FE(I)	Array for burnt increments.
FI(I)	Array for unburnt increments.
H	Piston height.
I	Used as a counter in all parts of the program.
II	Modifier produced from scaling routine.
K(I)	Array to store program logic flags.
L	Con rod length (127.5 mm).
LK$	String for plotter chip decider.
M	Number of readings in each data file (72).
MX	Input to scaling routine.
N	Engine speed (3000 rpm).
OP	Output of main menu.
P(I)	Array for pressure data.
PP	Output of plotting menu.
PX	Counter for maximum pressure.

Q	Output of pressure data input menu.
R	Rotational constant for plotting characters.
RA	Cylinder bore radius (35 mm).
RF	Radius of flame.
RN$	String for pressure data file name.
S	Size constant for plotting characters.
SS	Twice the stroke (66.7 mm).
T$	String used to label graph.
U$	String used to label graph.
V(I)	Array for volume increments.
VI(I)	Array for unburnt volume increments.
V1	Volume of given increment.
V2	Volume accumulator.
X	Plotting variable for X coordinates.
Y	Plotting variable for Y coordinates.

Computer listing for blowby simulation.

```
180 PRINT"    ***  CRANKCASE BLOWBY PROGRAM  ***"
190 INPUT"    HAVE YOU ACTIVATED THE PLOTTER CHIP
                    (SYS 9*4096)";LK$
200 IFLK$<>"Y"THEN SYS9*4096+3
210 DIMP(72),F(72),V(72),FI(72),FE(72),VI(72),K(5)
220 L=.1275:SS=.667:RA=.035:N=3000:DC=300:DI=2:M=72
230 PRINT"*********************************************"
240 PRINT"           ***  MAIN MENU  ***"
250 PRINT"       (1) INPUT PRESSURE DATA"
260 PRINT"       (2) CALCULATE BLOWBY CURVES"
270 PRINT"       (3) PLOT PRESSURE CURVE"
280 PRINT        (4) PLOT BLOWBY CURVE"
290 PRINT"       (5) STORE OUTPUT DATA"
300 PRINT"       (6) END"
310 PRINT"*********************************************"
320 INPUT"      PLEASE ENTER OPTION   1";OP
330 ONOPGOSUB430,1990,780,800,2270,350
340 GOTO 230
350 PRINT"            BLOWBY PROGRAM"
360 PRINT"        TYPE RETURN TO RESTART"
370 END
380 REM ************************
390 REM *                      *
400 REM *  PRESSURE DATA INPUT  *
410 REM *                      *
420 REM ************************
430 PX=0
440 PRINT"*****************************************"
450 PRINT"    PRESSURE DATA INPUT"
460 PRINT"*****************************************"
470 INPUT"    PLEASE INPUT RUN NUMBER     B224";RN$
475 IFRN$=""THEN430
480 PRINT"   IS THE PRESSURE DATA TO BE INPUTTED"
490 PRINT"       FROM: TAPE (1)"
500 PRINT"             DISK (2)"
510 PRINT"            TYPED (3)"
520 PRINT"*****************************************"
530 INPUT"   PLEASE TYPE IN NUMBER     2";Q
540 ONQGOTO550,565,630
550 PRINT"SEARCHING FOR ";RN$
560 OPEN1,1,0,RN$:GOTO580
565 PRINT"SEARCHING FOR ";RN$
570 OPEN1,8,2,"0:"+RN$+",S,R"
580 PRINT"LOADING ";RN$
590 FORI=1TOM
600 INPUT#1,P(I)
610 NEXTI
620 CLOSE1:GOTO650
630 PRINT"TYPE IN DATA THEN RETURN"
640 FORI=1TOM:PRINT"POINT";I:INPUT"";P(I):NEXTI
650 FORI=1TOM
660 IFP(I)>PXTHENPX=P(I)
670 NEXTI
680 REM ****************************
690 REM *                          *
700 REM *  3.D CURVE COEFFICIENTS  *
710 REM *                          *
720 REM ****************************
```

```
730 A$=LEFT$(RN$,1)
740 IFA$="B"THENA1=.3501:A2=-.0065:A3=.0151
750 IFA$="A"THENA1=.50797:A2=-.00965:A3=.00009
760 IFA$="D"THENA1=1.43155:A2=-.00612:A3=.02823
770 K(0)=1:K(1)=0:RETURN
780 IFK(0)<>1THENRETURN
790 GOTO810
800 IFK(1)<<>1THENRETURN
810 PRINT"****************************************"
820 PRINT"       ***  PLOTTING MENU  ***"
830 PRINT"       (1) PRESSURE PLOT WITH AXES"
840 PRINT"       (2) PRESSURE CURVE ONLY"
850 PRINT"       (3) BLOWBY PLOT WITH AXES"
860 PRINT"       (4) BLOWBY CURVE ONLY"
870 PRINT"       (5) PARTITION CURVE ONLY"
880 PRINT"       (6) RETURN TO MAIN MENU"
890 PRINT"****************************************"
900 INPUT"       PLEASE ENTER OPTION    6";PP
910 ONPPGOSUB1090,1100,1000,1010,990
920 RETURN
930 K(3)=0:K(4)=0:GOTO810
940 REM ***************************
950 REM *                         *
960 REM *  J.J PLOTTING ROUTINE   *
970 REM *                         *
980 REM ***************************
990 K(4)=1:GOTO1010
1000 K(3)=1
1010 IFK(1)<>1THENGOSUB1990
1020 IFK(0)<>1THENRETURN
1030 MX=FX:GOSUB1830
1040 PRINT"    PLOTTING BLOWBY"
1050 IFK(4)<>1THENGOSUB1400
1060 IFK(4)=1THENGOSUB1480:RETURN
1070 IFK(3)<>1THENRETURN
1080 C=8:D=25:AI=50:A$="BLOWBY FLOW INCREMENT (10-4M3 S-1)"
     :GOSUB1150:RETURN
1090 K(3)=1
1100 IFK(0)<>1THENRETURN
1110 MX=PX*1.6:GOSUB1830
1120 PRINT"    PLOTTING PRESSURES ":GOSUB1640
1130 IFK(3)<>1THENRETURN
1140 C=8:D=25:A$="CYLINDER PRESSURE (BAR)":AI=31.25:
     GOSUB1150:RETURN
1150 !HO
1160 X=45:Y=20:!MA,X,Y
1170 A=5:B=25:!XA,A,B
1180 X=45:Y=20:!MA,X,Y
1190 !YA,C,D
1200 X=51:Y=102;!MA,X,Y
1210 R=2:!RO,R
1220 S=3:!SZ,S
1230 !PR,A$
1240 X=85:Y=5:!MA,X,Y
1250 A$="CRANK ANGLE ( DEG A.T.D.C )"
1260 R=1:!RO,R
1270 !PR,A$
1280 Y=12:I+300
1290 FORX=40TO140STEP50
1300 C$=STR$(I)
1310 !MA,X,Y:!PR,C$
```

```
1320 I=I+60
1330 NEXTX
1340 X=33:I=0
1350 FORY=18TO218STEP50
1360 C$=STR$(I)
1370 !MA,X,Y:!PR,C$
1380 I=I+(AI*II):NEXTY
1390 !HO:RETURN
1400 X=45+((DC-300)/1.2)
1410 Y=20+(10000*F(1)/II)
1420 !MA,X,Y:!PD
1430 FORI=2TOM
1440 X=X+(DI/1.2)
1450 Y=20+(10000*F(I)/II)
1460 !DA,X,Y:NEXTI
1470 !HO:RETURN
1480 X=45+((DC-300)/1.2)
1490 Y=20+(10000*FI(I)/II)
1500 !MA,X,Y:!PD
1510 FORI=2TOM
1520 X=X+(DI/1.2)
1530 Y=20+(10000*FI(I)/II)
1540 !DA,X,Y:NEXTI
1550 !HO
1560 X=45+((DC-300)/1.2)
1570 Y=20+(10000*FE(1)/II)
1580 !MA,X,Y:!PD
1590 FORI=2TOM
1600 X=X+(DI/1.2)
1610 Y=20+(10000*FE(I)/II)
1620 !DA,X,Y:NEXTI
1630 !HO:RETURN
1640 X=45+((DC-300)/1.2):Y=20+(P(1)*1.6/II)
1650 !MA,X,Y:!PD
1660 FORI=2TOM
1670 X=X+(DI/1.2)
1680 Y=20+(P(I)*1.6/II)
1690 !DA,X,Y:NEXTI
1700 !HO:RETURN
1710 BB=(INT(1E7*BB))/100
1720 T$="ENGINE "+LEFT$(RN$,1)+" LOAD "
1730 U$=MID$(RN$,2,1)+">"+MID$(RN$,3)+" KW"
1740 X=70:Y=240:!MA,X,Y
1750 S=3:!SZ,S:R=1:!RO,R
1760 !PR,T$,U$
1770 !HO:RETURN
1780 REM **********************
1790 REM *                    *
1800 REM *  SCALING ROUTINE   *
1810 REM *                    *
1820 REM **********************
1830 IFMX<4THENII=.02
1840 IFMX>4ANDMX<=8THENII=.04
1850 IFMX>8ANDMX<=16THENII=.08
1860 IFMX>16ANDMX<=32THENII=.16
1870 IFMX>32ANDMX<=64THENII=.32
1880 IFMX>64THENPRINT"OUT OF PLOTTING RANGE":FORI=1TO3000:
     NEXTI:RETURN
1890 PRINT" SCALING FACTOR IS ";II
1900 INPUT" DO YOU WANT TO CHANGE THIS    N";Q$
1910 IFQ$<>"Y"THEN1930
```

```
1920 INPUT" NEW VALUE (.02,.04,.08,.16,.32)    .08";II
1930 RETURN
1940 REM ****************************
1950 REM *                          *
1960 REM *  CALCULATION SUBROUTINE  *
1970 REM *                          *
1980 REM ****************************
1990 IFK(0)=0THENRETURN
1995 IFK(1)=1THENRETURN
1997 PRINT"     CALCULATING BLOWBY"
2000 V2=0:V3=0:V4=0:FX=0:RF=0
2010 FORI=1TOM
2020 DA=DC+((I-1*DI):DB=ABS(DA-360):P(I)=P(I)-1
2030 F(I)=P(I)*(A1+A2*P(I))*EXP(-A3*DB):F(I)=F(I)/10000
2040 V1=F(I)/(3*N):V2=V2+V1:V(I)=V1*1E6
2050 IFF(I)>FXTHENFX=F(I)
2060 IFI<24THENFI(I)=F(I):FE(I)=0:GOTO2160
2070 RF=RF+(36/9000)
2080 AA=DA*3.141759/180:A=COS(A):H=L+SS*(1-A)/2
     -SQR(L^2+SS^2*(A^2-1)/4):H=H+.003
2090 IFRF<HTHENFI(I)=F(I):FE(I)=0:GOTO2160
2100 BR=SQR(RF^2-H^2)
2110 IFBR>(2*RR)THENFE(I)=F(I):FI(I)=0:GOTO2160
2120 BA=BR/(2*RR)
2130 IFBA=1THENBA=4*ATN(BA):GOTO2150
2140 BA=4*(ATN(BA/SQR(-BA*BA+1)))
2150 FE(I)=BA*F(I)/(2*3.141759):FI(I)=F(I)-FE(I)
2160 RI=FI(I)/F(I):VI(I)=RI*V(I):V(I)=V(I)-VI(I):V3=V3+VI(I)
2170 P(I)=P(I)+1:NEXTI
2180 K(1)=1:FX=10000*FX
2190 BB=V2*N/120:BC=V3*N/120
2200 PRINT"    BLOWBY =";BB"M3 S-1"
2210 V2=V2*1E6:V4=.81*(V2-V3)/V2:V5=1-V4
2220 PRINT"    INLET FRACTION =";V5
2230 PRINT" EXHAUST FRACTION =";V4
2240 PRINT"TYPE ANY KEY TO RETURN"
2250 GETX$:IFX$=""THEN2250
2260 RETURN
2270 IFK(0)<>1THENRETURN
2280 PRINT"    ************************************"
2290 PRINT"     IS THE PRESSURE DATA TO BE STORED
2300 PRINT"         ON: TAPE (1)"
2310 PRINT"             DISK (2)"
2320 PRINT"    ************************************"
2330 INPUT"         PLEASE TYPE IN NUMBER   2";Q
2340 IFQ>2THEN2330
2350 IFQ=1THEN2370
2360 IFQ=2THEN2380
2370 OPEN2,1,1,RN$:GOTO2390
2380 OPEN2,8,15,"0:"+RN$+",S,W"
2390 FORI=1TOM
2400 PRINT£1,P(I)
2410 NEXTI
2420 CLOSE2:RETURN
```